San Joaquin Valley Fog Measurements During the 1995 Integrated Monitoring Study

Jeffrey L. Collett, Jr.
Katherine J. Hoag
D. Eli Sherman
Aaron Bator

Research Supported by San Joaquin Valleywide Air Pollution Study Agency).

Colorado State University

DEPARTMENT OF ATMOSPHERIC SCIENCE

PAPER NO. 644

San Joaquin Valley Fog Measurements During the 1995 Integrated Monitoring Study

by

Jeffrey L. Collett, Jr.
Katherine J. Hoag
D. Eli Sherman
Aaron Bator

Department of Atmospheric Science
Colorado State University
Ft. Collins, Colorado 80523

Research Supported by
San Joaquin Valleywide Air Pollution Study Agency

July 1997

DISCLAIMER

The statements and conclusions in this report are those of the Contractor and not necessarily those of the California Air Resources Board, the San Joaquin Valleywide Air Pollution Study Agency, or its Policy Committee, their employees or their members. The mention of commercial products, their source, or their use in connection with material reported herein is not to be construed as actual or implied endorsement of such products.

EXECUTIVE SUMMARY

Fogs are important processors of atmospheric aerosols. Particles scavenged by fog drops can be efficiently removed to the ground via sedimentation. New particulate mass can also be formed as a result of chemical reactions within fog drops. Potentially significant reactions include aqueous phase oxidation of sulfur dioxide and nitrous acid to form sulfates and nitrates. The 1995 Integrated Monitoring Study (IMS 95) was designed to examine factors controlling particulate matter concentrations in California's San Joaquin Valley (SJV). As part of that effort, Sonoma Technology, Inc. (STI), Colorado State University (CSU), Carnegie Mellon University (CMU), and the National Center for Atmospheric Research (NCAR), joined together to conduct Technical Support Study Number 11: Investigating the dynamics and chemistry of fog formation and dissipation. As part of that effort, CSU conducted two SJV fog studies. This report documents the methodology of those studies and provides an overview of the findings. Separate TSS11 reports document the results of fog modeling by CMU and trace gas measurements by STI and NCAR. Further data analysis efforts are also underway through the joint efforts of STI, CMU, and CSU. Findings from these efforts will be provided in a future report.

APPROACH

In order to document temporal and spatial variations in SJV fogs and their ability to process aerosols, two separate fog measurement campaigns were conducted. Beginning December 8, 1995, three fog measurement sites were operated in the southern SJV at the IMS95 core sites of Bakersfield, Kern Wildlife Refuge (KWR), and Fresno. Following the conclusion of the IMS95 winter study, the fog sampling equipment was relocated to the Candelabra Tower in Walnut Grove, California, approximately 30 km south of Sacramento in the northern SJV.

The southern SJV study was designed to document fog composition at the three IMS95 core sites during as many events as possible. This included an analysis of temporal changes in fog chemistry and physics as well as an examination of variations in drop composition across the fog drop size spectrum. At each of the three locations CSU operated a bulk fogwater collector and one or more collectors capable of sampling two or three independent portions of the fog drop size spectrum for chemical analysis. The most heavily instrumented site was KWR, which featured a bulk fog sampler, two size-fractionating fog samplers, and a fog drop sizing probe. The Fresno and Bakersfield sites were each operated with one bulk fog sampler and one two-stage fog impactor. Sample times for bulk fog samples were typically an hour with two-hour sample times often used for the size-fractionating fog samplers.

Ten different fog episodes were sampled during the southern SJV study. There were two nights when widespread fog permitted sampling at all three sites. A total of 14 bulk fog samples were collected at Bakersfield during three fog episodes. Six episodes were sampled at KWR, where a total of 21 bulk fog samples were collected. At Fresno 25 bulk fog samples were collected during six fog episodes. Size-fractionated fog samples were also collected at the three sites during most of the sampled events.

The Candelabra Tower study was designed specifically to examine vertical variations in fog composition and aerosol processing. Three bulk fog collectors were operated by CSU during this study. One was located at the base of the 430 m Candelabra Tower and two were mounted on the tower. One collector was mounted at 140 m elevation on the tower, while the second was mounted at 230 m during one event and at 320 m during a second event. The fog measurements were complemented by aerosol (Berner impactor and Differential Mobility Analyzer) and trace gas (NH_3, HNO_3, SO_2, O_3, H_2O_2, NO and NO_y) measurements by CSU, CMU, STI, and NCAR and by meteorological measurements made by STI and CARB.

A total of two fog/low cloud events were sampled at the Candelabra Tower. During the first event, fog extended from above the top fog sampler to the ground. A total of four one-hour periods were sampled during this event. Two days later, low clouds were sampled by the upper two collectors, but no significant fog was present at the ground. A total of three one-hour periods were sampled during this event.

During both fog studies sample pH was measured on location, while sample aliquots were prepared for later analysis at CSU of the following species: Cl^-, NO_3^-, SO_4^{2-}, Na^+, K^+, NH_4^+, Mg^{2+}, Ca^{2+}, formate, acetate, propionate, pyruvate, oxalate, total organic carbon, dissolved organic carbon, S(IV), hydroxymethanesulfonate, formaldehyde, hydrogen peroxide, iron, and manganese.

MAJOR CONCLUSIONS

The fog measurement campaign has produced a number of significant findings. These include the following major conclusions:

- Although fog was forecast nearly every night of the southern SJV fog study, it did not form at the chosen sampling sites on most nights. Significant spatial heterogeneity in fog occurrence was observed, with observations suggesting that fog formed more frequently away from urban areas, particularly in areas receiving irrigation. Consequently, future studies of aerosol processing by fogs may be better served by locating fog sampling sites outside of urban boundaries.
- Fog pH was consistently high at all locations with a median observed bulk fog pH value above 6. Fogwater tended to be somewhat more basic at KWR than at Bakersfield or Fresno. The greatest range of pH values was observed at Bakersfield.
- The high pH values can be readily accounted for by large inputs of ammonia to the precursor aerosol and to the fog itself. Ammonium ion was the dominant species in the collected fog samples.
- Nitrate was generally present at much higher concentrations in the fog than was sulfate, although there were a few exceptions to this pattern at Bakersfield.
- On two of three nights sampled at Bakersfield rapid increases in fogwater S(IV) and sulfate concentrations were observed, each time accompanied by acidification of the fog. A similar phenomenon was also observed at the Candelabra Tower. These observations suggest that

plumes of sulfur dioxide may be present within the fogs, resulting in locally rapid aerosol sulfate production.

- Aside from these sulfur plumes, the major ion concentrations in collected fog samples were remarkably similar at the three southern SJV sites, despite the fact that Bakersfield and Fresno were urban locations, while KWR was at a rural, albeit polluted, location.
- Concentrations of some organic acids, formaldehyde, and total organic carbon content tended to be higher in urban than in rural SJV fogs.
- Fogwater loadings of major ions were observed to decrease over the course of two extended fog events, suggesting significant particulate removal via fog drop deposition.
- Secondary aerosol species (sulfate, nitrate, and ammonium) were observed to be enriched in small fog drops relative to large drop concentrations of these species. Small drops were also observed to be more acidic than large drops, with differences in large and small drop pH typically of the order of several tenths of a pH unit. These findings are consistent with previous observations of size-dependent fog drop composition in the SJV and elsewhere.
- Preliminary estimates of aqueous S(IV) oxidation rates during the study suggest that ozone is often the dominant oxidant, due to the extremely basic environment (pH typically greater than 6). Hydrogen peroxide concentrations were typically too low to make S(IV) oxidation by H_2O_2 competitive with oxidation by ozone.
- The high drop pH also appears capable of promoting rapid formation of S(IV)-aldehyde complexes, such as HMSA. Further data analysis is required to examine whether this complex formation is likely to result in decreased sulfate formation.
- The measured chemical heterogeneity present among the sampled fog drop populations suggests that accurate prediction of aqueous phase sulfate production rates may not be possible based simply on observations of the bulk fogwater composition. Information is required about the distribution of droplet pH values present.
- Significant vertical variations were observed in both fog/cloud liquid water content (LWC) and chemical composition. Increases in LWC with altitude were generally stronger than decreases in ion concentrations, indicating that greater amounts of material were present in the droplet phase at higher altitudes. This pattern could reflect enhanced aerosol scavenging higher in the fog/cloud, depletion of material near the surface due to droplet deposition, or both.
- Vertical gradients in oxidant concentrations (especially ozone), drop pH, and sulfur dioxide concentrations combine to produce variations in aqueous phase sulfate formation rates with altitude. In particular, strong increases in ozone with elevation were at times capable of driving much faster oxidation chemistry at the top of the fog layer than would be predicted based on surface measurements. This observation documents the need to monitor vertical gradients in fog and trace gas properties in any future study designed to examine mechanisms affecting winter SJV particulate levels.
- Increases in fogwater hydrogen peroxide concentrations following sunrise suggest that new peroxide is being photochemically produced, either in the gas phase or within the droplets themselves.

TABLE OF CONTENTS

TABLE OF CONTENTS

LIST OF FIGURES

LIST OF FIGURES

LIST OF FIGURES

LIST OF FIGURES

LIST OF TABLES

During winter 1995/96 Colorado State University conducted measurements of fog chemistry at four locations in California's San Joaquin Valley as part of the 1995 Integrated Monitoring Study (IMS 95). Ground-based measurements were made at three of the four study core sites (Bakersfield, Kern Wildlife Refuge (KWR), and Fresno) during the IMS 95 winter study in December and January. In early January sampling equipment was moved north to the Candelabra Tower, near Walnut Grove, California, where measurements were made of vertical variations in fog chemistry. This report provides documentation concerning the methods for fog sampling and analysis and provides an overview of the collected data. It begins with a description of measurement methods and data processing followed by presentation of an overview of findings from the measurement campaign.

1. Measurement Methods and Data Processing

1.1 Cloud/fog samplers used in IMS95

Four different cloud/fog sampler types were used in IMS95. One type collected "bulk" samples representative of the entire fog drop size distribution, while three other types collected multiple independent cloud drop size fractions. These collectors are described below. Sample times for bulk fog samples were typically one hour, but ranged from 20 minutes to several hours. Size-fractionated fog sample periods ranged from one hour to several hours, with typical times of approximately two hours.

1.1.1 The Caltech Active Strand Cloudwater Collector Version 2 (CASCC2)

The Caltech Active Strand Cloudwater Collector Version 2 (CASCC2) (Hoffmann et al., 1989; Collett et al., 1994; Demoz et al., 1996) was used to collect bulk fog samples at the three IMS95 winter core sites and from the Candelabra Tower. This instrument (see Figure 1-1) collects fog droplets by inertial impaction on a bank of Teflon cylinders. The cylinders are comprised of 508 μm diameter Teflon strand, wrapped around three Teflon-coated frames, for a total of six collector rows. The frames are enclosed in a Plexiglas housing and supported above a Teflon sample trough. Air is drawn through the CASCC2 at 5.8 m^3/min by a fan located at the rear of the collector. The theoretical 50% size cut for the CASCC2 corresponds to a drop diameter of 3.5 μm. As droplets impact on the Teflon collection strands, they coalesce and are pulled by gravity and aerodynamic drag down into the sample trough. Collected fogwater flows from the sample trough, through a Teflon sample tube, into a polyethylene sample bottle. During IMS95 the sample was retrieved manually at the end of each sample period.

Aliquots of CASCC2 samples were prepared for analysis of pH, major ions, S(IV), organic acids, trace metals, formaldehyde, and hydroperoxides at all sites. In some cases not all species were analyzed, especially when insufficient sample was available or insufficient time was available to preserve unstable species. Some samples collected at KWR and the Candelabra tower were also analyzed for hydroxymethanesulfonate (HMS), total organic carbon (TOC), and dissolved organic carbon (DOC).

1.1.2 The Size-fractionating Caltech Active Strand Cloudwater Collector (sf-CASCC)

The size-fractionating Caltech Active Strand Cloudwater Collector (sf-CASCC) (Munger et al., 1989; Demoz et al., 1996), is a larger version of the CASCC2 with an additional inlet designed to collect large fog drops. This collector, depicted in Figure 1-1, was deployed at the core site near

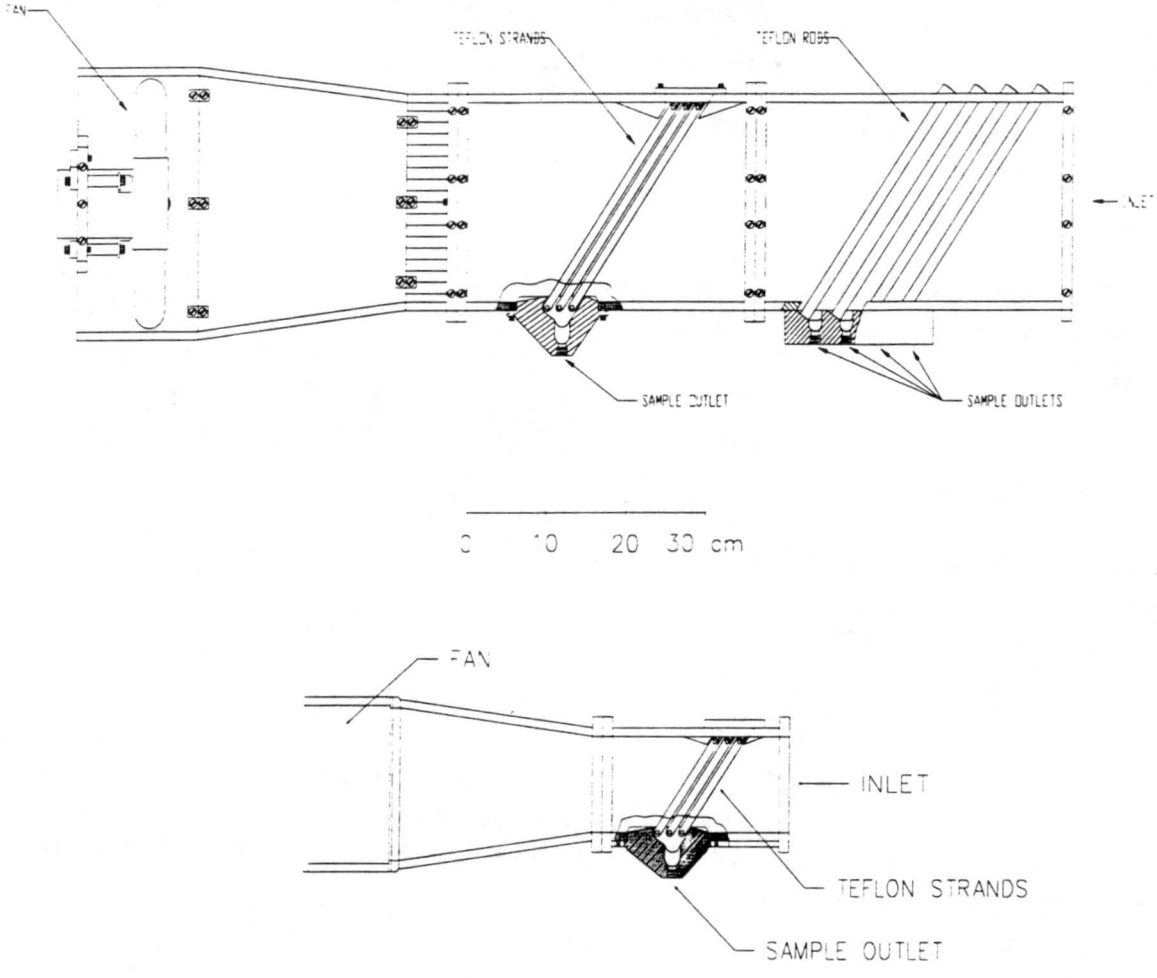

Figure 1-1. The CASCC2 (bottom) and the sf-CASCC (top)

the Kern Wildlife Refuge and at the Candelabra Tower. Air is drawn through the sf-CASCC at 19 m^3/min. The inlet of the sf-CASCC contains four rows of 12.7 mm diameter Teflon rods. The theoretical 50% size cut for this stage is 23 μm. The second stage of the collector contains six rows of 508 μm diameter Teflon strand and provides a 50% size cut of 4 μm. Both collector stages are contained in a Plexiglas housing. Sample from each collection stage drains through a collection trough into a polyethylene sample bottle via a Teflon sample tube. Samples are retrieved manually at the end of each sampling period.

Aliquots of sf-CASCC samples were prepared for analysis of pH, major ions, S(IV), organic acids, trace metals, formaldehyde, HMS, hydroperoxides and TOC as sample volume and time permitted. Some samples collected at KWR and the Candelabra tower were also analyzed for DOC.

1.1.3 The IESL impactor

A three-stage fog impactor was also deployed at the KWR core site and at the Candelabra Tower. The Institute for Environmental Studies Large (IESL) impactor, pictured in Figure 1-2, was used to collect three independent size fractions of fogwater. Details of the collector design are provided by Collett et al. (1995). The IESL impactor is a three-stage, cascade jet impactor. Impaction plates are constructed from Teflon, while the impactor housing and jet plates are made of Plexiglas. Each jet plate contains several cylindrical jets which accelerate air toward an impaction plate. Drops with sufficient inertia impact and are collected by the stage. Smaller drops pass through and are available for collection in a subsequent stage downstream. The IESL impactor features a total of seven impaction stages (size cuts of 30, 20, 15, 12, 10, 4, and 3 μm), three of which can be used simultaneously. Air is drawn through the IESL impactor by a Gast model R4110-2 regenerative blower, with the flow set at 1500 lpm based on the readout from a Sierra model 760 in-line mass flow meter. As the stage size cuts decrease from 30 to 3 μm, velocities increase from 137 to 1370 cm/s and the pressure drop increases from 0.01 to 1.1 mbar. The number of jets in each stage range from 21 to 213 while jet diameters range from 3.32 to 0.33 cm.

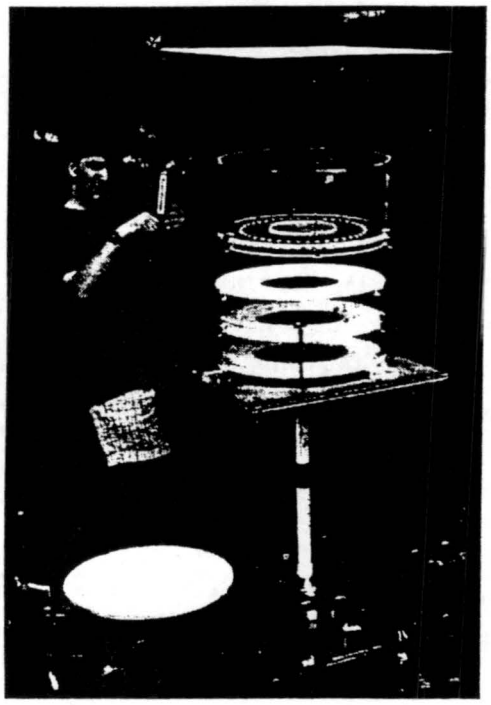

Figure 1-2. The three-stage IESL fog impactor.

The IESL impactor is 0.6 m in diameter and stands as tall as 1 m, depending on the size cuts chosen. Due to its size and weight, the IESL impactor is mounted on a mobile cart. In addition to the impactor, the cart houses the flow system and an overhead crane which is used to lift impactor stages for sample retrieval. Entry of precipitation into the impactor is minimized by a precipitation shield which mounts above the impactor inlet. An impaction stage is included in the inlet to remove any precipitation-sized particles (drops larger than 100 μm) that circumvent the precipitation shield. The height which the cart provides to the impactor helps minimize contamination from dust and debris disturbed at the ground during operation. Sample is retrieved manually at the end of each sampling period. Samples are retrieved by pipette and transferred to polyethylene sample vials.

Due to limited ground-based fog at the Candelabra Tower, samples were collected with this sampler only at KWR. Aliquots of samples collected by the IESL impactor were prepared for analysis of pH, major ions, S(IV), organic acids, trace metals, formaldehyde, HMS, hydroperoxides and TOC as sample volume and time permitted.

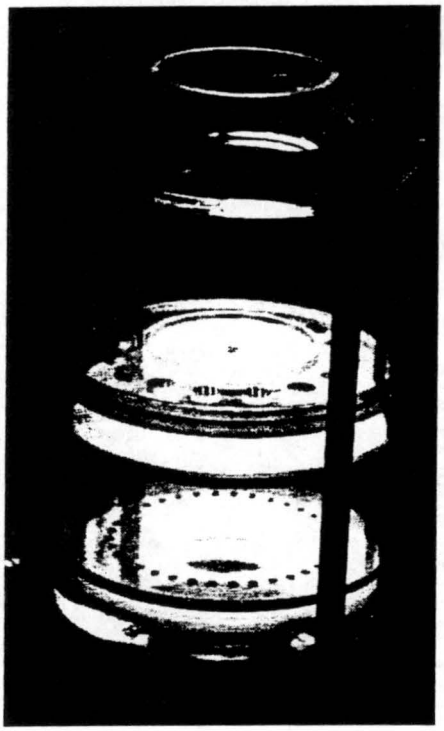

Figure 1-3. The 2-stage ETH fog impactor.

1.1.4 The ETH impactor

Two-stage jet impactors were used at Bakersfield and Fresno to collect separate samples of large and small fog drops. The ETH impactor (Collett et al., 1993, 1995), shown in Figure 1-3, contains two impaction stages in series. Air is drawn through the impactor by a regenerative blower. The flow rate is set by adjustment of a gate valve downstream of the impactor. The flow is checked by measuring the time to inflate a bag of known volume or by readout from an in-line volumetric flow meter. The ETH impactor is typically operated at flow rates between 300 and 400 lpm. The size cut of each stage is a weak function of flow rate in this range. Drops larger than 10 μm (depending on flow rate) are collected on the first stage, while drops with diameters between 3 and 10 μm (depending on flow rate) are collected on the second stage. Each stage consists of a Plexiglas jet plate and a Teflon impaction plate. Shallow troughs in the impaction plates help confine the collected sample to facilitate sample retrieval. Samples are manually retrieved at the end of each sampling period by disassembling the impactor and transferring the sample collected on each stage to a polyethylene sample vial using a pipette. Samples from the ETH impactors were analyzed for pH and major ions as sample volume permitted.

1.2 Other Measurements

In addition to collecting fog samples, CSU ran a Particle Measurement Systems CSASP-100-HV cloud drop sizing probe during some events at KWR and the Candelabra Tower. We also made some collections of trace gases and aerosols during the Candelabra Tower study. Brief descriptions of these measurements are provided below.

1.2.1 Fog drop size distribution measurements

A Particle Measurement Systems Classical Scattering Aerosol Spectrometer Probe (CSASP-100-HV) was used to measure the droplet size distribution during several fog events at KWR during the IMS-95 study. The CSASP uses a helium-neon laser to illuminate the sampling zone where the air flow is flowing perpendicular to the laser beam. If no particles are within the sample air flow then the laser terminates on a dump spot and no particles are counted. Particles

which pass through the sampling zone scatter light in proportion to their size around the dump spot of the laser and into the collecting optics where it is condensed onto a photo-detector.

The CSASP is capable of measuring the size distribution of fog droplets between 0.5 and 47 microns with four ranges. Each range contains 15 evenly spaced channels between each range maximum and minimum. Range 0 measures the distribution between 3 and 47 microns, Range 1 measures the distribution between 2 and 32 microns, Range 2 measures the distribution between 1 and 16 microns, and Range 3 measures the distribution between 0.5 and 8 microns. Range 1 provided the best coverage of drop size distributions measured during IMS95.

Field operations of the CSASP included field calibration checks with glass microspheres (Duke Scientific Corp., 15.7 ± 1.1 μm) before collecting data. The CSASP was operated to count particles in each range for 10 seconds, cycling through each range continuously until the CSASP was shut off. Post-processing of the data included selecting out only range 1 and then converting the particle counts/10 seconds to particle counts/cc of air sampled. The manufacturer's specified flow rate of 12.5 cc/sec was used to make the conversion. In some cases the number of droplets counted in a particular channel exceeded the maximum permitted.

1.2.2 Berner Low Pressure Impactor

Aerosol measurements were made at the Candelabra Tower using a Berner low pressure impactor (Hauke Model LPI/30/0.06). This aerosol cascade impactor features eight stages with size cuts ranging from 0.06 to 8 μm diameter and a blank stage. An inlet stage is designed to remove particles larger than 16 μm diameter. Flow through the impactor is controlled by a critical orifice at 28.2 lpm.

Tedlar substrates were used to collect impacting particles on each stage. The Tedlar substrates were coated with silicon spray to minimize particle bounce. Aqueous extracts of the substrates were analyzed by ion chromatography for major ions.

1.2.3 Annular Denuder System

Annular denuders (Oberholzer et al., 1992) were used to sample gaseous ammonia, nitric acid, and sulfur dioxide during the fog study at the Candelabra Tower. Flow rates through the denuders were controlled by critical orifices and measured using a flow meter. Three different coatings were used for the denuders. 0.2. M phosphoric acid was used to collect ammonia. 0.5 M potassium hydroxide was used to collect sulfur dioxide. 0.5 M sodium fluoride was used to collect nitric acid. Although the potassium hydroxide coating also collects nitric acid, the potential oxidation of nitrogen dioxide to nitric acid on this strongly basic coating makes use of the sodium fluoride coating preferable for nitric acid measurement in high NOx environments like the San Joaquin Valley.

The annular denuders were extracted with 3 ml of DI water after sampling. These aqueous extracts were analyzed by ion chromatography for ammonium, nitrate, and sulfate. A small

quantity of hydrogen peroxide was added to the sodium hydroxide denuder extract prior to analysis to ensure all sulfur was oxidized to sulfate.

The collection efficiency of the denuders depends on the gas sampled, ranging from approximately 82% for nitric acid to 96% for ammonia. As explained below, the Gormley-Kennedy solution to mass transfer in annular flow was applied to calculate efficiencies for each sampled gas and measured flow rate. Separate collection efficiency experiments made with the denuders have determined collection efficiencies close to the theoretical values. Calame et al. (1997) report experimental ammonia collection efficiencies of 99.0 and 97.6%, compared to a theoretically predicted value of 98.4% for their sampling conditions. Oberholzer (1992) reports an experimental ammonia collection efficiency of 93%, compared to a theoretically predicted value of 97% for his sampling conditions. Walke (1994) measured sulfur dioxide collection efficiencies between 91.4 and 94.7 % and nitric acid collection efficiencies between 91.4 and 96.4%, compared to theoretically predicted values of 89.9 and 89.1 %, respectively.

1.3 Chemical species analyzed in IMS95 fog samples

Several chemical species were analyzed in fog samples collected during IMS95. Some of these were analyzed in the field, while others were analyzed in the laboratory at Colorado State University. Several of the more unstable species were stabilized for later analysis immediately

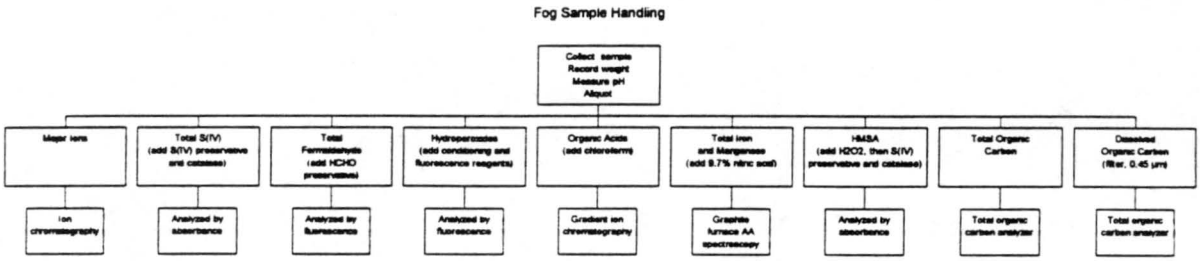

Figure 1-4. Fog sample handling procedures. Sample pH was measured on-site, while other species were aliquotted and preserved (as indicated) for later analysis in the laboratory.

after samples were collected in the field. All stored samples were refrigerated prior to analysis. Figure 1-4 illustrates how collected samples were split, preserved, and analyzed for the various chemical species. Descriptions of these procedures follow below.

1.3.1 pH

Fog sample pH was measured on-site using an Orion electronic pH meter (Model 250 or 290) equipped with a combination microelectrode (Microelectrodes, Inc. Model MI-710). Prior to sample measurement, the electrode was calibrated with pH 4 and 7 buffers.

1.3.2 Inorganic Ions and Low Molecular Weight Organic Acids

A Dionex DX-500 dual channel ion chromatograph was used for analysis of inorganic ions and low molecular weight organic acids. One channel is dedicated to analysis of cations (sodium, ammonium, potassium, magnesium, and calcium). The other channel switches between analysis for anions (chloride, nitrate, and sulfate) and selected organic acids (acetic, formic, oxalic, pyruvic, and propionic). Each channel of the DX-500 ion chromatograph (IC) is attached to an AS3500 autosampler which allows random access to the sampling vials. This permits analysis of the same set of calibration standards at the beginning and end of each run of samples. In addition, the autosampler can be programmed to automatically run duplicate samples. To make sure that the IC is running properly while unattended during a long run, periodic duplicates are run as are check standards. At the beginning of each run of samples, regardless of whether they are run for anions, cations or organic acids, a DI water blank is loaded. Then ten standards are run, followed by two commercial calibration check standards, and another blank sample. Ten samples are then run, the last of which is injected twice. After this duplicate, one of the standards is run. Samples continue to be run in groups of ten, ending with a duplicate injection followed by a standard injection, until the sample set to be analyzed is complete. At the end of the samples, standards are run again before turning off the instrument. This procedure provides a check on whether the response of the instrument changes during the course of a run as well as information on the reproducibility of the injections. Separate calibration curves are prepared for each analytical run. When appropriate, two calibration curves are determined from the ten calibration standards run, one representing a lower concentration range and the other a higher concentration range.

1.3.2.1 Operating Conditions for Cation Analysis

Cations are analyzed with a Dionex CS-12 Column preceded by a CG-12 guard column, with a Dionex Cation Self Regenerating Supressor (CSRS-1) operating in Auto Suppression Recycle Mode. Detection is with a Dionex conductivity detector. Injections are made by the AS3500 autosampler with a 50 µl sample loop.

The eluent used is 20 mM Methanesulfonic Acid, prepared from concentrated methanesulfonic acid (Kodak; Product Number CAT 116 5570) and water prepared from a Nanopure reverse osmosis - deionization system (hereafter referred to as DI water). The pump is primed for one minute at 9 ml/minute with the waste bypass valve open. The valve is then closed, and the system is started with a flow rate of 1 ml/minute and left to equilibrate for one hour before starting analyses. The time, pressure and total conductivity are recorded in a logbook at this point and hourly while the instrument is running. Expected background conductivity for the cation analysis is between 1 and 2 µS.

Previously prepared sample vials are then loaded into racks of forty for the AS3500 autosampler. If samples have not been previously prepared, 500 µl of each sample is pipetted into a sample vial and the top is securely screwed on. Sample vials are polypropylene 500 µL with screw-type polyethylene caps with Teflon septa.

Ten calibration standards are prepared from a stock solution prepared by dissolving appropriate amounts of reagent grade salts in DI water. Two calibration curves are used to determine the

concentrations of the samples. The lower is from 2 to 100 μN (microequivalents/liter) for each cation. If the sample concentration is above this range, a higher curve, extending up to 1600 μN is used.

1.3.2.2 Operating Conditions for Anion Analysis

Anions are analyzed with a Dionex AS4A-SC Column and AG4A-SC guard column. Supression of background conductivity is achieved using a Dionex Anion Self Regenerating Suppressor (ASRS-1), and detection is by a Dionex conductivity detector. An AS3500 autosampler is used to introduce the samples into the column. Sample loop volume is 25 μl. The anion eluent is 1.8 mM Na_2CO_3/1.7 mM $NaHCO_3$. The eluent is prepared from a stock solution of 180 mM Na_2CO_3/170 mM $NaHCO_3$ prepared from reagent grade salts and DI water.

The pump is primed for one minute at 9 ml/minute with the waste bypass valve open. The valve is then closed, and the system is then started with a flow rate of 2 ml/minute and left to equilibrate for one hour before starting analyses. The time, pressure and total conductivity are recorded in a logbook at this point and hourly while the instrument is running. The expected background conductivity for the anion analysis is 2.8 μS.

Previously prepared sample vials are then loaded into racks of forty for the AS3500 autosampler. If samples have not been previously prepared, 500 μl of each sample is pipetted into a 500 μl polyethylene sample vial and the top is securely screwed on. Sample vials are polypropylene 500 μL with screw-type polyethylene caps with Teflon septa.

Ten calibration standards are prepared from a stock solution prepared by dissolving appropriate amounts of reagent grade salts in DI water. Two calibration curves are used to determine the concentrations of the samples. The lower is from 2 to 100 μN for each anion, except chloride which is from 1 to 50 μN. If the sample concentration is above this range, a higher curve extending up to 1600 μN (800 μN for chloride) is used.

1.3.2.3 Operating Conditions for Organic Acid Analysis

Organic acids are analyzed on the same system as the anions, but with a different column and eluent combination. The organic acid column is a Dionex AS-11 column with an AG-11 guard column. Species are eluted from the column using a NaOH gradient.

500 μl of previously stabilized organic acid sample is pipetted into a glass autosampler vial and the top is securely screwed on. Sample vials are then loaded into racks of forty in the AS3500 autosampler.

Calibration standards are prepared by diluting a standard stock solution made by dissolving reagent grade salts in DI water. Two calibration curves are used to determine the concentrations of the samples. The lower is from 2 to 100 μN for each organic acid. If the sample concentration is above this range, a higher curve up to 1600 μN is used.

1.3.3 Total S(IV) and hydroxymethanesulfonate (HMS)

Since free S(IV) in cloudwater can be readily oxidized by H_2O_2, O_3 and O_2 in the presence of transition metals, samples are preserved as soon as possible after collection. Preservation is accomplished by adding a preserving solution containing formaldehyde, CDTA (trans-1,2-Cylohexylenedinitrilo-tetraacetic acid) and sodium hydroxide. The ratio of preservation solution to cloudwater is 1:15.

The principle of preservation is that S(IV) reacts rapidly with formaldehyde to form HMS (hydroxymethanesulfonate). HMS is stable in the preserved cloudwater samples since it is not easily oxidized. HMS formed in the preserved cloudwater can then be easily decomposed to free S(IV) before analysis. CDTA in the preservative solution prevents interference of trace metals in the S(IV) analysis. A catalase solution is also added to the samples to destroy any H_2O_2 in cloudwater, since aqueous oxidation of S(IV) by H_2O_2 is a very fast reaction and could interfere with the measurements. Preserved samples are kept at 4 ^{0}C until analysis for total S(IV) content.

It is also possible to analyze HMS contained in fog samples in a similar way. Before adding the preservative solution, however, hydrogen peroxide is added to rapidly oxidize any free S(IV) present in the sample. The sample is then preserved as described in the preceding paragraphs until it is analyzed for HMS content.

To analyze preserved S(IV) samples, HMS is first decomposed to HCHO and free S(IV) by adding strong base, and then free S(IV) and HCHO react with acidic pararosaniline to form a purple compound, which is measured spectrophotometrically using a Hitachi U-2000 UV/VIS spectrophotometer. A calibration curve relating absorbance to S(IV) concentration was prepared daily by analyzing calibration solutions prepared by diluting a stock solution of Na_2SO_3. Free S(IV) concentrations can be obtained by subtracting the HMS concentration from the total S(IV) concentration.

Due to limited available sample volumes, duplicate analyses could not be completed for S(IV) or HMS. Precision calculations were made using duplicate analyses of calibration standards.

1.3.4 Formaldehyde

Formaldehyde in fog samples can be preserved by adding bisulfite to form HMS. HMS can later be decomposed to formaldehyde to be analyzed. A formaldehyde preservation solution containing bisulfite is added on site. The volume ratio of preservative to sample is 1:10. This technique measures total formaldehyde ("free" formaldehyde plus HMS). The free formaldehyde concentration can be obtained by subtracting the HMS concentration (measured according to the procedure described in the preceding section) from the measured total formaldehyde concentration.

In the presence of small amounts of formaldehyde, 2,4-pentanedione and ammonia react with formaldehyde quantitatively to form a yellow product, diacetyldihydrolutidine (DDL). DDL can be measured by fluorescence. Since the amount of DDL produced equals the amount of

formaldehyde present in solution (provided 2,4-pentanedione and ammonia are in excess) the formaldehyde concentration can be determined from the amount of DDL. Analysis was completed using a Shimadzu RF-1501 fluorescence spectrophotometer and calibration standards prepared by diluting a stock solution of NaHMS. A new calibration was determined for each set of analyses. Approximately 20% of the samples were run in duplicate.

1.3.5 Hydroperoxides

The measurement of hydroperoxides using a fluorescence spectrophotometer measures both hydrogen peroxide and soluble organic hydroperoxides. For simplicity, hydrogen peroxide will be used here to denote hydroperoxides.

Hydrogen peroxide can be reduced by a hydrogen donor molecule, such as *p*-hydroxyphenylacetic acid (POPHA), in the presence of peroxidase. A dimeric product is formed which can be measured quantitatively by fluorescence. One molecular dimer is produced from one molecule of hydrogen peroxide. The hydrogen peroxide concentration in cloudwater can therefore be determined by measuring the dimer concentration. Hydrogen peroxide is very active chemically, however, requiring immediate analysis or preservation on site as soon as possible after cloudwater is taken from the collectors.

Hydrogen peroxide in fog samples was preserved on site by addition of *p*-hydroxyphenylacetic acid (POPHA) to form a stable dimer. The sample preservation is accomplished by adding 200 µl conditioning reagent and 200 µl fluorescent reagent to 1.0 ml cloudwater (or add conditioning and fluorescent reagents to cloud sample in a 1:5 ratio for smaller sample volumes). The conditioning reagent contains potassium hydrogen phthalate (KHP), which acts as a buffer (pH = 5.5), and EDTA, which can also act as a buffer (pH = 5.5) and prevents interference by metal ions.

Calibration standards were made from a reagent grade commercial 30% H_2O_2 solution (standardized by titration with potassium iodide) and DI water. A Shimadzu RF-1501 spectrofluorophotometer was used to measure the fluorescent intensity. Approximately 10% of the samples were analyzed in duplicate.

1.3.6 Total Fe and Mn

Total iron and manganese in fog samples were analyzed using a Zeeman-corrected Graphite Furnace Atomic Absorption Spectrophotometer (GFAAS). These metals are of importance due to their influence on aqueous phase S(IV) oxidation.

Trace metal aliquots of fog samples were stabilized in the field by acidification with 9.73% nitric acid (1 part acid added to ten parts fogwater). Standard methods for Zeeman corrected GFAAS of aqueous iron and manganese were used for the analysis. The method contains an auto-dilution program that can perform a calibration curve by injecting incremented amounts of a stock standard. Stock standards of 50 µg L^{-1} Fe and 80 µg L^{-1} Mn were prepared by dilution of

commercial standard Fe and Mn solutions. The following calibration standard concentrations were used:

Std.	Fe ($\mu g\ l^{-1}$)	Mn ($\mu g\ l^{-1}$)
1	5	8
2	10	16
3	20	24
4	30	48
5	40	64
6	50	80

Another low Mn concentration method was used for samples below the initial method's calibration range. The new standards for this method were 2, 4, 8, 10, and 20 $\mu g\ L^{-1}$.

All the samples were analyzed in duplicate; quality control parameters contained in the method regulate the amount the duplicates are allowed to differ before the run is stopped. Every 10 samples a zero and a standard were run again. The run proceeds past this point only if the new values are close to the previous responses. This prevents error due to the instrument drifting during a long series of samples.

1.3.7 Total Organic Carbon (TOC) and Dissolved Organic Carbon (DOC)

At the collection sites, the water available for organic carbon analysis was divided into two samples of approximately 2-3 ml each. The first sample was pipetted directly into a glass vial. This sample provided water for total carbon and total inorganic carbon analysis (with the difference between the two representing total organic carbon). The second sample was filtered through a 10 ml syringe with a 0.45 µm nylon twist-on filter (Gelman) into the glass vial. This sample provided water for analysis of dissolved carbon and dissolved inorganic carbon (with the difference representing dissolved organic carbon).

The collected organic carbon samples were analyzed using a Shimadzu TOC 5000a total organic carbon analyzer. The technique used to determine the total carbon (TC) content of a sample involves vaporization and decomposition of the sample in a 680° C furnace and measurement of the evolved CO_2. Inorganic carbon (IC) is determined by measurement of the CO_2 produced by reaction of the sample with 25% phosphoric acid. The instrument does not respond to elemental carbon, since it is not oxidized at the furnace temperature used.

The 2-3 ml sample volumes did not provide enough water for direct measurement of both TC and IC in the original sample vials. Thus it was necessary to dilute the samples. A dilution of 1:3 (sample:DI water) was chosen. The original sample provided two 400 µl volumes each of which was diluted with 1200 µl of DI water, thus providing samples for both TC and IC analysis.

Standards were prepared using 1000 ppm stock solutions of potassium hydrogen phthalate for TC and of sodium bicarbonate and sodium carbonate for IC. These stock solutions were

prepared using reagent grade salts and DI water. Two sets of four point calibration curves were run for both TC and IC spanning the ranges 0-20 ppm and 0-100 ppm. After calibration a deionized water sample was run to remove any residual material from the standards remaining in the sample lines.

At the beginning of a new batch of analyses, a check of the calibration curves was made using 5 and 10 ppm standards. If the standard check was within 10%, a DI water sample was run and then an analysis run was initiated. If the calibration check failed, a new calibration curve was generated before starting an analysis run.

All samples were analyzed in duplicate or triplicate. After each set of ten samples (TC and IC) a standard check was made using 10 ppm standards. If the standard check was within 10% the analysis run was continued, otherwise a new calibration curve was generated.

During analysis it was discovered that one batch of glass vials was contaminated. These vials were used for storing TOC and DOC aliquots made early in the study at the KWR site. Due to the contamination problems no TOC or DOC values are reported for these samples.

1.4 Quality Control, Quality Assurance and Data Validation

A variety of procedures were undertaken to minimize problems with information collected as part of this study and to quantify uncertainties in the data reported. Some of these procedures have been outlined in the preceding discussion of measurement methods and analytical techniques. Here we provided a brief summary of additional measures taken and report our findings of analytical precision, detection limits, and laboratory intercomparability.

1.4.1 Instrument Blanks

Following our standard operating procedures, the fog samplers used in the study were cleaned with DI water prior to each event. When possible, and in most cases, collector blanks were taken to test the adequacy of the cleaning procedures. Blanks were collected by spraying water onto the collection surfaces and allowing it to flow through the same path followed by actual samples. One limitation to this approach is that soluble gases are efficiently captured by the sprayed water and contribute to the chemical loading in the collected blank. Some aerosol particles may also contribute in this way, although their collection should be less efficient. A second point worth noting is that the collector is "cleaned" by collected fogwater during the course of an event. Consequently, a high blank may contribute much more to the first sample collected than to subsequent samples. Further, material rinsed off collection surfaces during blank collection is no longer present to contribute to the chemical loading of collected samples.

Due to these limitations, our standard procedures do not call for blank correcting sample concentrations. Instead we have chosen to flag samples for which corresponding blanks indicate potential contamination. This has been done on a species by species basis. Due to the absorption

of gaseous compounds by the sprayed DI water, we have excluded species coming predominantly from the gas phase from this flagging procedure.

Blanks were also collected from the Berner impactor and denuder runs. Berner impactor blanks were collected from the blank stage included in the instrument while denuder blanks were taken by extracting denuders that were prepared for sampling but not used. Analyses of the collected blanks were used in detection limit calculations for these measurements and to blank correct reported concentrations as described below.

1.4.2 Determination of Uncertainties and Detection Limits

As part of the analytical procedure of the study, values were determined for the uncertainty and detection limit of each species measured. Procedures and results are outlined below for the chemical species measured in fog and for the aerosol and gas measurements made at the Candelabra Tower.

1.4.2.1 Uncertainties and Detection Limits for the Fog Chemistry Measurements

As mentioned previously, no blank corrections were made to the fog chemistry measurements. Therefore the uncertainty and detection limits for the fog composition measurements are given by the uncertainties and detection limits for the analytical methods employed. Methods for calculating these quantities are outlined below and results of the calculations are presented in Table 1-1.

Analytical uncertainties are calculated and reported as relative standard deviations (RSD), in percent. The RSD (σ^*_s) for each species was calculated from large (>10 and usually >20) numbers of replicate sample analyses x_1 and x_2, except for S(IV) and HMS where replicate analyses of calibration standards were used due to insufficient available sample volumes. Equation 1-1 shows the formula used for calculating the RSD, where x_{bar} is the average value of all the replicates.

$$\sigma_s^* = \frac{\left[\left(\frac{1}{M}\right)\cdot\sum_{j=1}^{M}\left(\sigma_j'\right)^2\right]^{1/2}}{x_{bar}}\cdot 100 \qquad (1\text{-}1)$$

σ'_j is calculated as shown in Equation 1-2.

$$\sigma_j' = \frac{|x_1 - x_2|}{\sqrt{2}} \qquad (1\text{-}2)$$

The absolute uncertainties reported are the products of the calculated relative standard deviations and the reported concentrations.

Table 1-1. Calculated analytical uncertainties and detection limits for all chemical species.		
Species	**Analytical Uncertainty relative standard deviation % (# replicates, replicate conc. range, avg. replicate conc.)**	**Instrument Detection Limit (# replicates)**
Chloride	5.1 (21, 1.9-33.2 μN, 10.2 μN)	1.36 μN (15)
Nitrate	0.34 (21, 49.4-875.9 μN, 265.7 μN)	0.78 μN (15)
Sulfate	1.1 (21, 17.0-2408.5 μN, 168.6 μN)	1.27 μN (15)
Sodium	1.2 (21, 0 - 49.0 μN, 7.6 μN)	0.91 μN (19)
Ammonium	0.62 (21, 7.6 - 3129.7 μN, 603.2 μN)	1.15 μN (19)
Potassium	3.1 (21, 1.4 - 49.9 μN, 11.8 μN)	0.97 μN (19)
Magnesium	5.3 (21, 1.7 - 50.1 μN, 7.8 μN)	0.84 μN (19)
Calcium	4.2 (21, 2.5 - 143.6 μN, 30.4 μN)	0.90 μN (19)
Acetate	2.6 (19, 0 - 325.9 μN, 63.8 μN)	1.05 μN (7)
Propionate	7.9 (19, 0 - 54.3 μN, 17.9 μN)	2.02 μN (7)
Formate	0.74 (19, 0 - 124.3 μN, 44.7 μN)	1.97 μN (7)
Pyruvate	0.22 (19, 0 - 50.7 μN, 16.9 μN)	0.79 μN (7)
Oxalate	0.66 (19, 0 - 108.8 μN, 42.6 μN)	5.45 μN (7)
S(IV)	14.4 (36, 0.9-55.2 μM, 14.4 μM)	0.89 μM (18)
HMS	14.4 (36, 0.9-55.2 μM, 14.4 μM)	0.89 μM (18)
Formaldehyde	5.3 (45, 0.9 - 196.3 μM, 28.8 μM)	0.15 μM (13)
Hydrogen Peroxide	5.6 (18, 0.1 - 16.3 μM, 5.4 μM)	0.45 μM (8)
TOC	10.8 (81, 0 - 5.4 ppm, 2.0 ppm)	1.27 ppm (31)
TDOC	10.8 (81, 0 - 5.4 ppm, 2.0 ppm)	1.27 ppm (31)
Iron	5.0 (20, 0 - 1886.0 μg/l, 409.0 μg/l)	1.82 μg/L (17)
Manganese	8.6 (20, 7.3 - 57.6 μg/l, 22.1 μg/l)	0.22 μg/L (20)

Equation 1-3 was used for estimating instrument detection limits. As many blanks as possible were used for each calculation. In some cases no analyte was detected in the blanks and the detection limits had to be calculated by examining variability in analysis of a low concentration standard.

$$\Delta x_{\min} \geq t \cdot s_b \cdot \sqrt{\frac{N_b+N_s}{N_b \times N_s}} \qquad (1\text{-}3)$$

where t is the student t value at the 95% confidence level for the appropriate number of degrees of freedom, s_b is the standard deviation of the blanks, N_b is the number of blanks and N_s is the number of sample measurements. Detection limits were all calculated assuming a single sample analysis; lower detection limits are possible if replicate analyses are used.

1.4.2.2 Conversions, Uncertainties and Detection Limits for Aerosol and Gas Measurements

Chemical concentrations measured in denuder and impactor substrate extracts were converted to airborne concentrations prior to being reported. This section outlines the procedures used for

making these conversions, as well as the uncertainties in the reported values and the method detection limits.

Atmospheric Concentrations

The atmospheric concentrations of each species on each stage of the Berner low pressure impactor (C_{atmos}) were calculated from the extract concentrations ($C_{extract}$) and average blank extract concentration (C_{blank}) as follows:

$$C_{atmos} = \frac{(C_{extract} - C_{blank}) \cdot V_{extract}}{F \cdot t} \quad (1\text{-}4)$$

where the extract volume ($V_{extract}$) was 0.010 l, flow rate (F) was 28.2 lpm, and sampling times (t) ranged from 300 to 800 minutes.

The atmospheric concentration of a species sampled on a denuder (C_{atmos}) was calculated as follows:

$$C_{atmos} = \frac{(C_{extract} - C_{blank}) \cdot V_{extract}}{F \cdot t \cdot \eta} \quad (1\text{-}5)$$

where extract volume ($V_{extract}$) was 0.003 l, flow rates (F) were approximately 17 lpm (varied for each denuder type), and sampling times (t) ranged approximately from 300 to 700 minutes. The collection efficiency (η) of each gas sampled by the denuders was calculated using the Gormley-Kennedy equation as modified by Possanzini et al. (1983) for annular denuders. The equations are as follows:

$$\eta = 1 - \frac{C}{C_0} \quad (1\text{-}6)$$

where C_0 and C represent the gas concentrations entering and exiting the denuder, respectively, and their ratio is given by

$$\frac{C}{C_o} = 0.819\exp(-14.6272\Delta_a) + 0.0976\exp(-89.22\Delta_a) + 0.01896\exp(-212\Delta_a) \quad (1\text{-}7)$$

where

$$\Delta_a = \frac{\pi DL}{4F} \frac{d_1 + d_2}{d_2 - d_1} \quad (1\text{-}8)$$

and

D = diffusion coefficient ($cm^2 s^{-1}$)
L = length of denuder tube (cm)
F = flow rate ($cm^3\ s^{-1}$)
d_1 = outer diameter of inner tube
d_2 = inner diameter of outer tube

As described above, separate measurements have shown that the theoretical efficiency is an accurate representation of the denuder's actual performance.

Uncertainties

Relative uncertainties in blank corrected concentrations were calculated as

$$\sigma^{\star}_{s-b} = \frac{\sqrt{(\sigma^{'}_{b})^2+(\sigma^{\star}_{s}\times C_s)^2}}{C_{s-b}} \qquad (1\text{-}9)$$

where

$\sigma^{'}_{b}$ is the absolute uncertainty in the blanks
$\sigma^{\star}_{s}$ is the relative analytical uncertainty for a given species
C_s is the sample concentration
$C_{s\text{-}b}$ is the sample concentration minus the average blank concentration.

Relative uncertainties in calculated atmospheric concentrations were then calculated by incorporating estimates of uncertainty in the flow rate ($\sigma_F^{\star}$, for denuder and Berner impactor samples, estimated as 5%), the collection efficiency ($\sigma_\eta^{\star}$, for denuder samples only, estimated as 5%), and the extract volume ($\sigma_V^{\star}$, for denuder samples only, estimated as 2%) as

$$\sigma^{\star}_{at} = \sqrt{(\sigma^{\star}_{s-b})^2 + (\sigma^{\star}_{F})^2 + (\sigma^{\star}_{\eta})^2 + (\sigma^{\star}_{V})^2} \qquad (1\text{-}10)$$

Absolute uncertainties (σ_{at}') were then calculated as the product of the relative uncertainties and the atmospheric concentration:

$$\sigma^{'}_{at} = \sigma^{\star}_{at} \times C_{atmos} \qquad (1\text{-}11)$$

Detection Limits

Detection limits for extract concentrations measured on the stages of the Berner low pressure impactor were calculated as

$$\Delta x_{\min} \geq t \cdot s_b \cdot \sqrt{\frac{N_b+N_s}{N_b \times N_s}} \qquad (1\text{-}12)$$

where t is the student t value at the 95% confidence level for the appropriate number of degrees of freedom, s_b is the standard deviation of the blanks, N_b is the number of blanks and N_s is the number of sample measurements. Detection limits, calculated for a single measurement of the extract concentration, ranged from close to zero for nitrate to 10.8 μN for calcium. Atmospheric concentrations of species with extract concentrations below the detection limit were not reported.

Insufficient numbers of denuder blanks were available to calculate meaningful detection limits for this study. Since measured gas concentrations were much higher than typical detection limits for this method, and those blanks measured were very clean, we feel confident that the reported gas concentrations are well within the quantifiable range.

1.4.3 Checks on Laboratory Performance

Ion concentrations measured by CSU were checked by two methods. Internally, standard solutions containing known concentrations of the measured ions were purchased to use as spot checks on analytical performance. CSU also participated in a sample intercomparison with the CARB analytical laboratory in Sacramento. Results of these tests, provided below, indicate that CSU reported accurate values for ion concentrations measured in this study.

1.4.3.1 Internal Calibration Checks

CSU ion chromatography calibration standards were prepared by diluting stock solutions prepared from reagent grade salts and DI water. Analyses of the calibration standards were made daily to generate current calibration curves as explained above. NIST traceable cation and anion standards were purchased from Dionex corporation to provide a check on the accuracy of ion concentrations determined by ion chromatography analysis in the CSU lab. The standards purchased were combined five anion and combined six cation standards. Dilutions (1:100) of the Dionex standards were prepared and used as check standards periodically throughout the analysis of samples collected as part of IMS95.

Figure 1-5 depicts the ratios of measured ion concentrations to nominal ion concentration values for the Dionex check standards. Measured values for all ion concentrations were within 10% of the nominal concentrations, and six of the eight ions were measured within 5% of the nominal values. The greatest disagreement was for chloride (nominal value 8.3 μN, measured concentration 9.0 μN), a species which is somewhat difficult to quantify at concentrations below

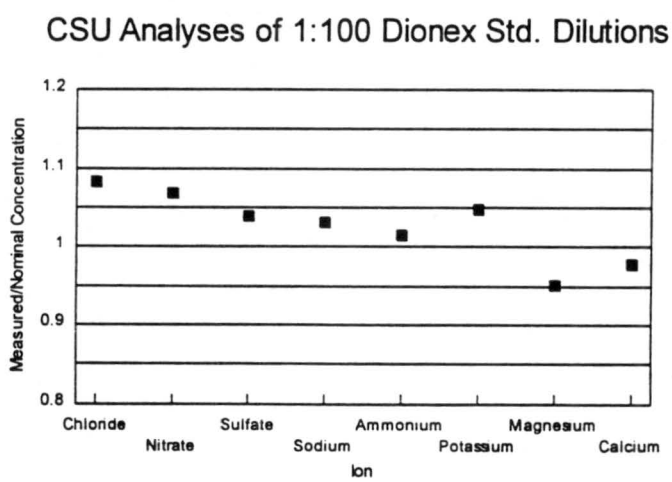

Figure 1-5. CSU analyses of calibration check standards made from NIST-traceable solutions purchased from Dionex Corporation.

Table 1-2. CSU Analyses of Dionex Check Standards

Ion	Nominal Concentration (μN)	Avg. Measured Concentration (μN)	Number of Measurements	RSD of Measurements (%)	Measured/Nominal
Chloride	8.32	9.01	5	11.5	1.08
Nitrate	16.13	17.21	5	3.6	1.07
Sulfate	31.23	32.46	5	3.2	1.04
Sodium	87.86	90.68	12	3.9	1.03
Ammonium	225.43	228.62	12	1.8	1.01
Potassium	51.15	53.59	12	4.2	1.05
Magnesium	168.72	160.40	12	2.2	0.95
Calcium	509.48	498.26	12	2.7	0.98

10 μN. Table 1-2 lists more complete information about the comparison, including the nominal and average measured ion concentrations of the check standards and the relative standard deviations (RSD) of the measurements.

1.4.3.2 Laboratory Intercomparison

As part of the study, CSU and the CARB inorganics analytical laboratory (Dr. Charles Cowell) in Sacramento participated in a laboratory intercomparison where samples were exchanged for ion analysis by both laboratories. CSU sent portions of six fog samples from IMS 95 to the CARB lab and the CARB lab prepared six anion and six cation synthetic samples which were sent to CSU for analysis.

Table 1-3 lists CSU's reported concentrations for the twelve synthetic samples prepared by CARB. Each sample was measured five times. The average concentration and standard deviation are shown for each sample and species. Also shown are the nominal concentration values reported by CARB (C. Cowell, CARB, personal communication). For most species and samples the concentrations reported by CSU show excellent agreement with the nominal concentration values. In many cases the reported concentrations are within a few percent of the nominal values. Two exceptions stand out. When nominal concentration values are very low (e.g., Anion samples B and E and Cation samples B and F where concentrations are 100 μg/l or less), the disagreement increases. There is also considerable disagreement between reported and nominal concentration values at all levels for calcium.

The increased disagreement between nominal concentrations and values reported by CSU at low concentration levels is not surprising for a number of reasons. First, concentrations below 100 μg/l are comparable to the analytical detection limit of the ion chromatograph for these species as operated for this study and are well below the concentration range for which the calibration curves were optimized (calibration ranges were selected to match likely fogwater concentrations of the analytes). Second, at such low concentrations the likelihood of observable effects of

Table 1-3. CSU Analyses of Synthetic Samples Provided by CARB

Sample		Nominal Anion Conc. (µg/l)	Chloride (µg/l)	Nitrate (µg/l)	Sulfate (µg/l)	Sample		Nominal Cation Conc. (µg/l)	Sodium (µg/l)	Ammonium (µg/l)	Potassium (µg/l)	Magnesium (µg/l)	Calcium (µg/l)
Anion A	average	1000	987.9	991.8	1024.9	Cation A	average	700	710.8	686.3	691.4	753.4	940.0
	std dev		28.9	22.3	36.4		std dev		2.6	4.9	9.6	9.6	32.7
	measured/nominal		0.99	0.99	1.02		measured/nominal		1.02	0.98	0.99	1.08	1.34
Anion B	average	100	111.8	71.1	112.7	Cation B	average	50	91.0	35.1	33.2	70.5	167.1
	std dev		8.9	9.6	15.5		std dev		3.3	4.3	2.2	1.9	2.8
	measured/nominal		1.12	0.71	1.13		measured/nominal		1.82	0.70	0.66	1.41	3.34
Anion C	average	1850	1784.9	1823.2	1855.4	Cation C	average	1000	985.1	961.6	961.8	1014.2	1252.0
	std dev		29.9	26.5	28.3		std dev		49.3	52.4	61.0	61.8	77.6
	measured/nominal		0.96	0.99	1.00		measured/nominal		0.99	0.96	0.96	1.01	1.25
Anion D	average	700	649.4	656.8	673.3	Cation D	average	400	398.8	367.3	373.0	435.7	577.1
	std dev		38.5	23.5	40.5		std dev		2.4	10.6	17.7	7.8	18.0
	measured/nominal		0.93	0.94	0.96		measured/nominal		1.00	0.92	0.93	1.09	1.44
Anion E	average	80	66.8	67.0	71.9	Cation E	average	1550	1501.7	1531.1	1483.5	1529.3	1732.0
	std dev		24.6	19.7	41.3		std dev		65.5	75.0	79.9	79.4	84.9
	measured/nominal		0.83	0.84	0.90		measured/nominal		0.97	0.99	0.96	0.99	1.12
Anion F	average	400	398.9	415.7	380.6	Cation F	average	100	94.7	87.7	86.9	127.8	235.0
	std dev		24.4	18.6	27.9		std dev		3.5	4.6	5.8	3.6	6.2
	measured/nominal		1.00	1.04	0.95		measured/nominal		0.95	0.88	0.87	1.28	2.35

contamination increases. Third, CARB shipped the samples unrefrigerated, increasing the likelihood that chemical and/or biological transformations might lead to changes in sample composition. CSU's standard operating procedures call for keeping all samples refrigerated until analysis. If one excludes samples in this low concentration range, one finds that reported anion values are all within 7% of the nominal concentrations, with an average disagreement just under 3%. Excluding samples with concentrations of 100 µg/l or below and excluding calcium, one finds a maximum disagreement of 9% and an average disagreement of 3.5% for the cation samples.

The disagreement between reported and nominal calcium values is not so readily explained. Values reported by CSU are consistently higher than the nominal concentration values reported by CARB. This is somewhat surprising, since CSU's internal checks described in the preceding section found calcium to be accurately measured. Further, as described below, CARB's analysis of the calcium levels in the fog samples substantially exceeded the values reported by CSU for all six samples. One possible explanation for these findings is that calcium was inadvertently introduced as a contaminant to the synthetic samples prepared by CARB and the fog samples measured by CARB. Calcium contamination could have occurred during handling in either lab, although the fact that CSU was able to accurately measure calcium in the Dionex check standards and reported lower calcium concentrations in the fog samples suggests that significant calcium contamination is probably not occurring there. One piece of information that might help clarify the situation would be the analytical results of the CARB lab for the synthetic samples they prepared, although it is not clear whether these samples were ever analyzed in their laboratory. In any case, we should keep in mind that calcium is generally a minor contributor to the fog composition and there is good evidence that the major species are accurately measured.

Table 1-4 illustrates the findings from the laboratory intercomparison of fog sample ion analysis. Both laboratories report similar values for nitrate, sulfate, and ammonium (with one exception). Reasonable agreement is also evident for sodium values. The agreement is poorer for chloride, potassium, magnesium and calcium concentrations. Values reported by CARB for chloride and

Table 1-4. Laboratory Intercomparison of Fog Composition. All concentrations are in μN.

Sample	Cl- CSU	CARB	Difference/Mean (%)
BCC1210#2	37.5	40.3	-7.3
FCC1209#2	16.1	18.0	-11.5
KCC0102#1	3.0	10.7	-112.0
KCL0101#1	3.2	13.2	-121.4
KCL0101#2	2.7	10.1	-115.6
KCL1209#3	7.1	9.9	-32.0

Sample	Na+ CSU	CARB	Difference/Mean (%)
BCC1210#2	9.3	8.2	12.1
FCC1209#2	3.9	4.0	-4.6
KCC0102#1	1.2	1.6	-27.5
KCL0101#1	2.5	2.5	0.5
KCL0101#2	2.3	2.0	14.4
KCL1209#3	9.6	8.0	18.2

Sample	NO3- CSU	CARB	Difference/Mean (%)
BCC1210#2	551.7	546.8	0.9
FCC1209#2	564.8	571.0	-1.1
KCC0102#1	128.6	114.5	11.6
KCL0101#1	76.4	75.8	0.8
KCL0101#2	97.3	100.0	-2.8
KCL1209#3	326.0	337.1	-3.4

Sample	NH4+ CSU	CARB	Difference/Mean (%)
BCC1210#2	1320.5	1380.6	-4.4
FCC1209#2	1014.8	1062.8	-4.6
KCC0102#1	226.3	244.4	-7.7
KCL0101#1	267.3	291.7	-8.7
KCL0101#2	314.7	388.3	-20.9
KCL1209#3	537.3	530.0	1.4

Sample	SO4= CSU	CARB	Difference/Mean (%)
BCC1210#2	197.2	189.0	4.3
FCC1209#2	94.0	87.0	7.8
KCC0102#1	30.4	27.3	11.0
KCL0101#1	28.4	25.8	9.5
KCL0101#2	88.2	86.2	2.3
KCL1209#3	50.4	52.0	-3.2

Sample	K+ CSU	CARB	Difference/Mean (%)
BCC1210#2	31.1	10.8	96.8
FCC1209#2	14.5	5.0	96.6
KCC0102#1	2.2	0.5	129.7
KCL0101#1	1.3	0.6	79.8
KCL0101#2	2.8	0.4	154.1
KCL1209#3	8.6	3.6	81.0

Sample	Ca2+ CSU	CARB	Difference/Mean (%)
BCC1210#2	6.8	21.3	-103.5
FCC1209#2	9.1	23.8	-89.5
KCC0102#1	3.8	19.4	-134.9
KCL0101#1	6.4	31.6	-133.1
KCL0101#2	5.0	21.3	-124.5
KCL1209#3	65.5	131.5	-67.0

Sample	Mg2+ CSU	CARB	Difference/Mean (%)
BCC1210#2	3.0	1.7	52.2
FCC1209#2	5.3	2.6	67.5
KCC0102#1	2.2	1.6	34.7
KCL0101#1	1.8	2.3	-23.0
KCL0101#2	2.5	1.4	55.4
KCL1209#3	8.9	6.8	26.1

calcium are consistently higher than those reported by CSU, while CARB values for potassium are consistently lower and magnesium values are lower in five of six cases. In many cases disagreement between the reported values is likely due to the low analyte levels being measured. For example, in samples where magnesium or chloride concentrations exceeded 5 μN, moderate agreement was observed between concentrations of these species reported by the two labs.There are several samples, however, where potassium or calcium concentrations exceed 10 μN, a level that should be accurately quantifiable, and large discrepancies are present between the values measured by the two laboratories. In the case of calcium, the fact that CARB reported no values below 19 μN despite the existence of CSU reported values as low as 4 μN, suggests the possibility of calcium contamination during sample handling.

1.4.4 Data Validation

Level 0 validation was described in our standard operating procedures and included collection of collector blanks, measurement of cloud collector flows, and record keeping of sampling procedures and events likely to affect data quality. These records were reviewed as part of data validation prior to submission of the final databases. The most common problem was lack of sufficient information about sample volume (for example if some sample was spilled during collection) to permit accurate calculation of fog liquid water content. In a few cases field records

indicated contamination of samples. Measurements for which level 0 data validation indicated problems were removed from the database.

It was our intent to collocate fog samplers during the study as part of a level I data validation effort. The CASCC2 samplers were all relocated for this purpose to Fresno during a break in IMS95 measurements in mid-December. Unfortunately no fog events occurred during this time and a side-by-side measurement comparison was not possible. A previous side-by-side comparison of five CASCC2 collectors constructed for a CARB fog monitoring network, however, reported excellent agreement among the collectors for sample mass and ion concentrations. A summary of these findings is presented in Table 1-5.

Table 1-5. Results of CASCC2 intercomparison (5 collectors) at San Pedro Hill, California in May 1989. Relative standard deviations are presented as a percentage of the mean value for each sample. Source: B. Daube, personal communication.

Species	Sample Mass (g)	H+ (μN)	NH4+ (μN)	Na+ (μN)	K+ (μN)	Ca2+ (μN)	Mg2+ (μN)	Cl- (μN)	NO3- (μN)	SO42- (μN)
Sample 1 avg.	125.2	515.3	458.3	175.1	7.3	43.3	49.3	205.7	546.4	489.5
Sample 1 rsd (%)	2.2	1.9	0.9	3.2	9	4.7	4	2.1	1	0.6
Sample 2 avg.	243.9	468	340.7	80.2	5.1	23.4	23.6	98.5	407.2	401.6
Sample 2 rsd (%)	2.9	4.1	1.4	5.8	14.5	8.1	5.7	5.9	0.8	0.5
Sample 3 avg.	161.1	1,047.2	848.6	73.7	6.6	45.8	26.5	143.4	1,027.1	902.4
Sample 3 rsd (%)	1.2	1.6	1.1	1.7	4.3	7.9	4.1	3.1	1.5	1.7

After sample analysis, a number of tests were applied as part of level II data validation. These tests are outlined below, along with an indication of flags applied to the submitted databases. Table 1-6 provides a summary for the southern San Joaquin Valley of the number of possible samples, the number of valid samples, and the number of samples above the limit of detection and the limit of quantitation (taken as three times the limit of detection). The fraction of samples not flagged for each species (% valid) ranged from a low of 54% for dissolved organic carbon (DOC) to a high of 93% for sodium, potassium and manganese. When flags due to high or low charge balances were excluded (in the SJV we have found that charge balances frequently are quite low when calculated as the sum of anions divided by the sum of cations (see below), presumably due to large concentrations of ionic species not analyzed), all species except total and dissolved organic carbon had total valid fractions of 89% or higher. In the Candelabra Tower study, 100% of the samples were determined valid except for total and dissolved organic carbon (with valid fractions of 88% each) and sodium (valid fraction of 94%). In the southern San Joaquin Valley study the fractions of samples above the detection limit were quite high, although smaller fractions of propionate, pyruvate, oxalate, and HMS were found to be above the limit of quantitation. At the Candelabra Tower, most species were measured at concentrations above the limit of quantitation, although magnesium, pyruvate, propionate, oxalate, and HMS concentrations were below this level in more than half the samples.

Table 1-6. Southern San Joaquin Valley fog sample statistics. The Limit of Quantitation (LOQ) is taken as three times the Limit of Detection (LOD).

Species	# samples	# flagged	# flagged excluding charge balance	# valid samples (#samples - #flagged)	% valid	% valid (excluding charge balance)	# above LOD	% above LOD	#above LOQ	% above LOQ
Cl-	111	20	7	91	82	94	111	100	95	86
NO3-	111	20	4	91	82	96	111	100	111	100
SO42-	111	20	5	91	82	95	111	100	111	100
Na+	113	20	6	93	82	95	107	95	92	81
NH4+	111	20	4	91	82	96	111	100	111	100
K+	113	20	5	93	82	96	110	97	103	91
Mg2+	113	20	4	93	82	96	112	99	96	85
Ca2+	113	22	8	91	81	93	113	100	111	98
Acetate	76	10	0	66	87	100	76	100	76	100
Propionate	76	10	0	66	87	100	59	78	30	39
Formate	76	10	0	66	87	100	76	100	75	99
Pyruvate	76	10	0	66	87	100	60	79	19	25
Oxalate	76	10	0	66	87	100	69	91	18	24
S(IV)	92	9	9	83	90	90	90	98	68	74
HMSA	57	6	6	51	89	89	47	82	29	51
HCHO	92	4	4	88	96	96	92	100	92	100
H2O2	87	2	2	85	98	98	84	97	68	78
TOC	18	6	6	12	67	67	18	100	18	100
DOC	13	6	6	7	54	54	13	100	13	100
Fe	88	9	9	79	90	90	88	100	88	100
Mn	85	6	6	79	93	93	83	98	83	98

1.4.4.1 Collector Blanks

As mentioned previously, there are several limitations to the information gained by taking fog collector blanks. Foremost among these is the uptake of soluble gases by the DI water sprayed onto collection surfaces. Nonetheless, there are times when collector blanks reveal that collector cleaning procedures were inadequate. We have set flags in the submitted database to identify the following situations:

- Chloride, sulfate, sodium, potassium, or calcium concentrations in a collector blank are > 5 μN and > 50% of the ion concentration measured in the first subsequent sample collected.
- Fe blank concentration >50 μg/l and >50% of the following fog sample Fe concentration
- Mn blank concentration >5 μg/l and >50% of the following fog sample Mn concentration

1.4.4.2 Charge Balance

If all ionic species present in a sample are accurately measured, the ion charge balance should sum to zero (the electroneutrality condition). In many environments, especially highly polluted ones like the San Joaquin Valley, many charged species are present in solution which are not measured by conventional methods. This situation is exacerbated by high fog pH values, such as those present in SJV fogs, due to increases in solubility of many gaseous compounds. In general, most of the charged species not accounted for tend to be anions, so that measured species tend to show an excess of positively charged species in the ion balance.

With these limitations in mind, we established the following criteria for examining samples with large ion imbalances:

- in cases where complete inorganic ion analysis and low molecular weight organic acid analysis was completed and the sum of anion charges divided by the sum of cation charges was below 0.70 or above 1.15, the sample was reanalyzed. If the charge balance ratio still fell outside these bounds it was flagged in the database. Numerous samples fell into this category and were reanalyzed. Upon reanalysis we generally found the charge ratio little changed, suggesting that the charge imbalance was due to unmeasured species, rather than to inaccuracies in sample analysis. Some of the missing species are likely of an organic nature. Others probably include carbonate, bicarbonate, and nitrite, which were not specifically analyzed.
- samples where low molecular weight organic acid analysis was not completed, and the anion/cation charge balance ratio was below 0.35 or above 1.5, were flagged in the database.

1.4.4.3 Concentration Comparisons

Hydroxymethanesulfonate (HMS) is one species contributing to total S(IV) and dissolved organic carbon (DOC) is a subset of total organic carbon (TOC). Consequently we expect sample analysis to show that HMS and DOC concentrations are less than or equal to S(IV) and TOC concentrations, respectively.

In order to test for cases when HMS concentrations were significantly larger than S(IV) concentrations, we applied a one-tailed test using the parameter

$$Z = \frac{[HMS\text{–}S(IV)]}{\sigma_{HMS\text{–}S(IV)}} \tag{1-13}$$

where

$$\sigma_{HMS\text{–}S(IV)} = \sqrt{\sigma_{HMS}^2 + \sigma_{S(IV)}^2} \tag{1-14}$$

and σ_{HMS} and $\sigma_{S(IV)}$ represent the absolute uncertainties of the HMS and S(IV) measurements. A 5% significance level was used for the test, corresponding to a critical Z value of 1.645. When Z was computed to exceed this critical value, a flag was applied to the sample in the database. The same approach was used to flag samples when DOC was found to significantly exceed TOC concentrations.

1.4.4.4 Size-fractionated Sample Comparisons

If the fog drop size spectrum is sampled in multiple fractions, the concentrations of a conserved chemical species contained in the sampled size fractions should average together (weighted by the liquid water content in each size fraction) to give the bulk fog concentration of that species. In other words, the concentration of a conserved chemical species in a bulk fog sample should fall between its concentrations in large and small drop fractions. If it does not, it suggests that

the species is not truly conserved upon mixing, or that some sampling or analysis artifact was encountered (e.g., evaporation of one or more sample fractions).

We compared bulk fog concentrations of sulfate (collected by CASCC2 samplers) with large and small drop fraction (collected by the size-fractionating CASCC) sulfate concentrations for corresponding sample periods. Size-fractionated samples for which the bulk sulfate concentration did not fall between the small and large drop sulfate fractions were flagged in the database.

1.4.4.5 S(IV) over range

A flag was applied when the measured sample concentration of a species exceeded the highest calibration standard concentration. This flag only needed to be applied for a few S(IV) concentrations measured in Bakersfield fog samples.

2. Review of Findings

Three different reviews of San Joaquin Valley fog chemistry have been conducted from the measurements made during IMS95. These are presented below as separate sections. The first is an overview of findings in the southern San Joaquin Valley; the second is an overview of fog chemistry from the Candelabra Tower study. These two sections are updated versions of papers presented at the A&WMA Air Toxics Meeting in Research Triangle Park, North Carolina in May 1996. They have been updated by including level-II validated data. The third is an overview of sulfur oxidation in San Joaquin Valley fogs, including north-south variations in the southern San Joaquin Valley, vertical variations observed at the Candelabra Tower, and the effect of chemical heterogeneity among droplet populations. This section was written to include findings presented at the AAAR Annual Meeting in Orlando, Florida in October 1996.

2.1 Preliminary Findings of Fog Chemistry in the Southern San Joaquin Valley During IMS95

Persistent radiation fogs often form in California's San Joaquin Valley during periods of winter air stagnation (Holets and Swanson, 1981). The fogs influence ambient aerosol concentrations both by accelerating the removal of particles and by enhancing particle growth through aqueous phase chemical reactions (Jacob et al., 1986, 1987; Waldman and Hoffmann, 1987; Pandis and Seinfeld, 1989). Preexisting particles which are scavenged by fog drops can be deposited at the surface by droplet removal processes, including sedimentation. Aqueous phase reactions in regional fogs have been demonstrated to produce significant quantities of particulate sulfate (Jacob et al., 1986). Aqueous phase nitrate formation is generally considered unimportant in typical clouds and fogs; however, conditions in the San Joaquin Valley are probably more conducive to aqueous phase nitrate formation warranting further investigation of the potential importance of this mechanism.

Characterization of both droplet removal processes and aqueous phase sulfate production in past studies have been hampered by a lack of information about variations in droplet composition

across the fog drop size spectrum. Recent work in the SJV and elsewhere has revealed that variations in droplet composition across the drop size distribution can enhance sulfate production significantly, particularly in environments where ozone or oxygen (catalyzed by iron and manganese) are the dominant aqueous phase S(IV) oxidants (Collett et al., 1994; Hegg and Larson, 1990). Because droplet removal processes are drop size dependent, variations in drop composition across the drop size spectrum can also bias the contributions of fog drop deposition to favor those chemical species which tend to be enriched in large fog drops. Species which are preferentially associated with small fog drops are removed with lower efficiency.

The purpose of the study described here was to characterize fog chemistry and physics in the southern San Joaquin Valley. The fog study comprised a portion of the 1995 Integrated Monitoring Study (IMS95), part of the Phase 1 planning effort for the California Regional PM10 Air Quality Study (CRPAQS). An overview of IMS95 is presented by Solomon et al.(1996). The approach of the fog study was to sample fog at multiple locations in the region, looking at variations in fog composition with time, in space, and as a function of drop size. The results will be used to investigate the effects of fogs on particulate concentrations in the region, both directly and as input to modeling activities, as well as to provide baseline data for planning a more comprehensive future study in the region. In this section we describe measurements of fog chemistry at three ground-based sites in the southern San Joaquin Valley.

2.1.1 Experimental Procedure

Fog collection in the Southern San Joaquin Valley during IMS95 was performed at three locations. Two sites were in urban locations: Fresno and Bakersfield, California. The third was located at a rural site near the Kern Wildlife Refuge (KWR), west of Delano, California. These sites, subsequently referred to as Fresno, Bakersfield and KWR, were selected because of their use as core sites for the winter component of IMS95. Sampling equipment used at these sites and analytical methods used to characterize the composition of collected samples were described above.

The Bakersfield and Fresno sites were both equipped with two fog collectors, one for bulk fogwater collection (all drop sizes collected together) and the other for separate collection of small and large drop size fractions. The KWR site was instrumented with three fog collectors, one for bulk fogwater collection and two for size-dependent fog drop sampling. An optical probe (PMS CSASP-100-HV) for measurement of the fog drop size distribution was also deployed at this site.

The goal of the study was to characterize fog composition at all three locations during as many fog events as possible. Simultaneous operation of the various collectors at each site was intended to provide information about bulk fog composition and variations in drop composition with drop size. Sample time intervals were selected to balance the desire to obtain information about temporal changes in fog composition and to match sampling periods between different fog collectors.

2.1.2 Results and Discussion

Although weather conditions during the study period were not as conducive to extensive fog formation as they are in a typical winter, it was still possible to sample fog on several nights during the four week study. Overall, ten different fog episodes were sampled during the study. There were two nights when widespread fog permitted simultaneous sampling at all three sites. A total of 14 bulk fog samples were collected at Bakersfield during three fog episodes. Six episodes were sampled at KWR, where a total of 21 bulk fog samples were collected. At Fresno 25 bulk fog samples were collected during six fog episodes.

The weather forecast called for the possibility of fog formation nearly every night during the study; however, fog did not form on many of those occasions and when it did form it was generally quite localized. We experienced several nights where locally dense fogs were located at locations other than the sampling sites. In particular we noted that dense fog often formed outside urban boundaries, especially in irrigated regions, while skies remained clear at the sampling sites.

Figure 2-1 depicts the pH of bulk fog samples collected with the CASCC2 collectors at the three southern SJV sites during the study. The plot in Figure 2-1 provides a quick overview of the number of fog episodes at each site and whether episodes occurred simultaneously at more than one location. Each week of the study had at least one episode which could be sampled, with the most extensive fog occurrence near the beginning and end of the study. Figure 2-1 also provides an overview of the variability, or lack thereof, in the fog pH at each site (both within an event and between events) and the difference in pH between sites. It is apparent that fog at all locations was generally basic in comparison to typical background atmospheric water pH values (a pH of 5.6 is expected from equilibrium with atmospheric carbon dioxide with other naturally occurring acids at times depressing the background pH several tenths of a pH unit lower). Frequency distributions of bulk fog sample pH values for the three sites are depicted in Figure 2-2. There is an apparent tendency in this data set, consistent with expectations, for fogwater to be somewhat more basic at the rural KWR site than at the two urban sites. There also appears to be a larger range of acidities in Bakersfield fog than at Fresno.

Because the fog pH was consistently high at all locations we do not expect sulfur oxidation to be limited by the presence of hydrogen peroxide (Seinfeld, 1986). Further evaluation of available oxidant concentrations (including hydrogen peroxide and ozone) and catalysts (including Fe and Mn) will permit an assessment of the relative importance of different sulfur oxidation pathways to aqueous phase sulfate production. This issue is addressed in more detail in a subsequent section of this report.

Fogwater acidity in the region has been shown previously to be governed by a balance between acidic inputs from nitric and sulfuric acids and basic inputs of ammonia (Jacob et al., 1986). In samples collected this year, the inorganic composition of the fog is again dominated by nitrate, sulfate and ammonium with ammonium levels generally in excess of the sum of nitrate and sulfate. Figure 2-3 illustrates the relative contributions of the major inorganic ions to the fog composition for a typical sample. As in this sample, nitrate concentrations were typically several

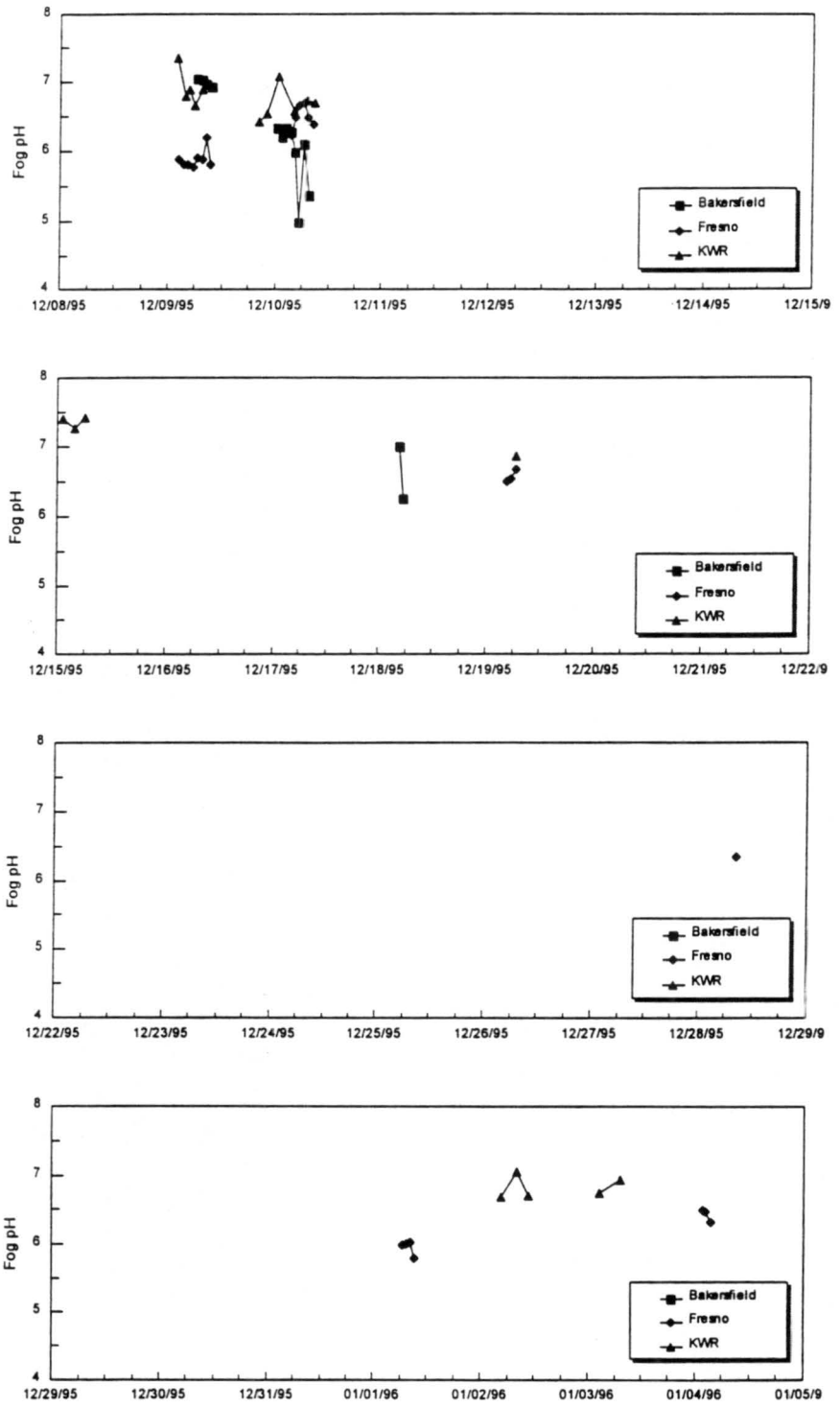

Figure 2-1. Fog pH values measured in bulk fog samples collected with the CASCC2 collectors at the three IMS95 core sites. Points are plotted at the midpoint of each sampling interval.

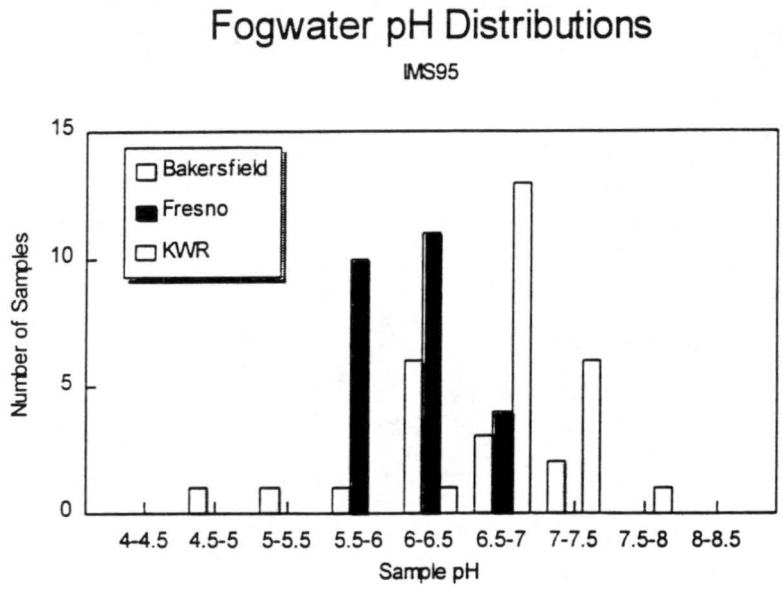

Figure 2-2. Frequency distributions of pH values observed in CASCC2 bulk fog samples from the three IMS95 core sites.

times higher than sulfate concentrations, with a few noted exceptions at Bakersfield (discussed below), and inorganic anions were typically insufficient to balance contributions from inorganic cations. At the high pH values observed in these fogs low molecular weight organic acids are quite soluble and also contribute substantially to the anion side of the charge balance. Acetate and formate were often present at significant concentrations (up to a few hundred micronormal), with smaller contributions from propionate and oxalate. Small concentrations of pyruvate were also measured.

Figures A-1 through A-21 depict the concentrations of all species (except pH) measured in fog samples collected at the three core sites. In general, concentrations of major ions in the fog samples were similar at all three locations, with the exception of periods of elevated sulfate in the Bakersfield fogs. Organic acids, especially acetate, formate and propionate, appear to be somewhat more concentrated in the urban fogs than in fog collected at KWR (see Figures A-9 to A-13. Fog concentrations of formaldehyde (Figure A-15) were somewhat higher at the urban locations. There also appears to be a tendency for higher S(IV) concentrations at the urban sites, particularly at Bakersfield (Figure A-14). Formaldehyde concentrations were typically much higher than S(IV) concentrations in the fog samples, suggesting that hydroxymethanesulfonate (HMS) formation may be important. Modest concentrations of HMS, up to 20 μM, were measured in fog samples from KWR (see Figure A-16).

Measured aqueous hydroperoxide concentrations (Figure A-17) ranged from approximately 1 to 25 μM. Peroxide concentrations in fog samples exhibited a decrease from south to north on the morning of December 9, but no clear trend among sites was present the next morning. There also appears to be a tendency for peroxide concentrations to increase after sunrise, perhaps reflecting photochemical production in the gas phase or within the droplets themselves. Concentrations of

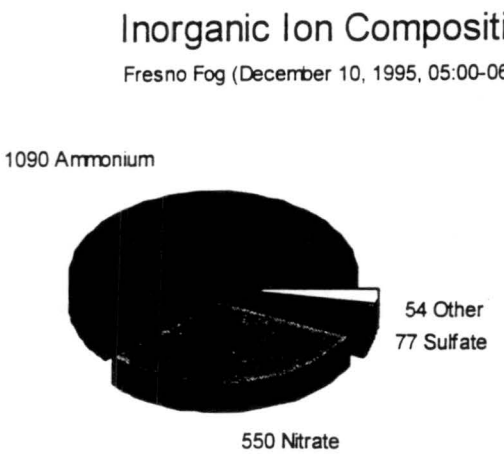

Figure 2-3. Inorganic composition of a typical fog sample from IMS95. The species included in the slice labeled "Other" are Cl^-, Na^+, K^+, Ca^{2+}, and Mg^{2+}.

iron and manganese show no clear trends between sites, with iron concentrations typically running around a few hundred μg/l and manganese concentrations a factor of ten smaller (see Figures A-18 and A-19). It is difficult to draw any conclusions from the few TOC (Figure A-20) and DOC (Figure A-21) measurements made. Measurements of TOC in Fresno fog samples on three nights averaged approximately 35 ppm, while concentrations measured on two (different) nights at KWR were generally between 5 and 10 ppm.

Figure 2-4 depicts concentrations of ammonium, nitrate, and sulfate in bulk fog samples collected at the three sampling sites on December 9 and 10, 1995. Aside from the December 10 concentration spikes at Bakersfield, the fog composition is roughly comparable at the three sites. One remarkable feature depicted in Figure 2-4 is the rapid fluctuations in pH in the Bakersfield fog observed on the morning of December 10, 1995. In Figure 2-5 fogwater concentrations of sulfate, nitrate, ammonium, and total S(IV) are plotted, together with pH, for this episode. The rapid changes in pH occur at times where dramatic changes in the sulfur composition of the sample are observed. For example, between the fourth and sixth samples, the S(IV) concentration increases from a few μM to approximately 300 μM and the sulfate concentration increases by more than a factor of ten, from just over 100 μN to more than 1300 μN. During the same time period the fog pH drops from 6.3 to 5.0, despite the fact that the ammonium concentration increased significantly, presumably as greater quantities of gas phase ammonia dissolved into the acidifying droplets. During the hour following the rapid sulfur buildup, the sulfur concentrations relax back toward their previous values and the fog pH climbs again. During this entire period the nitrate concentrations show a much smaller increase and decrease. These observations suggest that the site was influenced during a portion of the fog episode by a strong plume of sulfur dioxide superimposed on a background composition that is otherwise relatively constant. A similar rapid rise in sulfur concentrations, accompanied by a drop in fog pH, was observed at Bakersfield on the morning of December 19, 1995. The existence of such

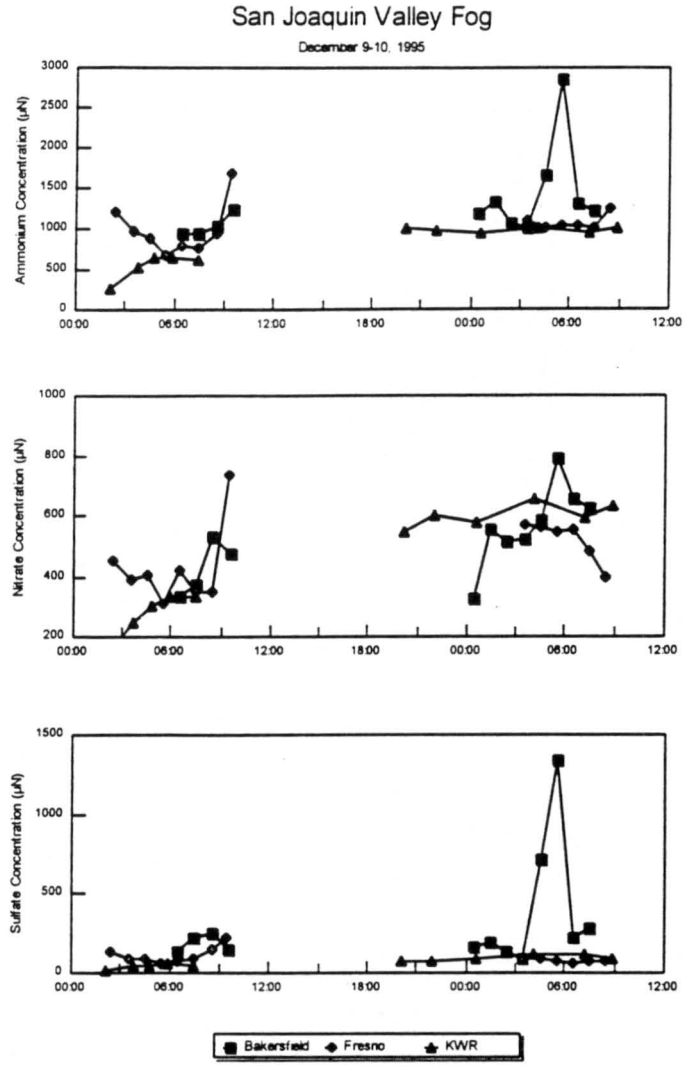

Figure 2-4. Concentrations of ammonium, nitrate, and sulfate measured in fog samples collected with the CASCC2 collectors at the three IMS95 core sites on the mornings of December 9 and 10, 1995. Points are plotted at the midpoint of the sampling intervals.

strong gradients in sulfur concentrations in the fog indicates that significant sulfate production in fogs in the region may occur over rather limited spatial domains.

The Fresno fog concentrations on December 9 exhibit a U-shaped profile with time, with high concentrations at the beginning and end of the fog and lower concentrations in between (see Figure 2-4). This pattern is often seen in fogs as the fog drops grow by condensation following fog formation and later evaporate as the fog dissipates, reflecting the dilution and concentration of fog solutes during growth and evaporation. In order to examine whether the observed changes in the Fresno fog simply reflected this phenomenon, we multiplied the aqueous phase concentrations of ammonium, nitrate and sulfate in each sample by the average fog liquid water content for that sampling period to obtain a loading of each species in the aqueous phase per unit volume of air. Liquid water contents were calculated from the collection rate of the CASCC2

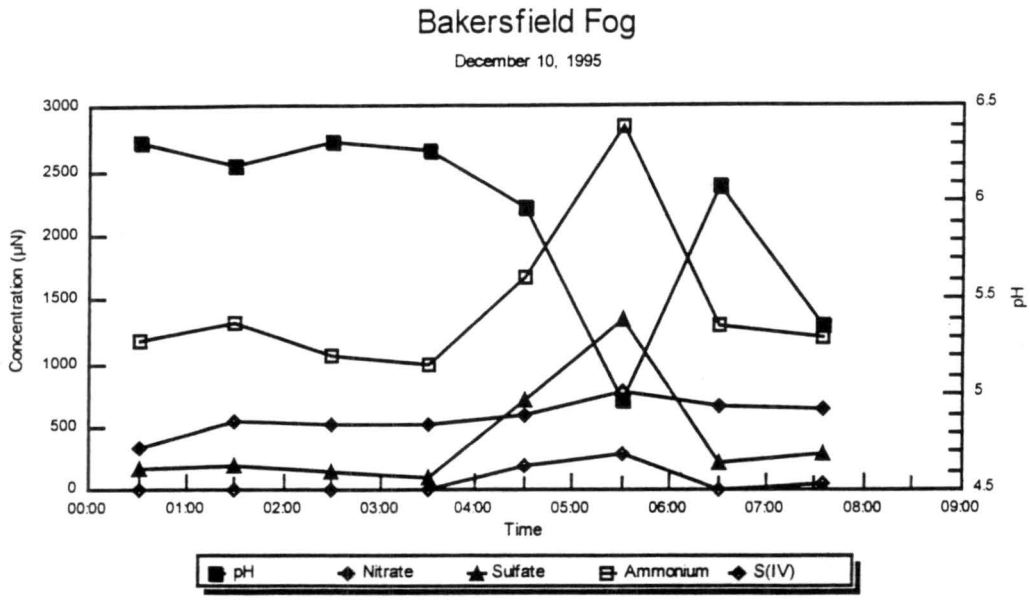

Figure 2-5. Temporal changes in fog composition at Bakersfield on the morning of December 10, 1995. Samples were collected with the CASCC2 and are plotted at the midpoint of each sampling interval

sampler using an approach outlined by Demoz et al.(1996). The calculated loadings of ammonium, nitrate, and sulfate in the Fresno fog sampled on December 9 and 10, 1995 are depicted in Figure 2-6. On both nights concentrations of all three species decrease with time, suggesting significant loss by deposition to the surface. This is consistent with observations at the site of significant droplet flux to exposed surfaces.

2.1.3 Summary

Fog was successfully sampled at three locations in the southern San Joaquin Valley during several fog episodes. Frequent observations of fog occurrence at locations other than the fixed sampling sites suggests that fog processing of atmospheric aerosols and trace gases occurred in the region during a greater fraction of the time than is represented by our data set. Preliminary analysis of the data revealed fog that was generally basic at all three locations, with ammonium and nitrate generally dominating the inorganic composition Sulfur inputs to the fog were relatively more important at Bakersfield than at sites farther north. On two of three foggy nights in Bakersfield rapid increases in fogwater sulfur concentrations were observed, each time accompanied by acidification of the fog. Observations of significant fogwater deposition at Fresno during a dense fog episode early in the study are consistent with observations that reveal total loadings of fogwater sulfate, nitrate, and ammonium decreasing over the course of the episode.

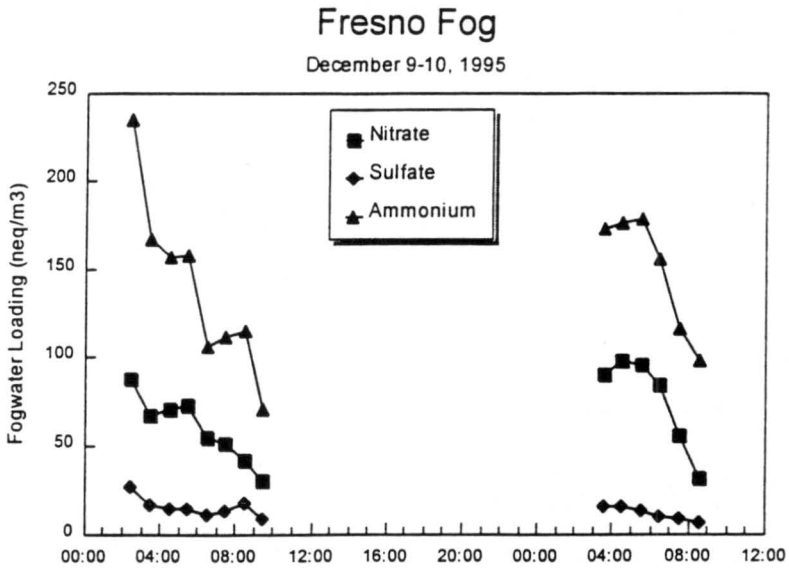

Figure 2-6. Fogwater loadings of ammonium, nitrate and sulfate at Fresno on the mornings of December 9 and 10, 1995. The fogwater loading of a species is its aqueous phase concentration multiplied by the fog liquid water content, and represents the total amount of that species in the aqueous phase per unit volume of air.

2.2 Vertical Variations in Fog Chemistry in the Northern San Joaquin Valley During IMS95

Fogs are known to play an important role as processors of atmospheric particles. They contribute to particle production through aqueous phase reactions that can be much faster than their gas phase counterparts (Seinfeld, 1986). For example, oxidation of sulfur dioxide to sulfate occurs much more quickly in solution than in the gas phase under typical conditions. Fogs also enhance particle removal, since particulate material scavenged by fogs is removed fairly quickly by deposition of the relatively large fog drops (Waldman et al., 1987).

Winters in California's San Joaquin Valley typically feature extended periods of air stagnation, often accompanied by dense fog formation and high atmospheric particle loadings (Holets and Swanson, 1981; Jacob et al., 1986). During the winter of 1995-96, the winter portion of the 1995 Integrated Monitoring Study (IMS95-W), part of the Phase 1 planning effort for the California Regional PM10 Air Quality Study (CRPAQS), was conducted in the southern San Joaquin Valley to gather preliminary information on mechanisms governing the build-up of particle concentrations in the region (Solomon et al., 1996). As part of that effort, a fog study was conducted to examine the influence of fogs on regional particulate levels. The fog study included examination of variations in fog chemistry and physics in space and time, as well as variations across the fog drop size spectrum. In the previous section we describe those efforts in the southern San Joaquin Valley where three ground-based stations were used to sample fog. Here we describe efforts to characterize vertical variations in fog chemistry and physics using a

television broadcast tower (the Candelabra Tower) in the northern San Joaquin Valley as a sampling platform.

In most fog sampling campaigns, fogwater collection is conducted on or near the ground. Little is known about how the fog chemistry and physics change away from the surface. Models of San Joaquin Valley fog and cloud chemistry suggest that significant vertical variations exist in fog/cloud chemistry and physics (Jacob et al., 1989; Pandis and Seinfeld, 1989). Knowledge of such vertical variations is essential to accurately predicting particle formation in the fog. Entrainment of reactive materials, including key oxidants such as ozone and hydrogen peroxide, from clear air above the foggy boundary layer may accelerate sulfate production near the top of the fog compared to what is observed in the oxidant-depleted environment near the surface (Pandis and Seinfeld, 1989). From a practical standpoint, information about the occurrence or absence of significant vertical variations in fog properties can also provide a basis for determining the necessity of making measurements away from the surface in a more comprehensive future winter particulate study in the region.

2.2.1 Experimental Procedure

Sampling was conducted at the 430 m high Candelabra tower in Walnut Grove, California, located in the northern San Joaquin Valley approximately 30 km south of Sacramento. Although the Candelabra tower currently serves mainly as a backup broadcast tower, three additional tall towers nearby are usually broadcasting. Access to the tower is provided by a small personnel elevator which can also be used to transport small to moderately sized pieces of equipment. The elevator can hold one or two people and takes about 20 minutes to run the length of the tower. An enclosed room at the top of the tower was available to house some instrumentation. Power was installed at several additional levels to permit operation of fog samplers and other equipment.

Fog was sampled using Caltech Active Strand Cloudwater Collectors Version 2 (CASCC2), described in detail above. Two CASCC2 collectors were mounted on the tower with a third installed on a 3 m stand at the surface. Although it was possible to relocate the tower-based collectors to several elevations, this was not practical at night during fog due to safety considerations.

Samples from the three CASCC2 samplers were collected over matching one hour sampling periods, with 30-60 minute gaps between samples. The timing scheme was dictated by the transit speed of the elevator and the desire to get samples to the field lab at the bottom of the tower for pH measurement and trace species stabilization as soon as possible following collection. The sample pH was measured on site using a portable pH meter and glass combination microelectrode calibrated with pH 4 and 7 buffers. Aliquots were removed from each sample for individual stabilization of trace species including S(IV), formaldehyde, hydroxymethanesulfonate (HMS), soluble hydroperoxides, organic acids, total organic carbon, iron, and manganese. The aliquots and any remaining sample were refrigerated until analyses could be completed. In addition to the species mentioned above, samples were analyzed for Na^+, NH_4^+, K^+, Mg^{2+}, Ca^{2+}, Cl^-, NO_3^-, and SO_4^{2-} by ion chromatography.

In addition to the fog measurements, several trace gas and aerosol measurements were made at the site. The Berner aerosol impactor described previously was used to collect samples at the surface for characterization of the size-dependent aerosol composition prior to fog formation. Annular denuders, also described above, were operated at the surface prior to anticipated fog events in order to characterize surface concentrations of sulfur dioxide, nitric acid, and ammonia. Several continuous monitors were also operated at the site. Soluble gas phase hydroperoxides were monitored continuously at the top and bottom of the tower as were SO_2, NO_y and O_3.

Meteorological conditions were characterized by tower-mounted instruments at several elevations and by rawinsonde launches. Unfortunately, the strong electromagnetic fields emitted by the active broadcast towers nearby interfered with several of the rawinsonde measurements, even when the launch site was relocated several tens of km away.

A time lapse video system was installed on top of the Candelabra Tower to provide a record of fog/cloud presence, an estimate of the elevation of the top of the cloud or fog layer, and visual information about the dynamics of the cloud/fog top and its interactions with the clear air above. Lights at known elevations on a nearby tower provided a reference for determining the approximate location of the fog/cloud top at night.

2.2.2 Results and Discussion

Fog or low clouds were sampled at the Candelabra Tower during two separate periods within the study. Unfortunately an extension of the prior study in the southern San Joaquin Valley delayed the start of the tower work past the peak fog period and limited the number of events available for study at the tower. On the morning of January 12, 1996, fog was sampled at the ground and at two elevations on the tower. After that morning, no significant fog was observed at the ground. Low-lying stratus clouds did occur again and were sampled at two elevations on the tower on the morning of January 14, 1996. An overview of results from these two fog/cloud events is presented below.

CASCC2 collectors were deployed at the ground and at 140 and 230 m elevation on the tower on the morning of January 12, 1996. Collection at all three elevations began at 06:00 with the first sample collected at 07:00. Two additional samples were collected at all three elevations between 07:30 and 08:30 and between 09:00 and 10:00. By 10:00 the fog had lifted from the ground; however, an additional pair of samples was collected from the two tower-mounted collectors between 10:30 and 11:30. Figure 2-7 presents the liquid water content values for the three sampling elevations during this fog episode. Liquid water content was calculated from the collection rate of the CASCC2 as described elsewhere (Demoz et al., 1996). The calculated liquid water content depends on the collected fogwater mass, the sample time, the collection efficiency of the CASCC2, and the assumed drop size distribution. It is difficult to assign a general uncertainty value to LWC's obtained in this way, but the authors' experience suggests a relative standard deviation on the order of 20% is probably reasonable. Not surprisingly, the highest liquid water contents, as high as 0.3 g m^{-3}, were observed at the highest sampling location. Liquid water content decreased toward the ground, with the average values during the

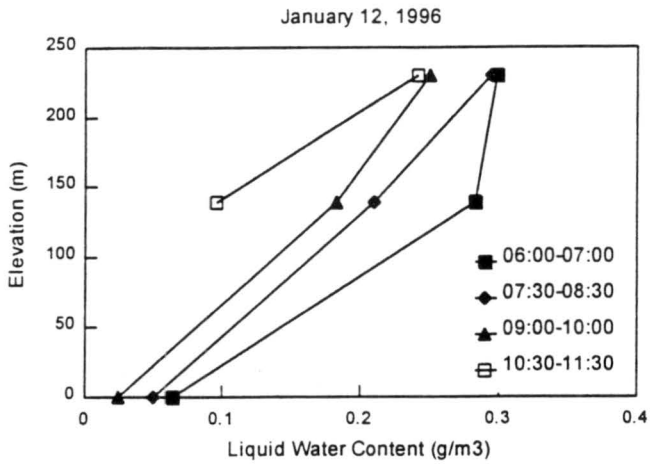

Figure 2-7. Liquid water contents measured at the Candelabra Tower on January 12, 1996.

three sampling periods at the surface all well below 0.1 g m^{-3}. The liquid water content at all three elevations decreased with time over the course of the morning.

Figure 2-8 depicts vertical profiles of fog pH and fogwater concentrations of ammonium, nitrate and sulfate at the three sampling elevations between 06:00 and 07:00 during the same fog episode. Concentrations of ammonium, nitrate and sulfate decrease with elevation, especially between the ground and the first sampling platform. There is also a slight decrease in pH apparent between the ground and the first sampling platform. Figure 2-9 illustrates ammonium, nitrate and sulfate concentrations observed at the ground and from the highest collector (230 m) over the course of the morning. Major ion concentrations at these elevations were remarkably stable over time, despite the significant changes observed in liquid water content. Similar stability was observed for the fog composition at the middle collector elevation (140 m). The product of the fog liquid water content and the concentration of any species yields the loading of that species: the total concentration of the species in the aqueous phase per unit volume of air. Figure 2-10 depicts the fogwater loadings of ammonium, nitrate and sulfate at the ground and at 230 m elevation on the morning of January 12. The loadings of all three species at both elevations appear to decrease with time. This suggests that material was being removed from the cloud with time, either by transport out of the column we were sampling (by advection or surface deposition) or by complete evaporation of some drops, releasing particulate material. Future efforts to model this episode will provide further insight into the relative importance of these possible explanations.

One of the reasons for looking at vertical variations in fog composition was to determine whether entrainment of material, particularly oxidants, from above the fog top could affect particle processing by the fog. Aqueous phase soluble peroxide concentrations from the morning of January 12, 1996 for the three sampled elevations are plotted in Figure 2-11. A gradient in peroxide concentrations is apparent, but concentrations appear highest at the ground, rather than higher in the fog as we might expect if the predominant source was entrainment from clear air

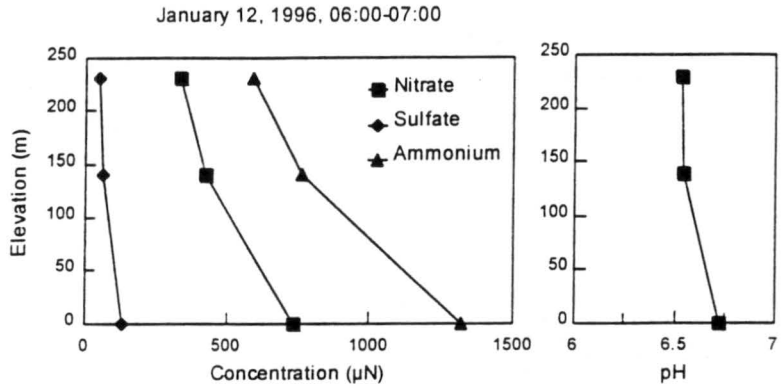

Figure 2-8. Vertical profiles of major ion concentrations and pH in fog sampled at the Candelabra Tower on January 12, 1996.

above the fog top. There also appears to be an increase in peroxide concentrations after sunrise, consistent with photochemical production either in the gas phase or in the droplets themselves. Separate analyses of the gas phase peroxide measurements made at the top and bottom of the tower can provide better insight into vertical gradients in available peroxide concentrations. Ozone data from the top and bottom of the tower will also be quite interesting since, for the high pH values observed in these fogs, ozone is probably a more important oxidant for aqueous phase sulfate production. Although the trace gas data are being presented in a separate report, the vertical gradients in ozone and peroxides are addressed in section 2.3 below in the context of looking at sulfate production rates vs. elevation.

Another interesting observation from the morning of January 12 is that S(IV) and peroxides were observed to coexist in the fog, contrary to conventional wisdom. This reflects significant

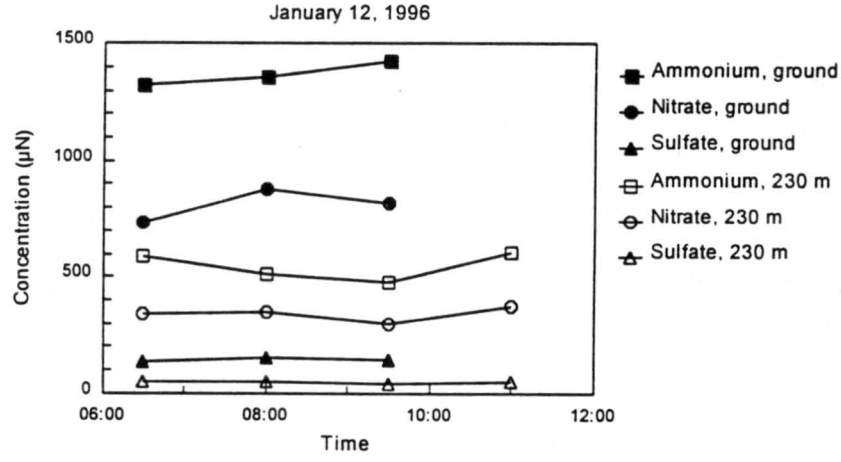

Figure 2-9. Temporal changes in major ion concentrations in fog sampled at the ground and at 230 m elevation at the Candelabra Tower on January 12, 1996. Points are plotted at the midpoint of each sampling period.

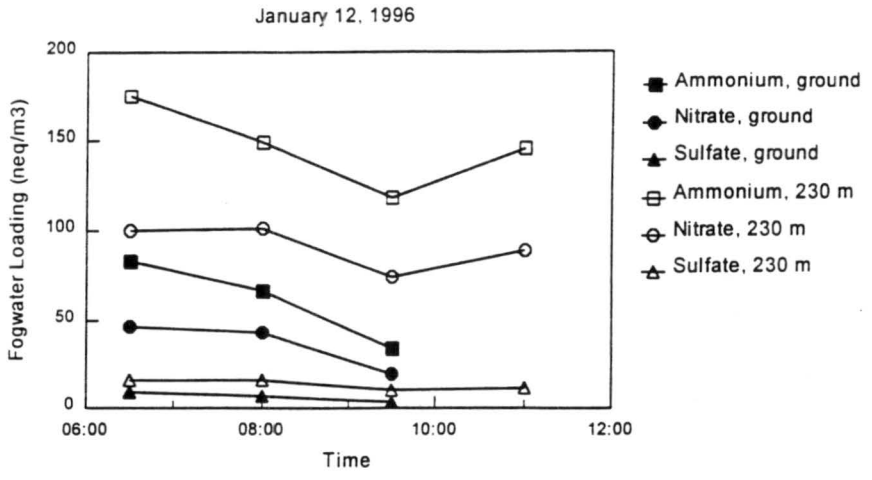

Figure 2-10. Temporal changes in fogwater loadings of major ions in fog sampled at the ground and at 230 m elevation at the Candelabra Tower on January 12, 1996. The fogwater loading of a species is defined as the concentration of that species in the fogwater multiplied by the fog iquid water content and represents the total amount of that species in the aqueous phase per unit volume of air. Points are plotted at the midpoint of each sampling interval.

formation of a relatively stable S(IV)-aldehyde complex, due to the relatively slow rate of S(IV) oxidation by hydrogen peroxide at high pH compared with the rate of complexation of S(IV) by formaldehyde (Rao and Collett, 1995). The complex between S(IV) and formaldehyde, hydroxymethanesulfonate (HMS), is measured along with free S(IV) in the total S(IV) analysis. Separate measurements of HMS indicate it comprised the major fraction of S(IV) measured in

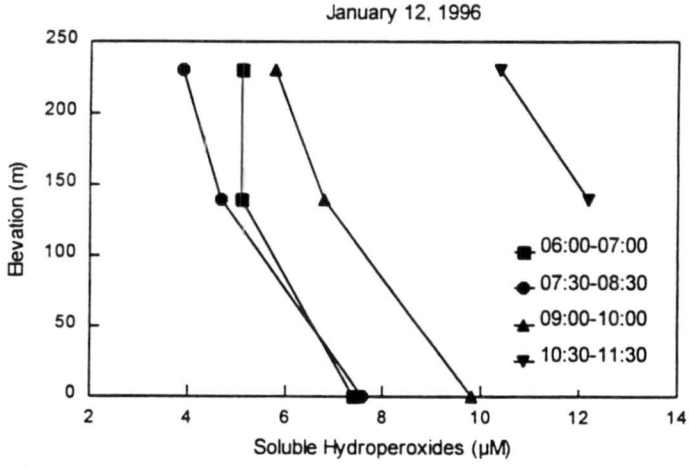

Figure 2-11. Vertical concentration profiles of concentrations of soluble hydroperoxides measured in fog sampled at the Candelabra Tower on the morning of January 12, 1996. The analysis technique used is sensitive to hydrogen peroxide and to soluble organic hydroperoxides.

this event. Measurements of formaldehyde in the fog samples show it present in large excess, relative to S(IV), suggesting a significant potential for further HMS formation if additional sulfur dioxide is added to the system.

A low cloud deck hung over the northern San Joaquin Valley on the morning of January 14, 1996. Although no significant fog was present at the surface, clouds could be collected from two CASCC2 collectors mounted at 140 and 320 m elevation on the tower. Three pairs of samples were collected between 05:00 and 10:00. As on the morning of January 12, the liquid water content was observed to increase with height in the cloud layer, with values close to 0.1 g m^{-3} at 140 m and about three times that level at 320 m. Concentrations of major ions during the first two sample periods were roughly constant at both elevations. During the final hour of sampling, however, a significant change was evident. Figure 2-12 depicts concentrations of sulfate, S(IV) and nitrate as a function of time at both elevations. While nitrate concentrations are rather constant through the entire sampling period at both elevations, sulfate concentrations increase substantially at both elevations between the second and third samples. The sulfate increase is paralleled by an increase of similar proportion in S(IV) concentrations. These observations, which occur despite the absence of any significant change in the cloud liquid water content, are not unlike those seen at Bakersfield in the southern San Joaquin Valley, as described in the previous section. It appears that the clouds at the tower during the final sampling period were influenced by a sulfur plume that was superimposed on an otherwise constant background composition (as reflected by the stability of the nitrate concentrations). An increase in the ammonium concentration in parallel with the occurrence of the sulfur peak, together with the absence of a significant change in the cloud pH at this time, suggests that sufficient excess ammonia was available to neutralize the additional sulfate produced. The existence of such sharp gradients in sulfur concentrations suggests that an understanding of particle production in regional fogs may require considerable knowledge about spatial variability in concentrations of S(IV) available to be oxidized. Sharp increases in formaldehyde and HMS concentrations between samples two and three further reinforce the need to consider the competition between formaldehyde and oxidants for dissolved sulfur dioxide in this high pH environment.

Preliminary analysis of the time lapse video footage filmed from the top of the Candelabra tower reveals the existence of a very dynamic interface between the fog/cloud top and the clear air above. The interface often looks much like a strongly boiling pot of water. At one point a wave is observed to sweep across the entire field of view, appearing almost as an ocean wave sweeping in to shore. These observations suggest that entrainment of material from above the cloud/fog may provide a significant source of oxidants or other materials to the foggy/cloudy surface boundary layer.

2.2.3 Summary

Two fog/cloud events were sampled from the 430 m tall Candelabra Tower near Walnut Grove, California in the northern San Joaquin Valley. Cloud collectors located at multiple elevations were used to characterize vertical variations in fog/cloud chemistry and physics. Both liquid water content and fog/cloud chemical composition were observed to vary with height, although ion concentration decreases away from the surface were not as strong as increases in liquid water

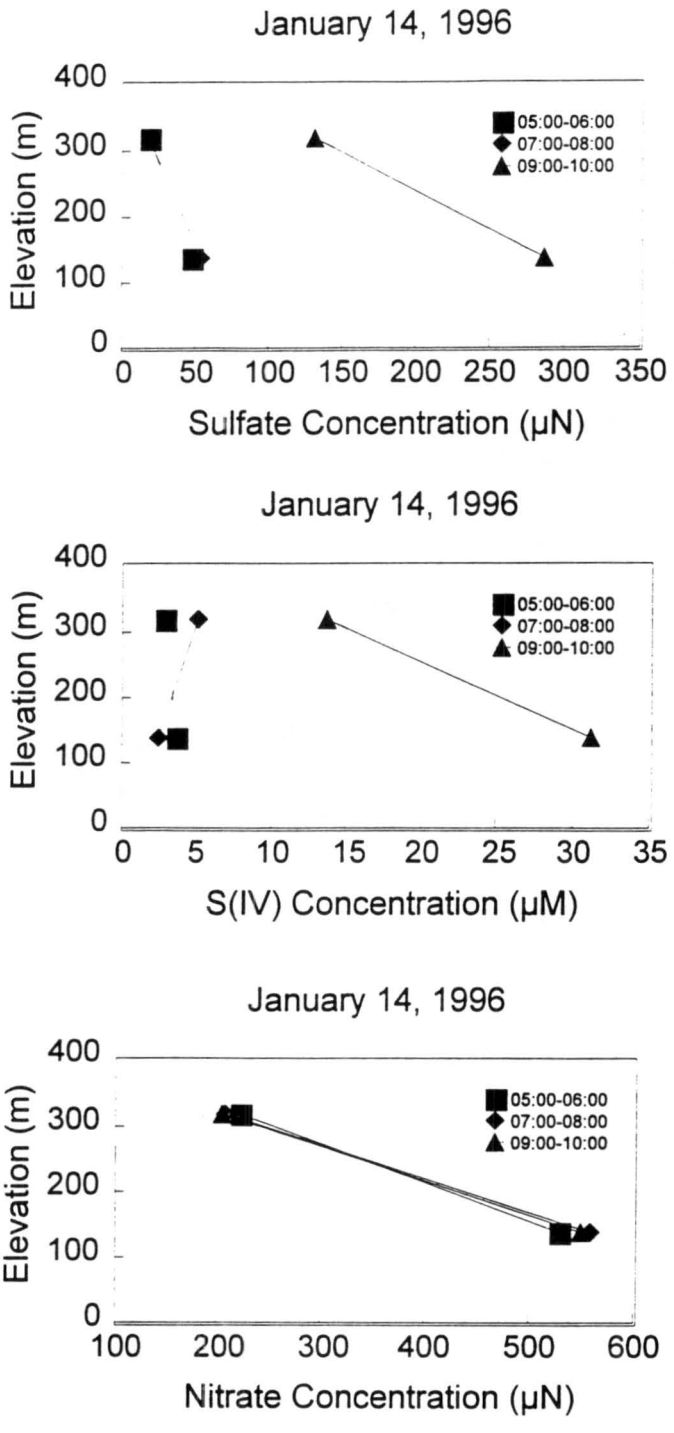

Figure 2-12. Vertical concentration profiles of sulfate, S(IV) and nitrate measured in cloudwater collected at the Candelabra Tower on the morning of January 14, 1996.

content. The fog composition at each sampled elevation was remarkably constant over the sampled episodes, with the exception of a strong increase in reduced and oxidized sulfur concentrations at the end of one event. Time lapse video footage of the cloud/fog top reveals a very dynamic interface that suggests that significant entrainment of material into the fog/cloud from above is likely.

2.3 A Preliminary Examination of Sulfate Production in SJV Fogs during IMS95

One important way fogs act as aerosol processors is through aqueous phase sulfate production. Fog drops absorb sulfur dioxide from the air which is then oxidized to sulfate more rapidly than occurs in the gas phase. There are several pathways through which this reaction takes place. These include oxidation by hydrogen peroxide, ozone and oxygen. The oxygen pathway is enhanced by the presence of Fe(III) and Mn(II) which catalyze the reaction. Both this pathway and the ozone pathway exhibit rates which are strongly pH dependent. The rate of aqueous phase oxidation by hydrogen peroxide, by contrast, is effectively pH independent. One consequence of this is that oxidation by hydrogen peroxide tends to be the dominant mechanism for aqueous phase sulfate production in many environments where fogs and clouds are acidic (see Fig. 2-13) and sufficient hydrogen peroxide is present in the atmosphere or produced photochemically within the droplets. In the more basic conditions often observed in San Joaquin Valley (SJV) fogs, it is not immediately obvious which oxidation pathway is likely to dominate sulfate production and quite possible that the dominant oxidation mechanism varies in time and space.

This section investigates the rates of these three aqueous phase S(IV) oxidation mechanisms and their temporal and spatial variability in the SJV using data collected in the southern San Joaquin Valley of California at the core sites of Bakersfield, Fresno, and Kern Wildlife Refuge (KWR)

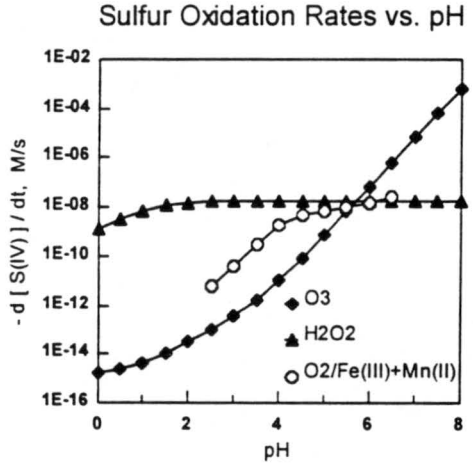

Figure 2-13. A comparison of sulfur oxidation rates for conditions typical of the San Joaquin Valley. Assumed conditions are H_2O_2 = 200 ppt, SO_2 = 1 ppb, O_3 = 5 ppb, [Fe(III)] = 1.5 μM, [Mn(II)] = 0.25 μM. Rate laws are taken from O_3 - Hoffmann, 1986, H_2O_2 - Seinfeld, 1986, O_2 / Fe(III)+Mn(II)- Ibusuki and Takeuchi, 1987.

during IMS95. Vertical variations in fog chemistry and sulfate production are also considered using data collected at the Candelabra Tower near Walnut Grove, California in January 1996. Details of the various fog collection methods and instruments mentioned can be found in the preceding sections of this report.

A second topic considered here is the effect of variations in fog drop composition across the droplet size spectrum on sulfate production. Two effects are possible. First, if droplet composition (especially pH or catalyst concentrations) varies with drop size, then sulfate production rates may also vary with drop size. Second, due to the nonlinear nature of the rate laws involved, it is likely that the net rate of sulfate production in the fog will not be accurately predicted from the average droplet composition. Collett et al. (1994) have demonstrated that use of bulk fog/cloud drop composition tends to underpredict sulfur oxidation by ozone in chemically heterogeneous cloud or fog drop populations. Similar findings have also been reported for the metal-catalyzed pathways (Rao and Collett, 1997). In cases where hydrogen peroxide is the dominant oxidant, little effect of nonuniform drop chemistry on sulfate production is expected.

2.3.1 Calculations

The following rate laws were used to calculate sulfate production for various oxidants:

- H_2O_2 : $-d[S(IV)]/dt = k\,[H^+]\,[H_2O_2]\,[HSO_3^-] / (\,1+13[H^+]\,)$ (Seinfeld, 1986)

- O_2 / Fe(III)+Mn(II): $-d[S(IV)]/dt = k\,[Fe(III)]\,[Mn(II)]\,[S(IV)]\,[H^+]^{0.67}$ for pH > 4.2 (Ibusuki and Takeuchi, 1987. This rate law includes a synergistic catalytic effect due to the simultaneous presence of Fe(III) and Mn(II)).

- O_3: $-d[S(IV)]/dt = [O_3](\,k_1[SO_2H_2O] + k_2[HSO_3^-] + k_3[SO_3^{2-}])$ (Hoffmann, 1986)

Gas measurements or assumed typical winter SJV gaseous concentrations of SO_2, H_2O_2 and O_3 were used to calculate aqueous phase concentrations of these species using Henry's Law. $[H^+]$ (from pH), total aqueous phase iron and total aqueous phase manganese were measured in actual fog samples. The collection of the samples and the chemical analyses are described in detail in previous sections of this report. Dissolved [Fe(III)] was assumed to represent 25% of the total iron measured and dissolved [Mn(II)] was assumed to comprise 100% of the total manganese measured.

Aqueous phase sulfur oxidation rates were calculated using the compositions of bulk fog samples collected using CASCC2 fog collectors in the southern SJV. For the purpose of these calculations we assumed gas phase concentrations of SO_2 (1 ppbv), H_2O_2 (200 pptv) and O_3 (5 ppbv), based on measurements during IMS95 and previously studied SJV fog episodes. For samples taken at the Candelabra Tower, measurements of these gases at 439 m and at the ground were used to construct an assumed linear concentration vs. height profile.

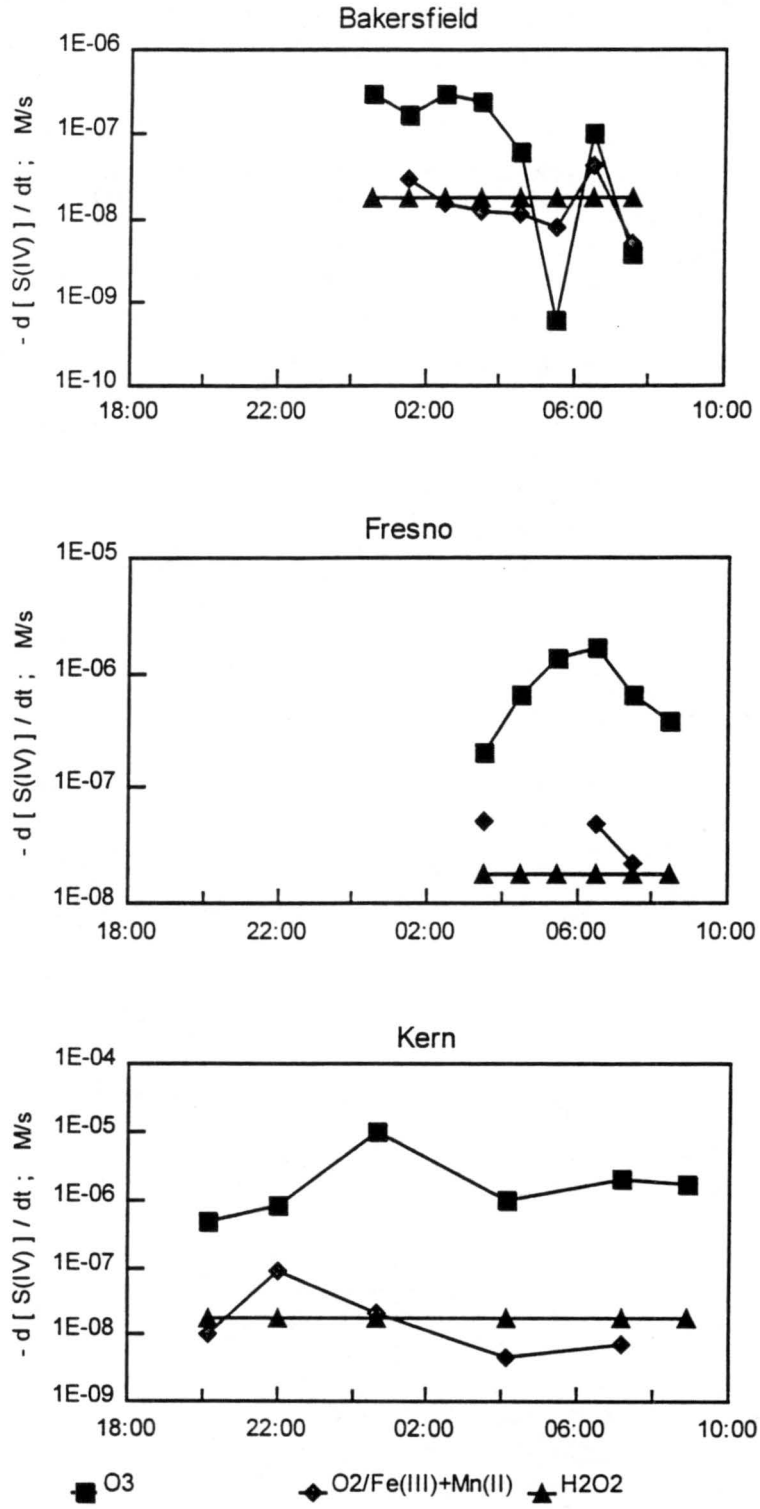

Figure 2-14. Calculated rates of aqueous phase S(IV) oxidation by three main oxidants at the three fog sampling sites in the southern San Joaquin Valley on December 9-10, 1995.

The measured compositions of size-fractionated samples collected using the size-fractionating CASCC at the Kern Wildlife Refuge core site were used to calculate sulfate production occurring in small drops and in large drop fractions. Aqueous S(IV) concentrations and oxidant concentrations used in these calculations were calculated from assumed gaseous concentrations of SO_2 (1 ppbv), H_2O_2 (200 pptv) and O_3 (5 ppbv) as described in the preceding paragraph. The average sulfate production rate in the fog was calculated as a liquid water content weighted average of the small and large drop oxidation rates. This rate was then compared to the sulfate production rate calculated from a liquid water content weighted average drop composition to determine the enhancement in sulfate production resulting from the presence of two chemically distinct droplet populations.

For the ozone pathway, acidity differences between drops enhance sulfate production. For the metal-catalyzed pathway, variations in acidity and catalyst concentrations both change the sulfate production rate, and lead to a more complicated effect. No effect is expected for the peroxide pathway since its oxidation rate is pH independent. Therefore, if the peroxide pathway is not dominant, accurate prediction of sulfate production requires knowledge of chemical differences between drops.

2.3.2 Results and Discussion

Figure 2-14 shows the sulfate production rates calculated for bulk fog samples collected at the three fog collection sites in the southern San Joaquin Valley on the night of December 9-10, 1995. As illustrated in the figure, the ozone pathway rate is typically one to two orders of magnitude faster than the rates of the other two oxidation pathways, despite the very low ozone concentrations typically present at the surface during these stagnation events. Exceptions to this observation occur for two samples collected at Bakersfield on the morning of December 10 when oxidation appears to be dominated by hydrogen peroxide. The change in the dominant oxidation mechanism results from sharp decreases in fogwater pH at these times. The fogwater acidification was accompanied by large increases in fogwater concentrations of S(IV) and sulfate probably resulting from advection of a sulfur rich plume to the site and rapid aqueous phase conversion of S(IV) to sulfuric acid. Clearly our assumption of typical gaseous concentrations is probably inappropriate for these sample periods and needs to be replaced with actual gas concentration measurements to more accurately calculate sulfate production rates.

Vertical profiles of the sulfate production rates were investigated using bulk samples collected at the Candelabra Tower and assumed linear SO_2, H_2O_2 and O_3 concentration profiles constructed from measurements made with continuous monitors at the top and bottom of the tower (see Figure 2-15). The results, presented in Figure 2-16, clearly show that in the fog sampled on January 12, 1996, ozone was the dominant oxidant as the rate of S(IV) oxidation by ozone greatly exceeded rates calculated for the other two pathways.

Figure 2-17 shows time series of vertical profiles of fog pH and the rate of sulfur oxidation by ozone for the morning of January 12. At the beginning of the fog event, the pH is higher at the surface, but, due to the strong increase in ozone with elevation, the sulfate production rate is determined to vary little with elevation. As the fog event continues, the pH increases aloft while

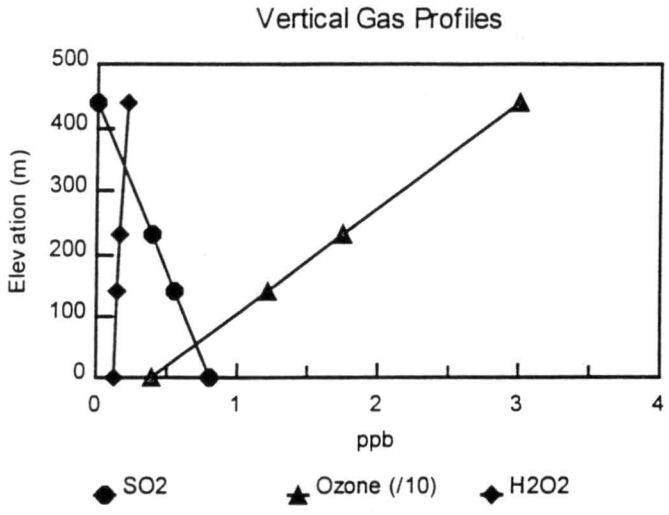

Figure 2-15. Vertical profiles of SO_2, O_3, and H_2O_2 at the Candelabra Tower site on January 12. 1996. The top and bottom points on each curve represent measured concentrations at the top of the tower and at the ground, respectively. Lines are plotted representing linear interpolations between the measured concentrations, with intermediate points on the curves representing the interpolated concentrations corresponding to the heights of the two tower-based fog samplers.

the pH at the ground decreases, yielding a pattern where sulfate production increases strongly with altitude. This strong vertical gradient in sulfate production occurs despite the decrease in gaseous SO_2 with height.

Figure 2-18 depicts the preferential enrichment of accumulation mode aerosol species in small fog drops observed during IMS95. The small drops also were typically more acidic than the large drops. As mentioned above, nonuniform distributions of drop acidity and catalyst concentrations can affect rates of aqueous phase sulfur oxidation. Calculations of the effect of chemical heterogeneity among the sampled fog drop populations on sulfate production suggest sulfur oxidation is probably significantly underestimated when rate calculations are based on average droplet composition. Figure 2-19 shows rates of sulfur oxidation by ozone calculated for the small and large drop fractions sampled at KWR on December 9-10, 1995. Due to the higher pH measured in large drops, sulfate production occurs much more rapidly in large drops than in small drops. Also presented in the figure is the liquid water content weighted average oxidation rate in the fog. Since most of the liquid water was contained in the large drop fraction, the average oxidation rate in the fog closely approximates the large drop oxidation rate. Contrast this result with the calculated "bulk" fog oxidation rate, representing the oxidation rate calculated using the average drop composition, which is several times slower.

Figure 2-20 presents the pH difference measured between the large and small fog drop fractions along with the oxidation rate enhancement factors, resulting from the measured differences between small and large drop compositions, for the three oxidation pathways as well as the sum of these three pathways. The greatest enhancement was calculated to occur for the ozone pathway, with smaller enhancement expected for the metal catalyzed pathway during this period.

No oxidation rate enhancement results for the peroxide pathway, since its rate is independent of pH. Due to the dominant role of ozone as an oxidant in this event, the enhancement in the total oxidation rate closely parallels that calculated for the ozone pathway, with calculated enhancements ranging from factors of one to eight. The calculated enhancement of sulfate production due to chemical variations among droplets, large as it is, really represents a lower

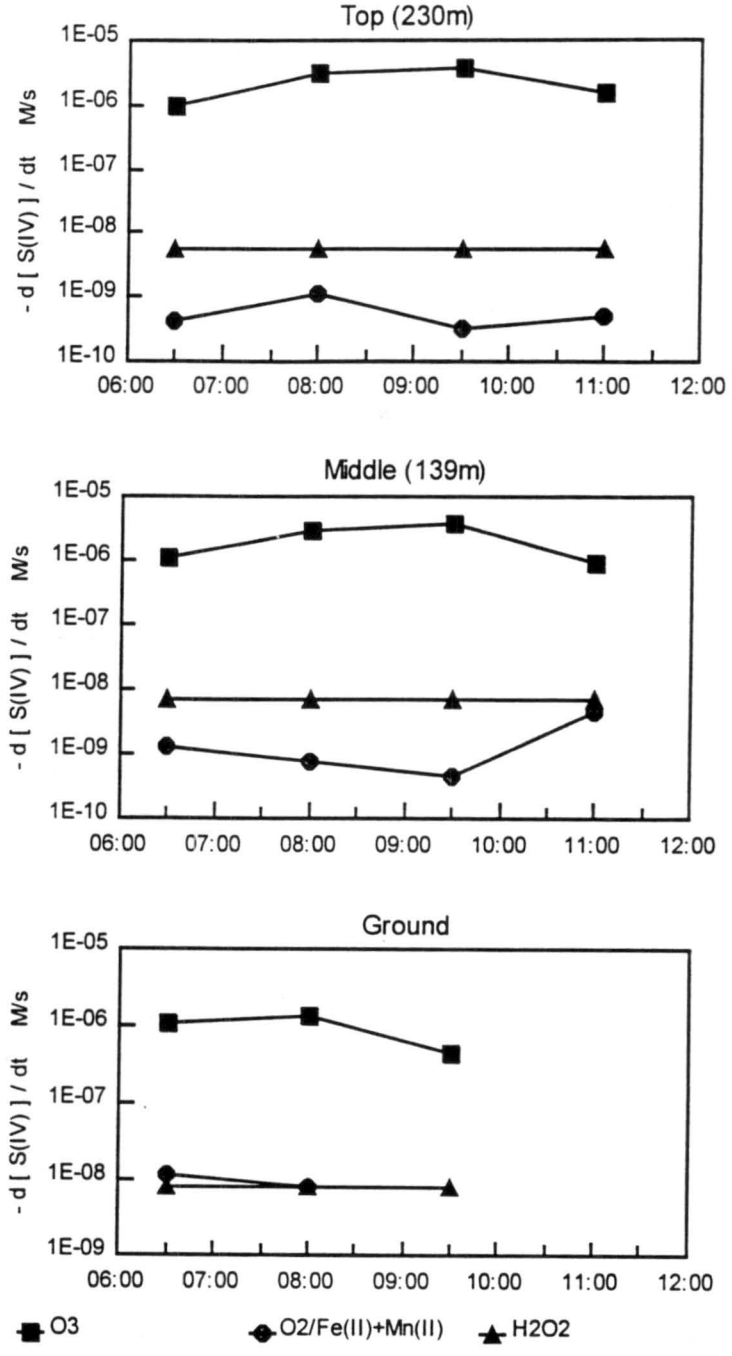

Figure 2-16. Calculated aqueous phase sulfate production rates at the three fog sampling levels at the Candelabra Tower on January 12, 1996.

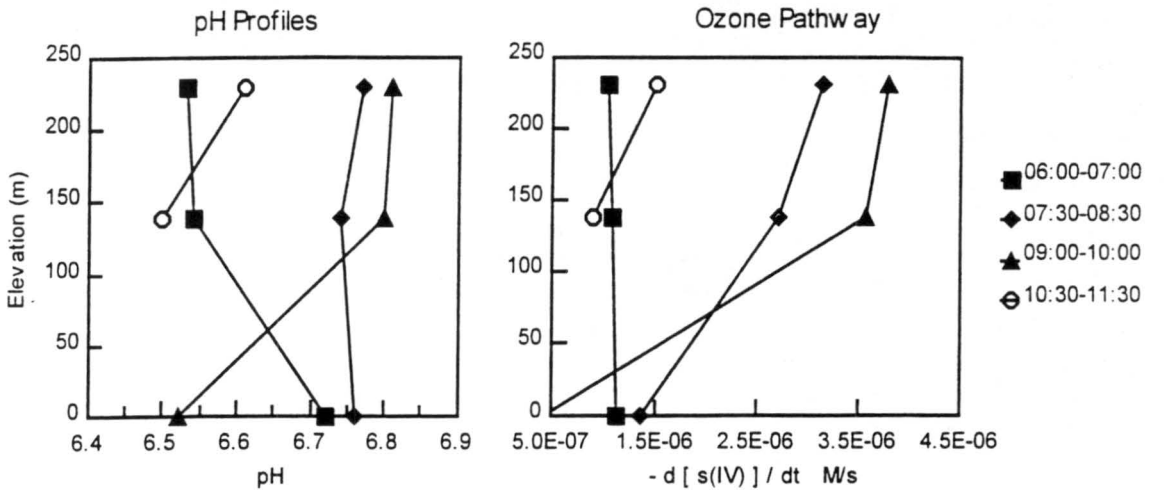

Figure 2-17. A time series of the measured vertical pH profile and the calculated vertical rate profile of aqueous S(IV) oxidation by ozone on January 12, 1996 at the Candelabra Tower.

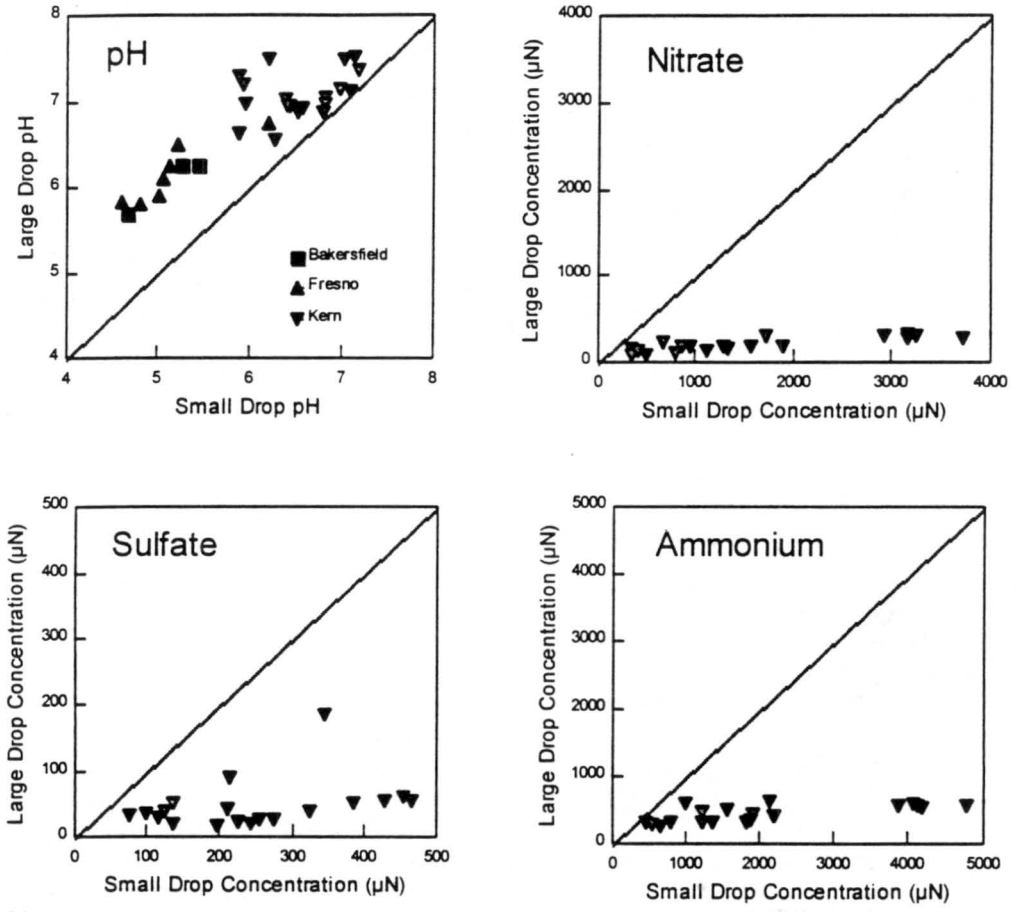

Figure 2-18. Small and large fog drop concentrations of major ions and pH. Ion concentrations and pH were measured in sf-CASCC samples at the Kern Wildlife Refuge core site, while pH was measured in ETH impactor samples at Bakersfield and Fresno.

bound on this effect. There are certainly many more than two independent drop compositions present within the cloud. The more heterogeneity that is present, the greater the enhancement of sulfur oxidation by ozone will be.

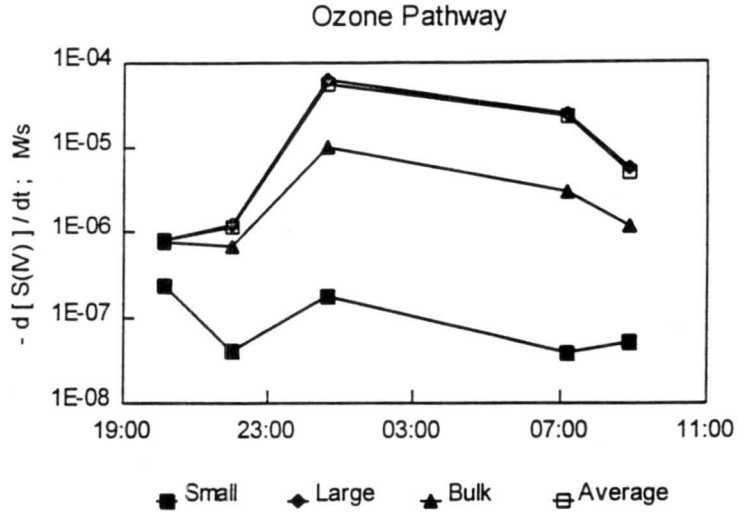

Figure 2-19. A comparison of rates of aqueous phase S(IV) oxidation by ozone at the Kern Wildlife Refuge site on December 9-10, 1995. Shown are calculated values for sulfate production rates using bulk sample pH, small drop pH, large drop pH, and a volume weighted average pH from large and small $[H^+]$. Samples were collected with a sf-CASCC.

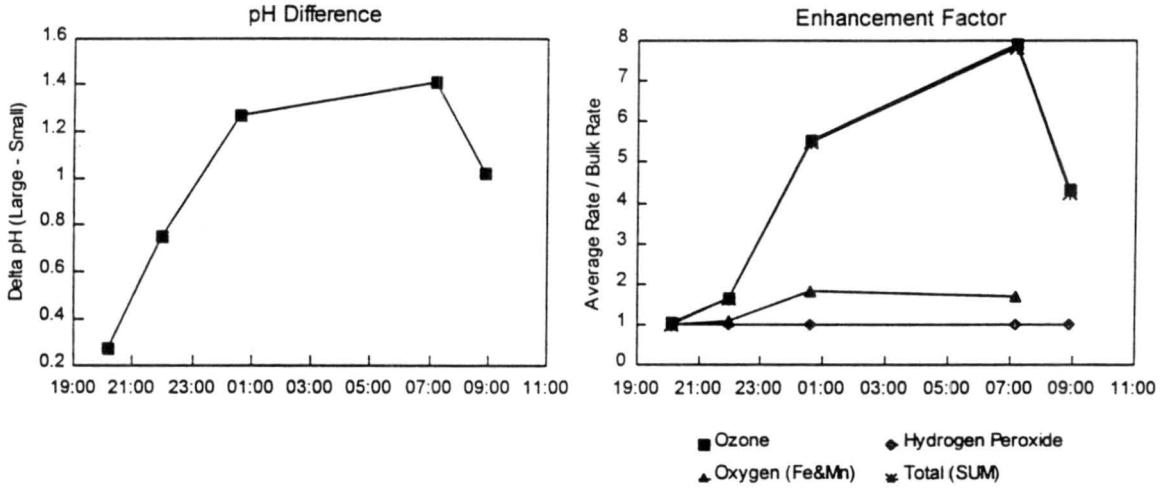

Figure 2-20. A time series of the difference in pH between the large and small drop fractions and the amount heterogeneous drop chemistry (based on differences in small and large drop pH and metal catalyst concentrations) enhances sulfate production relative to the rates expected from the average drop composition. Samples were collected with the sf-CASCC at the Kern Wildlife Refuge site on December 9-10, 1995.

2.3.3 Summary

These preliminary calculations, analyzing a portion of the IMS95 fog data set, suggest that ozone is typically the dominant oxidant for aqueous phase sulfate production in the region. Significant variations in sulfate production rates were found to occur as a function of altitude and as a function of drop size. In the cases studied, sulfate production was at times observed to increase strongly with altitude above the surface and with drop size. Due to the nonlinear nature of the relevant oxidation rate laws, use of average droplet composition to predict sulfur oxidation rates was found to cause significant underprediction of aqueous phase sulfate production in SJV fogs. Further work is needed to consider additional fog episodes not yet examined and to refine estimates made here by including measured gas concentrations. There is also a need to consider in some detail the complexation of aqueous S(IV) by formaldehyde and its effect on sulfate production in the region.

3. Summary

During IMS95 Colorado State University successfully sampled fog and low clouds at four locations in the San Joaquin Valley. Quality control and quality assurance checks indicate that high quality samples were collected and analyzed accurately and precisely. Databases containing fog data from the study have been submitted to the California Air Resources Board.

A preliminary analysis of the fog data reveals the following key findings:

- Fog sampled at all sites during the study was alkaline, with pH values generally above 6.
- The high pH promotes rapid oxidation of aqueous S(IV) by ozone as well as rapid formation of aqueous aldehyde-S(IV) complexes. Peroxide concentrations were typically too low to make S(IV) oxidation by peroxides competitive with oxidation by ozone in the alkaline conditions encountered.
- Significant vertical variations were observed in fog/cloud liquid water content and chemical composition. These vertical gradients, coupled with measured vertical gradients in oxidant concentrations, are capable of producing substantial vertical variations in aqueous phase aerosol formation rates.
- The chemical composition of large and small fog drops was observed to differ significantly. Small drops were typically enriched in accumulation mode aerosol species, relative to large drops. Small drops also were found to be more acidic, with differences at times exceeding one pH unit. The observed variations in drop composition across the fog drop size spectrum are capable of significantly affecting aqueous phase aerosol formation processes and may also alter rates of deposition.

Additional work is planned to consider the implications of the fog observations upon aerosol processing during winter stagnation episodes in more detail. Part of this work will take the form of numerical modeling of fog physics and chemistry, led by Spyros Pandis of Carnegie Mellon University. The combined approach of modeling and comprehensive fog chemistry

measurements will provide new insight into the relative importance of aerosol formation and removal during winter fog episodes.

4. Acknowledgements

We are grateful to O. Graf and X. Rao for assistance during the field campaign. E. Andrews and S. M. Cox are gratefully acknowledged for assistance with chemical analysis of collected samples. L. W. Richards is gratefully acknowledged for his assistance arranging operations at the Candelabra Tower Site. The assistance of both L. W. Richards and S. Pandis in planning the tower study is acknowledged. We are grateful to Transtower, Inc. for providing access to the Candelabra Tower. P. Solomon and K. Magliano are gratefully acknowledged for their instrumental roles in arranging infrastructure for sampling at the three IMS 95 core sites and coordinating the measurement program. Funding for this work was provided by the San Joaquin Valleywide Air Pollution Study Agency. The statements and conclusions in this report are those of the Contractor and not necessarily those of the California Air Resources Board, the San Joaquin Valleywide Air Pollution Study Agency, or its Policy Committee, their employees or their members. The mention of commercial products, their source, or their use in connection with material reported herein is not to be construed as actual or implied endorsement of such products.

5. References

Calame, L., Gang, X., Hand, J., Hoag, K., Moore, K., Sherman, D. and Straub, D. (1997) Aerosol Characterization: A Limited Study in Fort Collins, Colorado, AT680 Final Report, Department of Atmospheric Science, Colorado State University, Fort Collins, Colorado.

Collett, Jr., J., Oberholzer, B. and Staehelin, J. (1993) Cloud chemistry at Mt. Rigi Switzerland: Dependence on drop size and relationship to precipitation chemistry. *Atmos. Environ.* **27A**, 33-42.

Collett, Jr., J. L., Bator, A., Rao, X. and Demoz, B. (1994) Acidity variations across the cloud drop size spectrum and their influence on rates of atmospheric sulfate production. *Geophys. Res. Lett.* **21**, 2393-2396.

Collett, Jr., J., Iovinelli, R. and Demoz, B. (1995) A three-stage cloud impactor for size-resolved measurements of cloud drop chemistry. *Atmos. Environ.* **29**, 1145-1154.

Demoz, B., Collett, Jr., J. L. and Daube, Jr., B. C. (1996) On the Caltech Active Strand Cloudwater Collectors. *Atmos. Res.* **41**, 47-62.

Hegg, D. A. and Larson, T. V. Tellus 1990 42B, 272-284.

Hoffmann, M. R. (1986) On the kinetics and mechanism of oxidation of aquated sulfur dioxide by ozone. *Atmos. Environ.* **20**, 1145-1154.

Hoffmann, M. R., Collett, Jr., J. L., and Daube, Jr., B. C. (1989) Characterization of cloud chemistry and frequency of canopy exposure to clouds in the Sierra Nevada. Final report prepared for the California Air Resources Board, Sacramento, CA.

Holets, S. and Swanson, R. N. (1981) High-inversion fog episodes in central California. *J. Appl. Meteor.* **20**, 890-899.

Ibusuki, T. and Takeuchi, K. (1987) Sulfur dioxide oxidation by oxygen catalyzed by mixtures of manganese (II) and iron (III) in aqueous solutions at environmental reaction conditions. *Atmos. Environ.* **21**, 1555-1560.

Jacob, D. J., Munger, J. W., Waldman, J. M. and Hoffmann, M. R. (1986) The H_2SO_4-HNO_3-NH_3 system at high humidities and in fogs. 1. Spatial and temporal patterns in the San Joaquin Valley of California. *J. Geophys. Res.* **91**, 1073-1088.

Jacob, D. J., Shair, F. H., Waldman, J. M., Munger, J. W. and Hoffmann, M. R. (1987) Transport and oxidation of SO_2 in a stagnant foggy valley. *Atmos. Env.* **21**, 1305-1314.

Jacob, D. J., Gottlieb, E. W. and Prather, M. J. (1989) Chemistry of a polluted cloudy boundary layer. *J. Geophys. Res.* **94**, 12975-13002.

Munger, J. W., Collett, Jr., J., Daube, Jr., B. and Hoffmann, M. R. (1989) Chemical composition of coastal stratus clouds: dependence on droplet size and distance from the coast. *Atmos. Environ.* **23**, 2305-2320.

Oberholzer, B. (1992) Untersuchungen ueber den einfluss von anorganischen Spurenstoffen auf die zusammensetzung des Niederschlages waehrend winterlichen Feldmessungen an der Rigi (Zentralschweiz), Dissertation No. 9854, Swiss Federal Institute of Technology, Zurich, Switzerland.

Possanzini, M., Febo, A. and Liberti, A. (1983) New design of a high-performance denuder for the sampling of atmospheric pollutants. *Atmos. Environ.* **17**, 2605-2610.

Pandis, S. N. and Seinfeld, J. H. (1989) Mathematical modeling of acid deposition due to radiation fog. *J. Geophys. Res.* **94**, 12911-12923.

Rao, X. and Collett, Jr., J. L. (1995) The behavior of S(IV) and formaldehyde in a chemically heterogeneous cloud. *Environ. Sci. Tech.* **29**, 1023-1031.

Seinfeld, J. H. (1986) *Atmospheric Chemistry and Physics of Air Pollution.* Wiley, New York.

Solomon, P.A., Thuillier, R. H., Magliano, K., et al. (1996) 1995 Integrated Monitoring Study: Study objectives and design, in *Proceedings of the 1996 A&WMA/U.S. EPA Symposium on Measurement of Toxic and Related Air Pollutants*, Air and Waste Management Association, Pittsburgh, Pennsylvania.

Waldman, J. M. and Hoffmann, M. R. (1987) Sources and Fates of Aquatic Pollutants, in ACS Advances in Chemistry Series No. 216, R. A. Hites and S. J. Eisenreich Eds.; American Chemical Society, New York, pp. 79-129.

Walke, E. (1994) A Study of the ETH Annular Denuder System. Senior Report, Department of Chemical Engineering, University of Illinois, Urbana, Illinois.

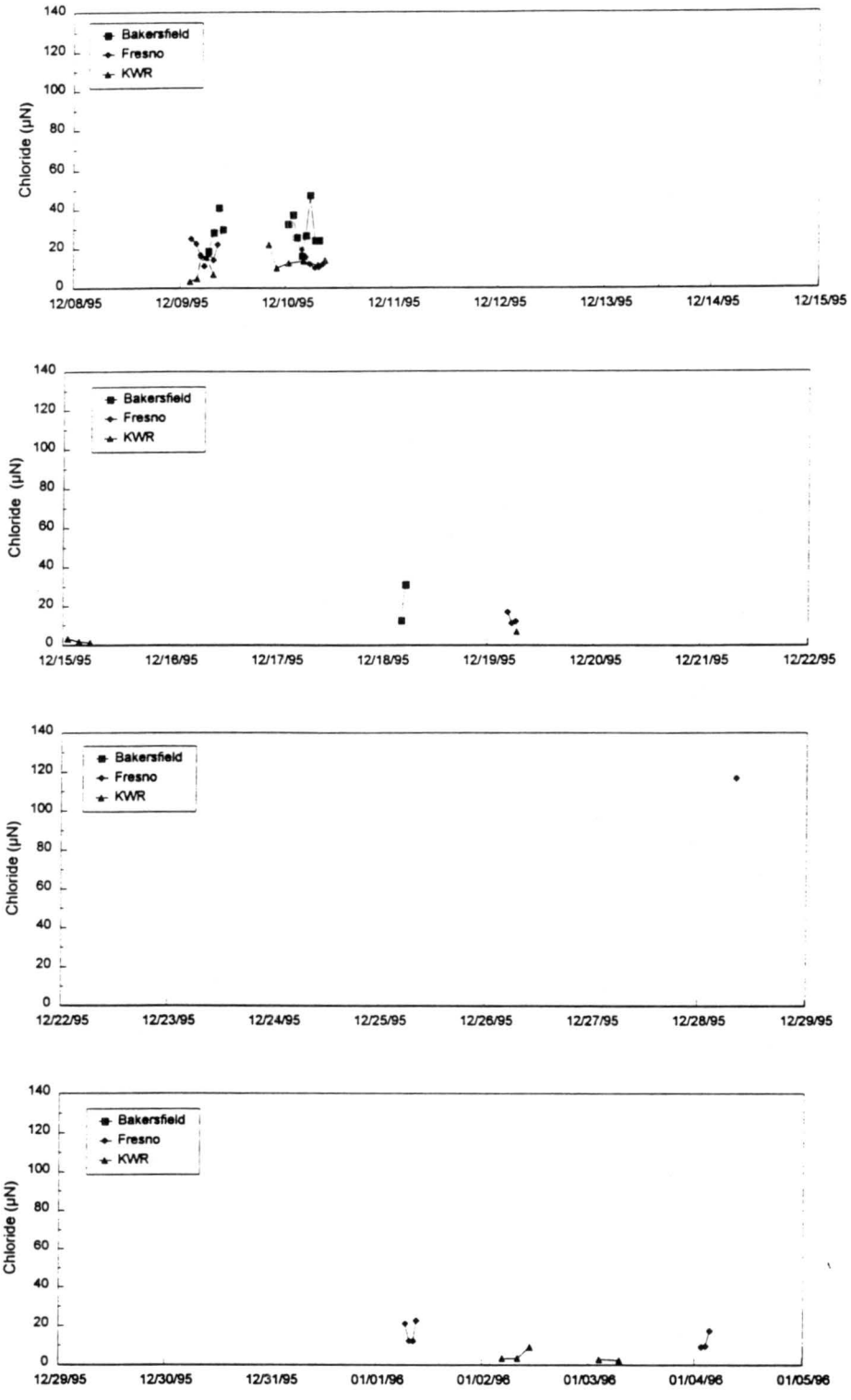

Figure A-1. Chloride concentrations measured in bulk fog samples collected with the CASCC2 collectors at the three IMS95 core sites.

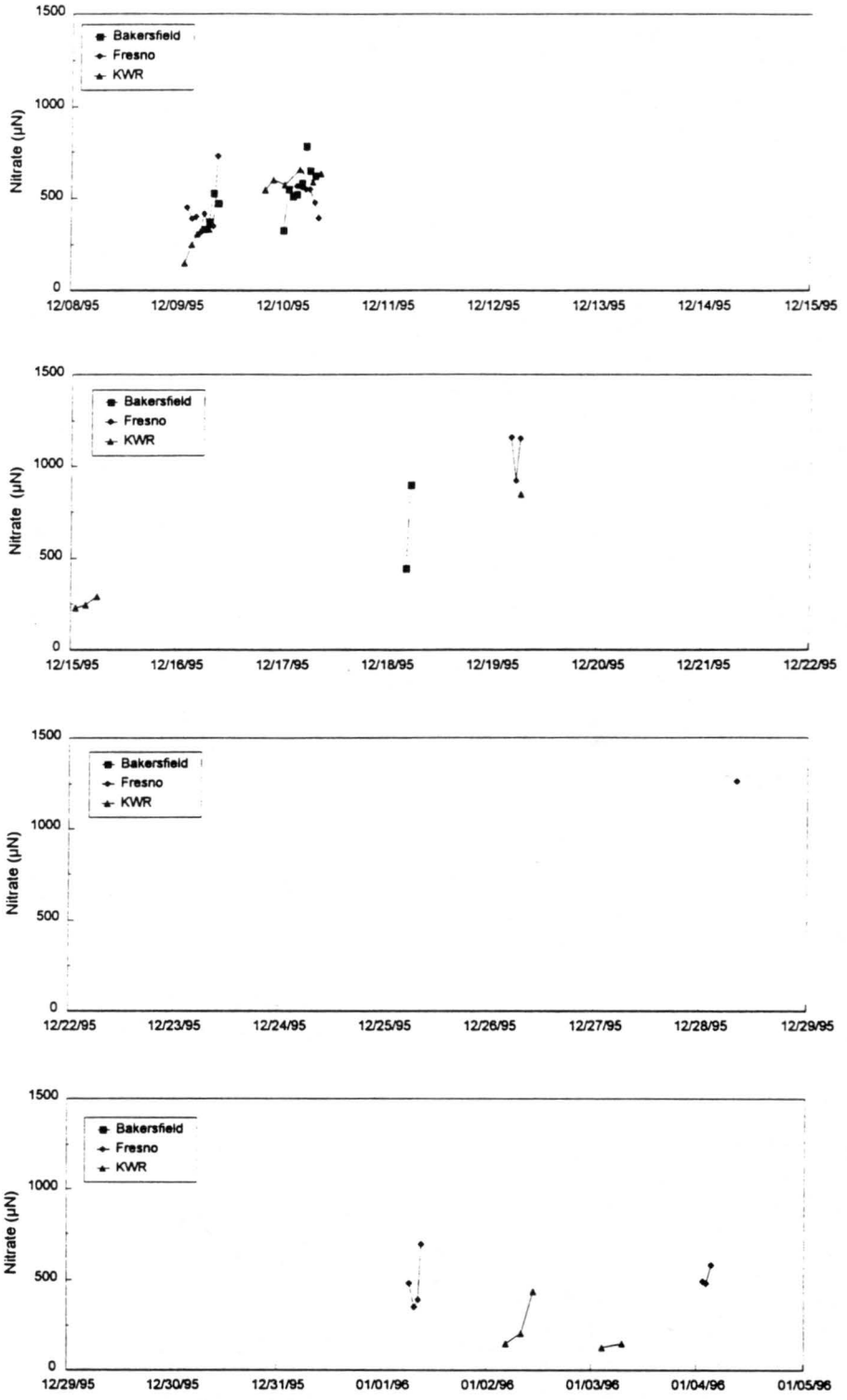

Figure A-2. Nitrate concentrations measured in bulk fog samples collected with the CASCC2 collectors at the three IMS95 core sites.

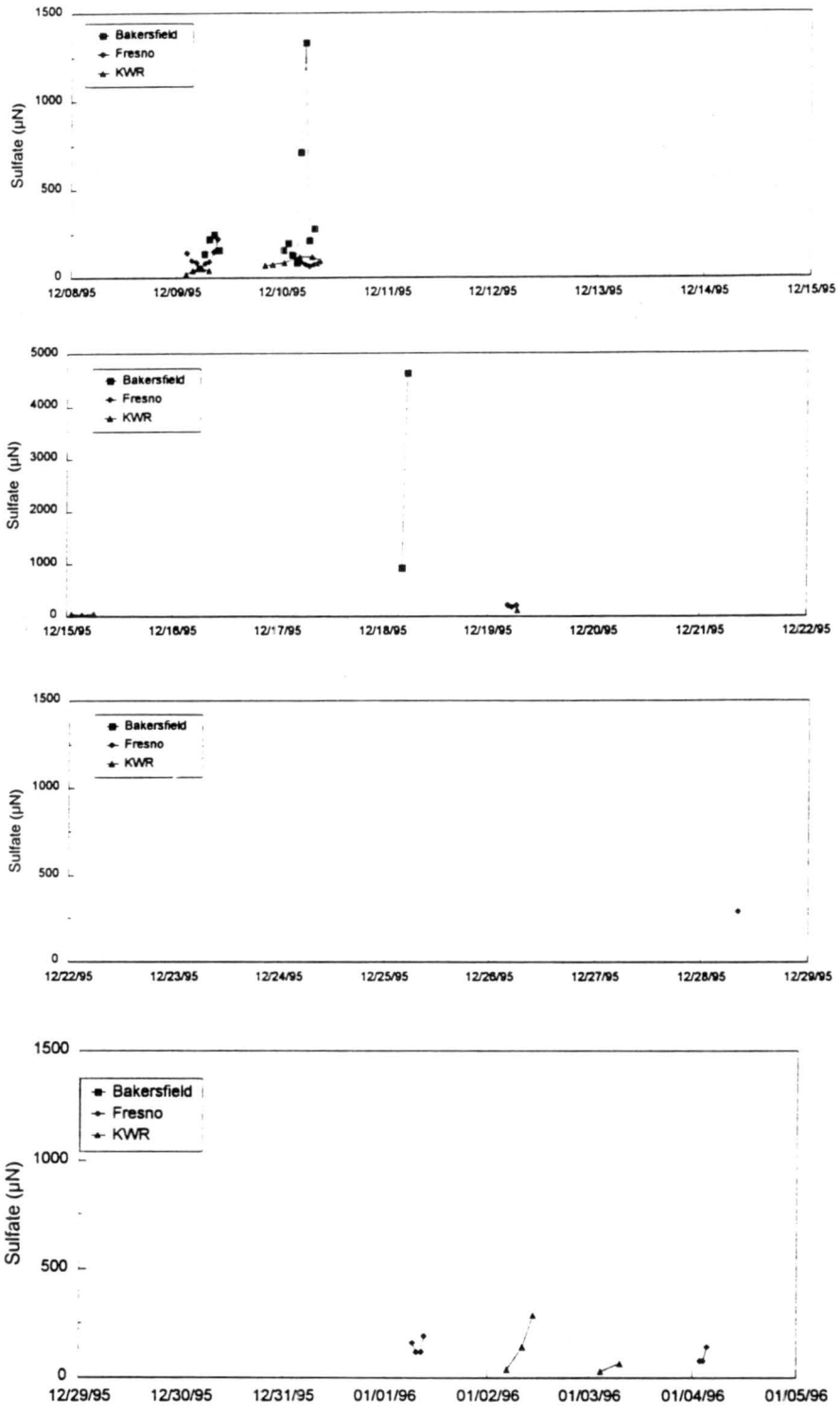

Figure A-3. Sulfate concentrations measured in bulk fog samples collected with the CASCC2 collectors at the three IMS95 core sites.

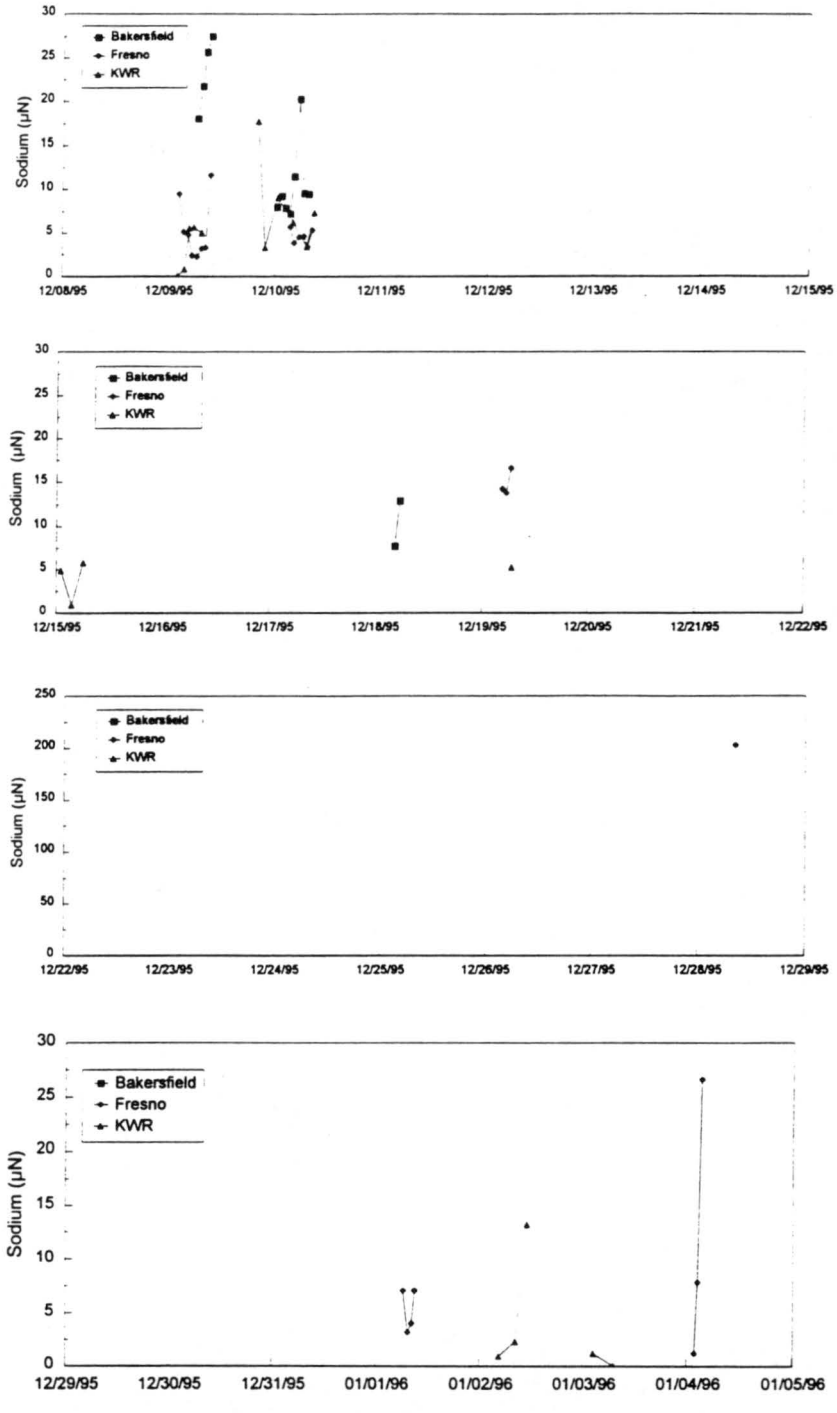

Figure A-4. Sodium concentrations measured in bulk fog samples collected with the CASCC2 collectors at the three IMS95 core sites.

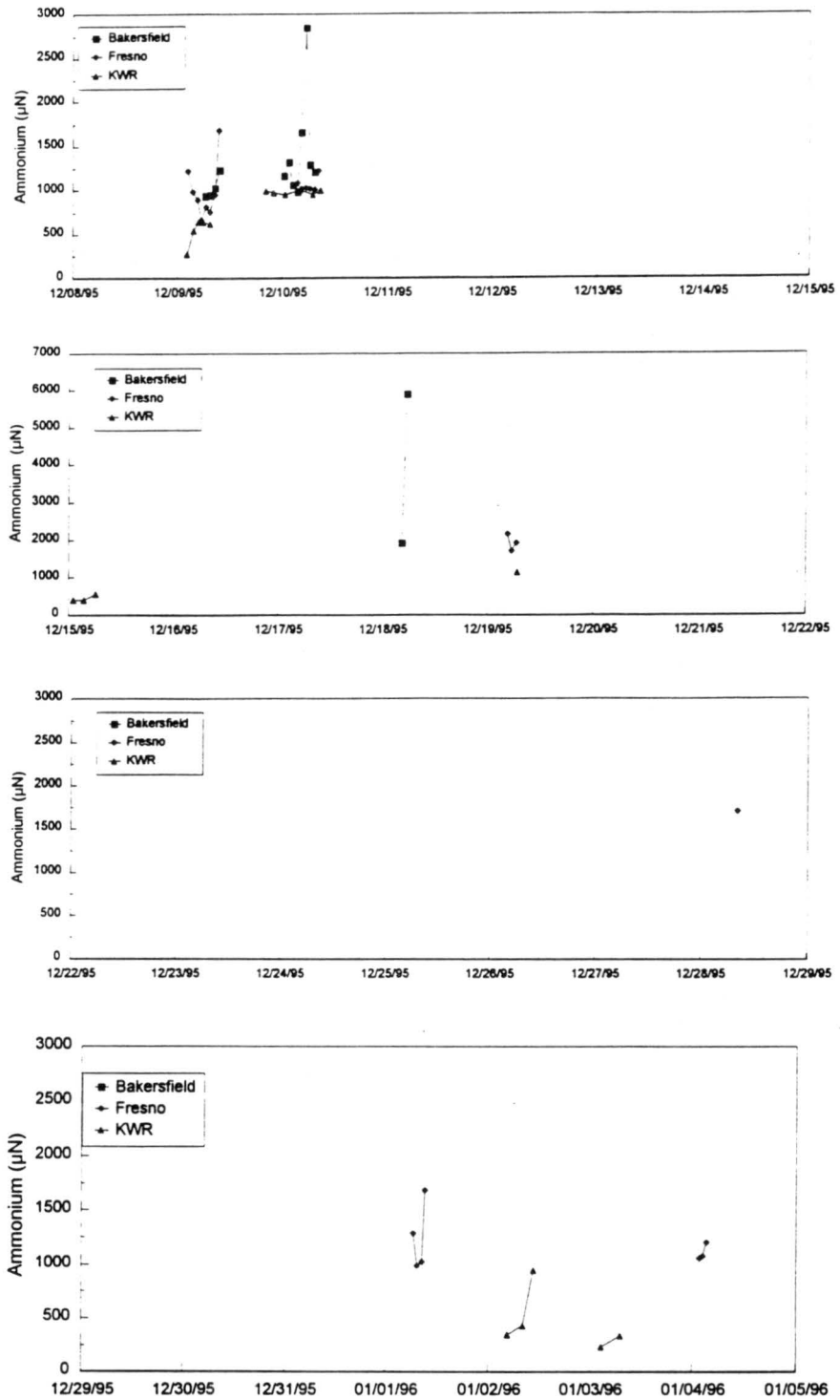

Figure A-5. Ammonium concentrations measured in bulk fog samples collected with the CASCC2 collectors at the three IMS95 core sites.

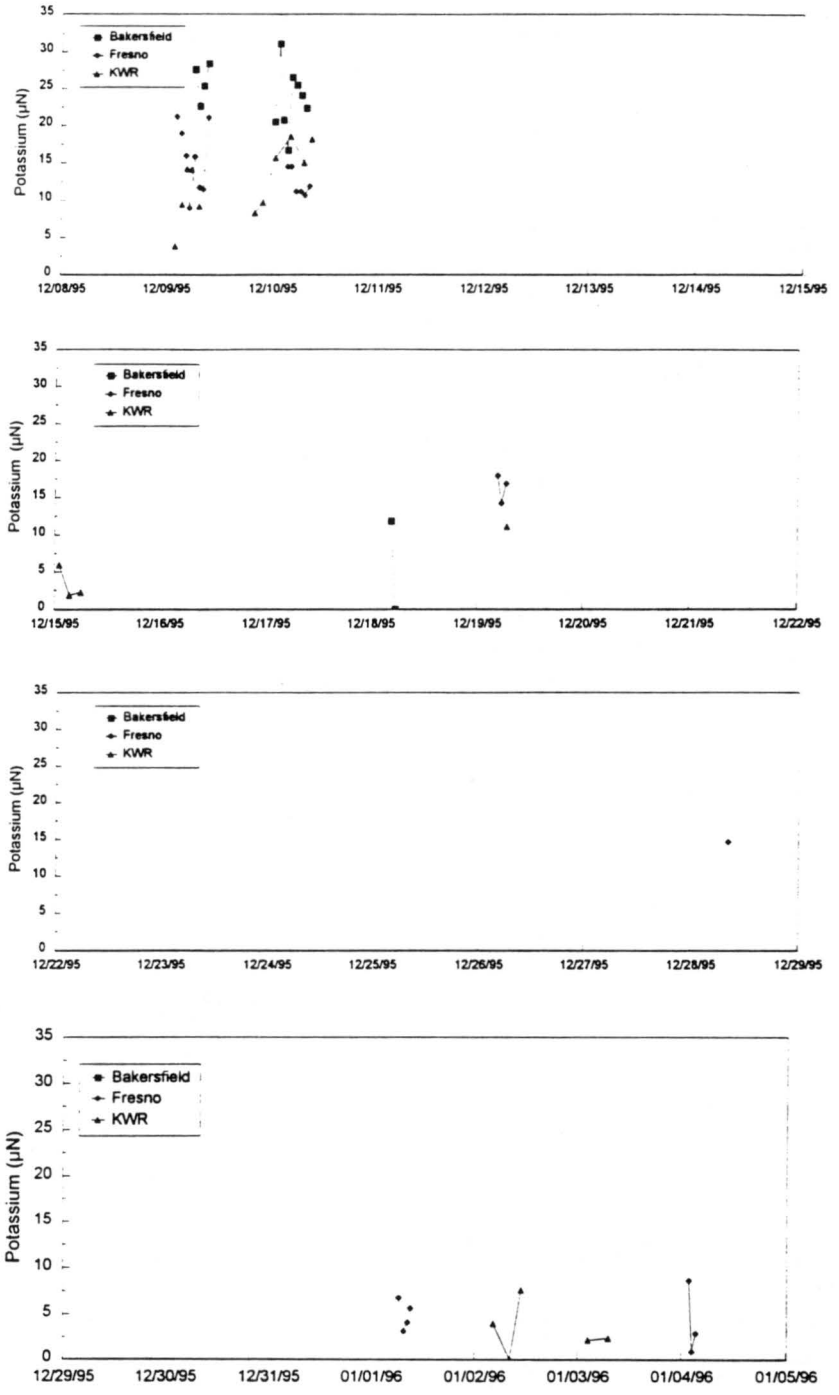

Figure A-6. Potassium concentrations measured in bulk fog samples collected with the CASCC2 collectors at the three IMS95 core sites.

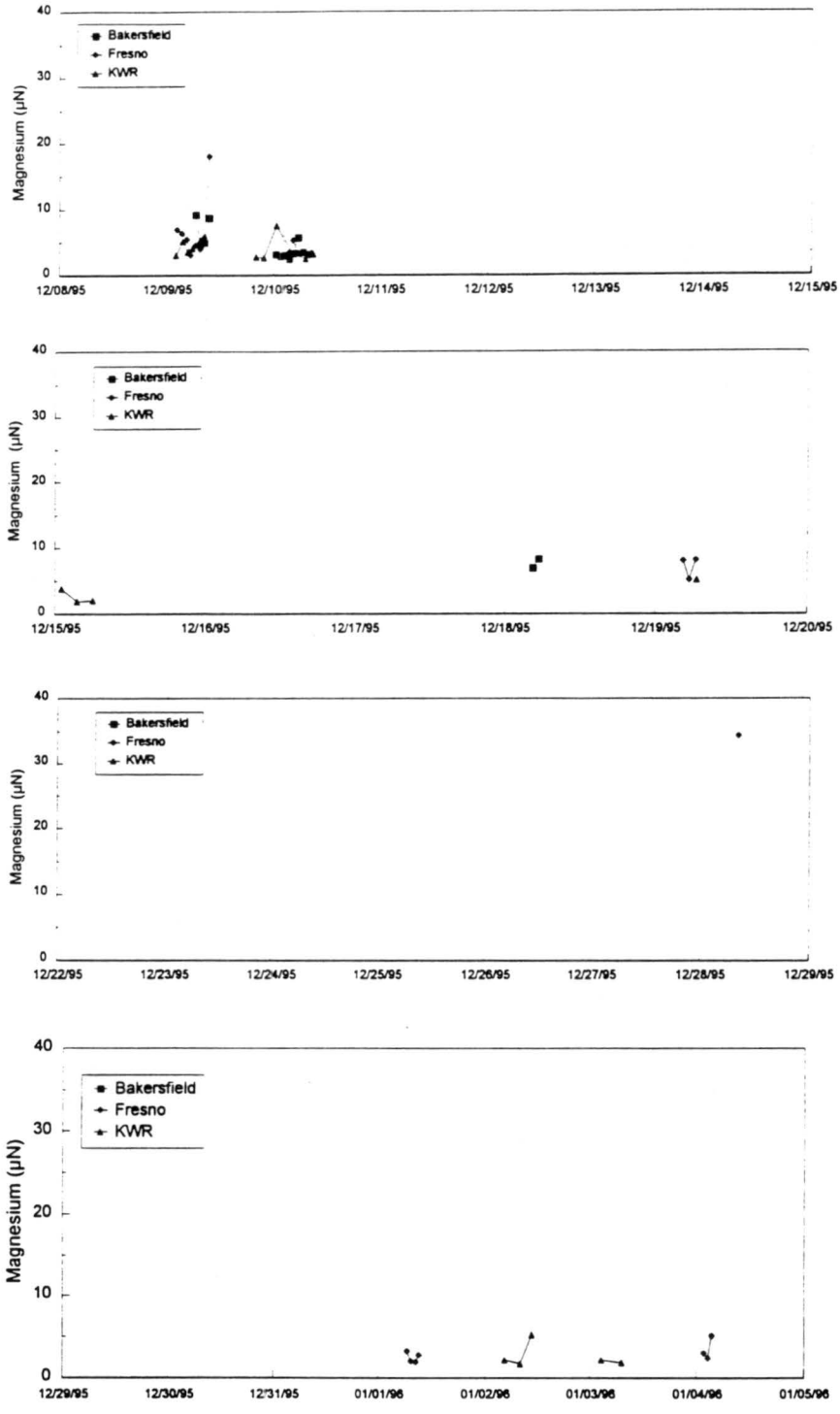

Figure A-7. Magnesium concentrations measured in bulk fog samples collected with the CASCC2 collectors at the three IMS95 core sites.

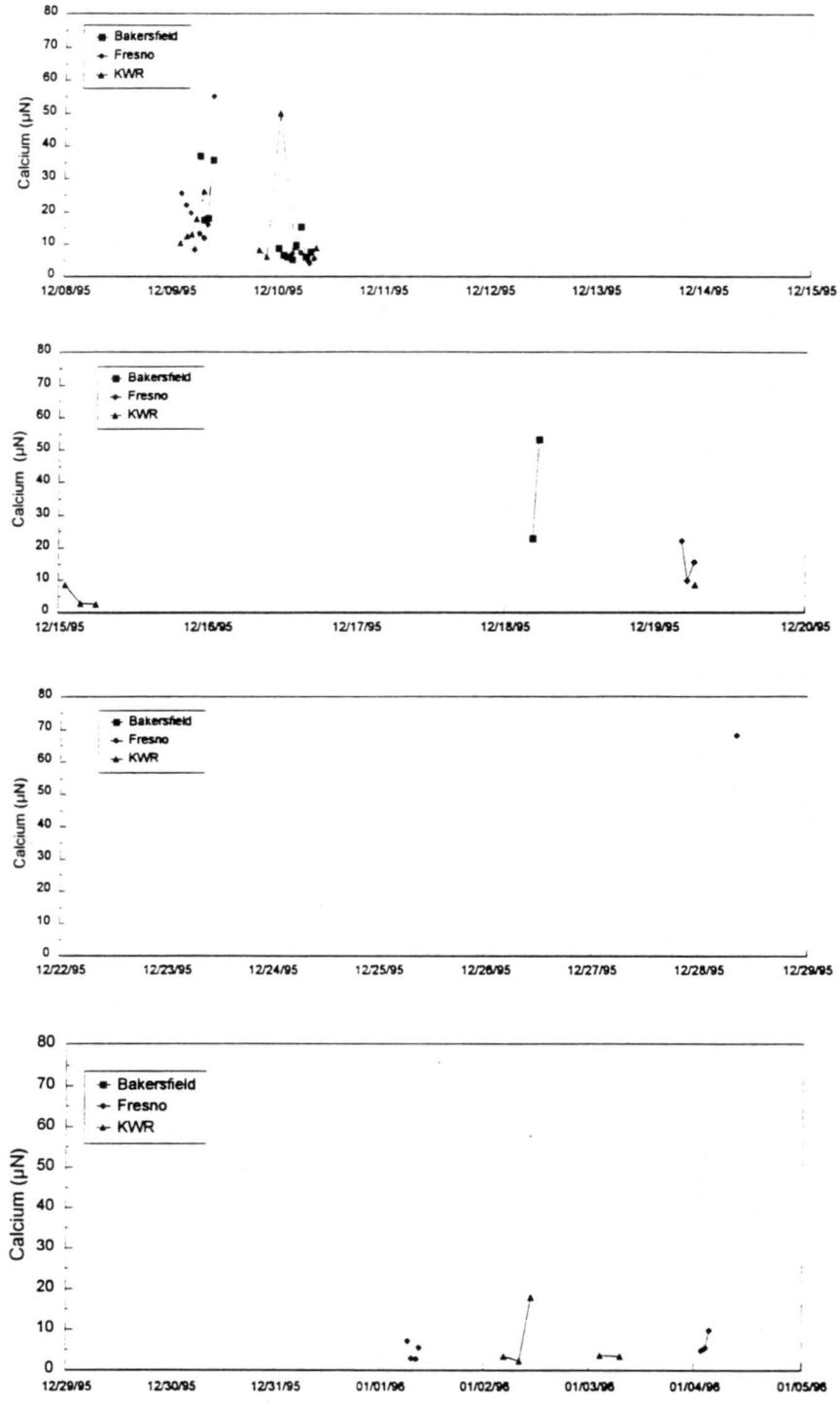

Figure A-8. Calcium concentrations measured in bulk fog samples collected with the CASCC2 collectors at the three IMS95 core sites.

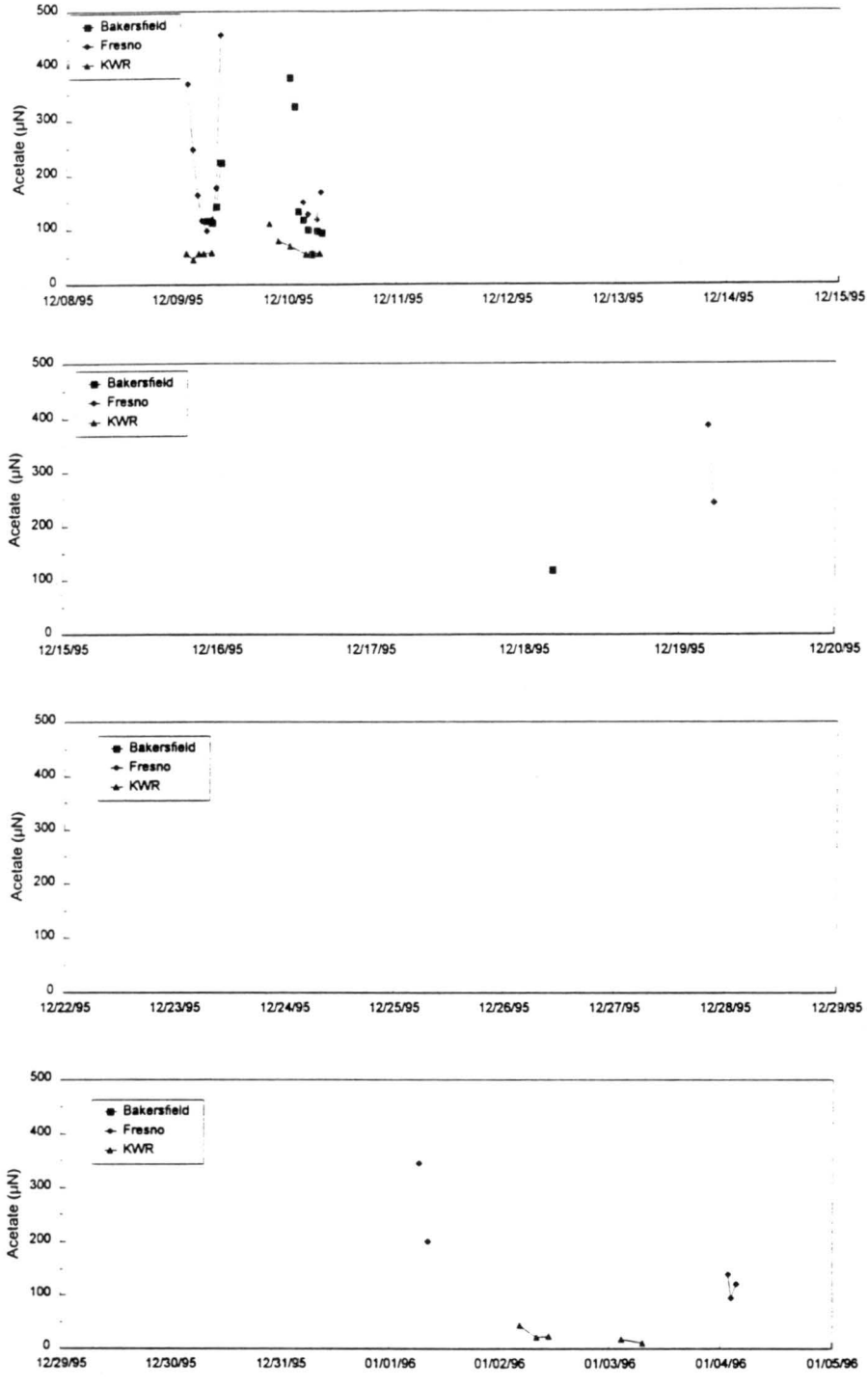

Figure A-9. Acetate concentrations measured in bulk fog samples collected with the CASCC2 collectors at the three IMS95 core sites.

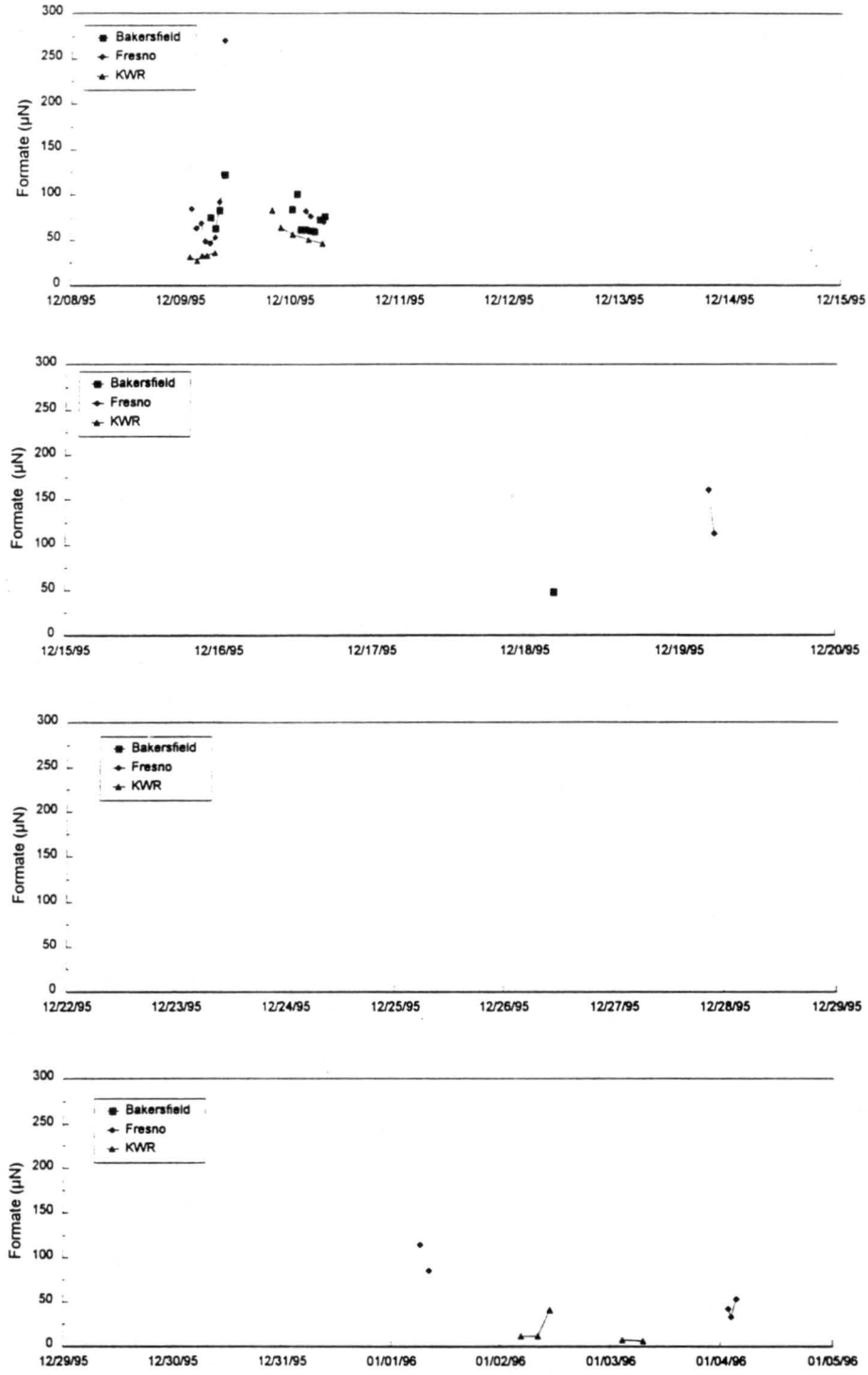

Figure A-10. Formate concentrations measured in bulk fog samples collected with the CASCC2 collectors at the three IMS95 core sites.

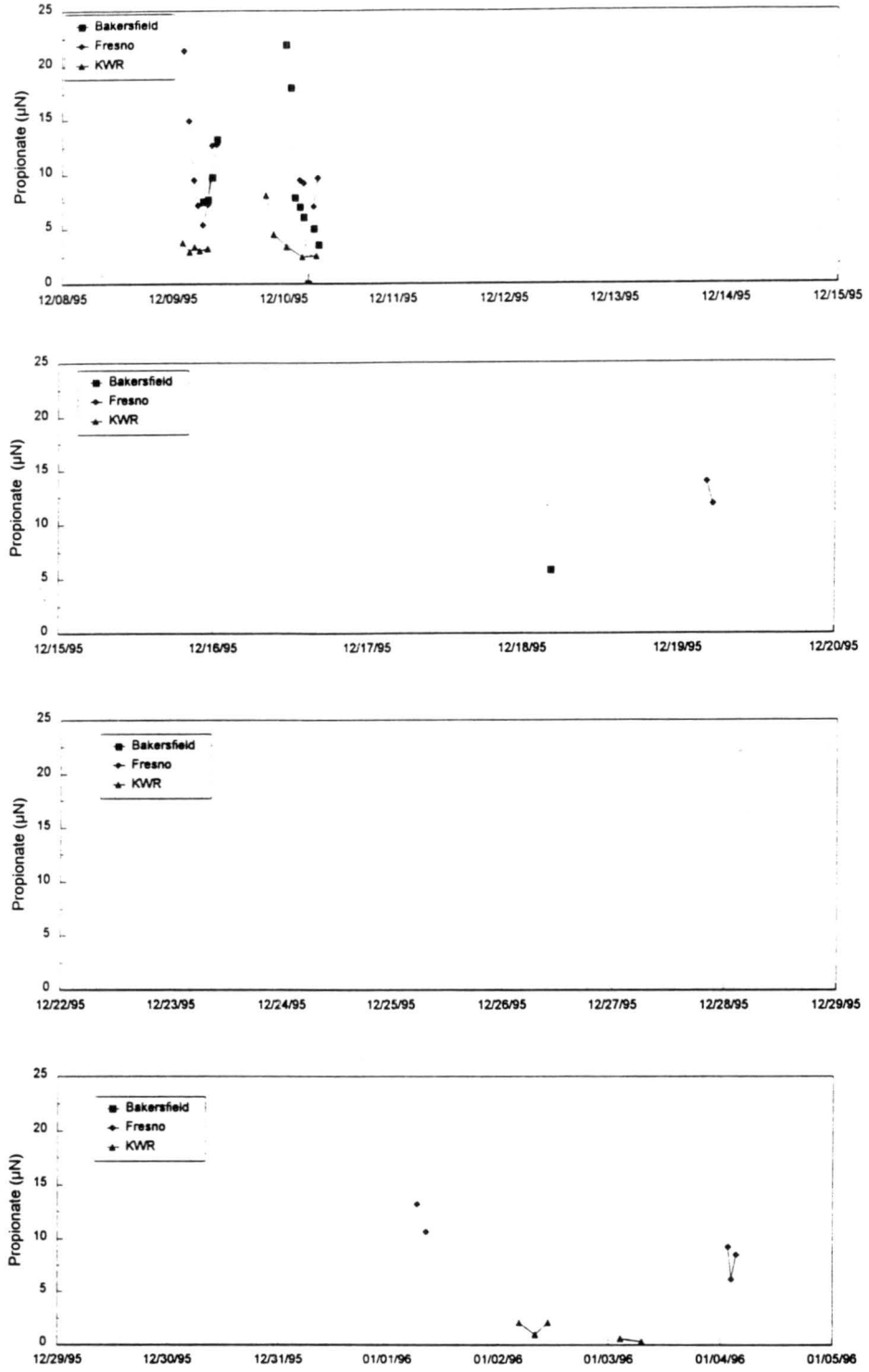

Figure A-11. Propionate concentrations measured in bulk fog samples collected with the CASCC2 collectors at the three IMS95 core sites.

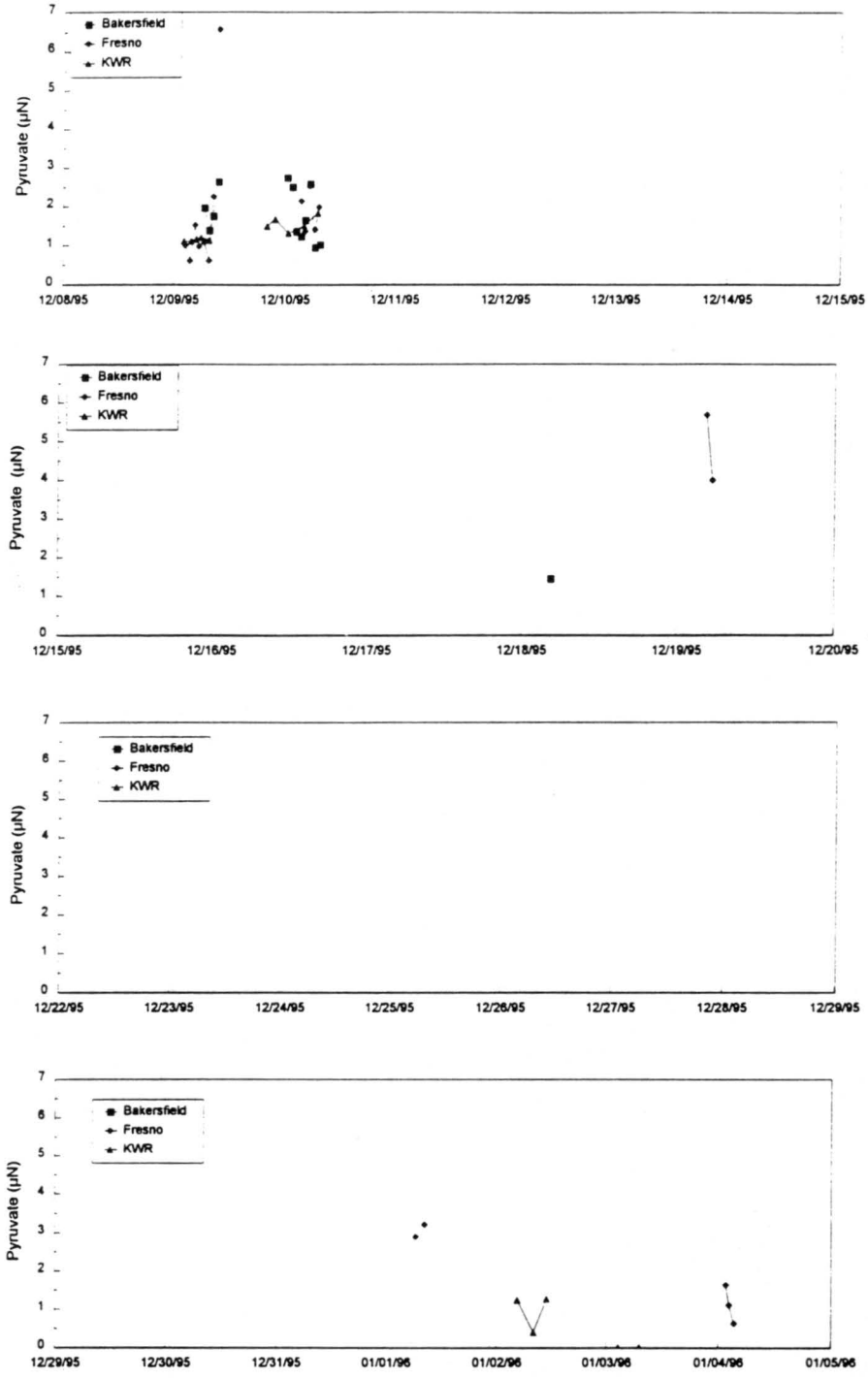

Figure A-12. Pyruvate concentrations measured in bulk fog samples collected with the CASCC2 collectors at the three IMS95 core sites.

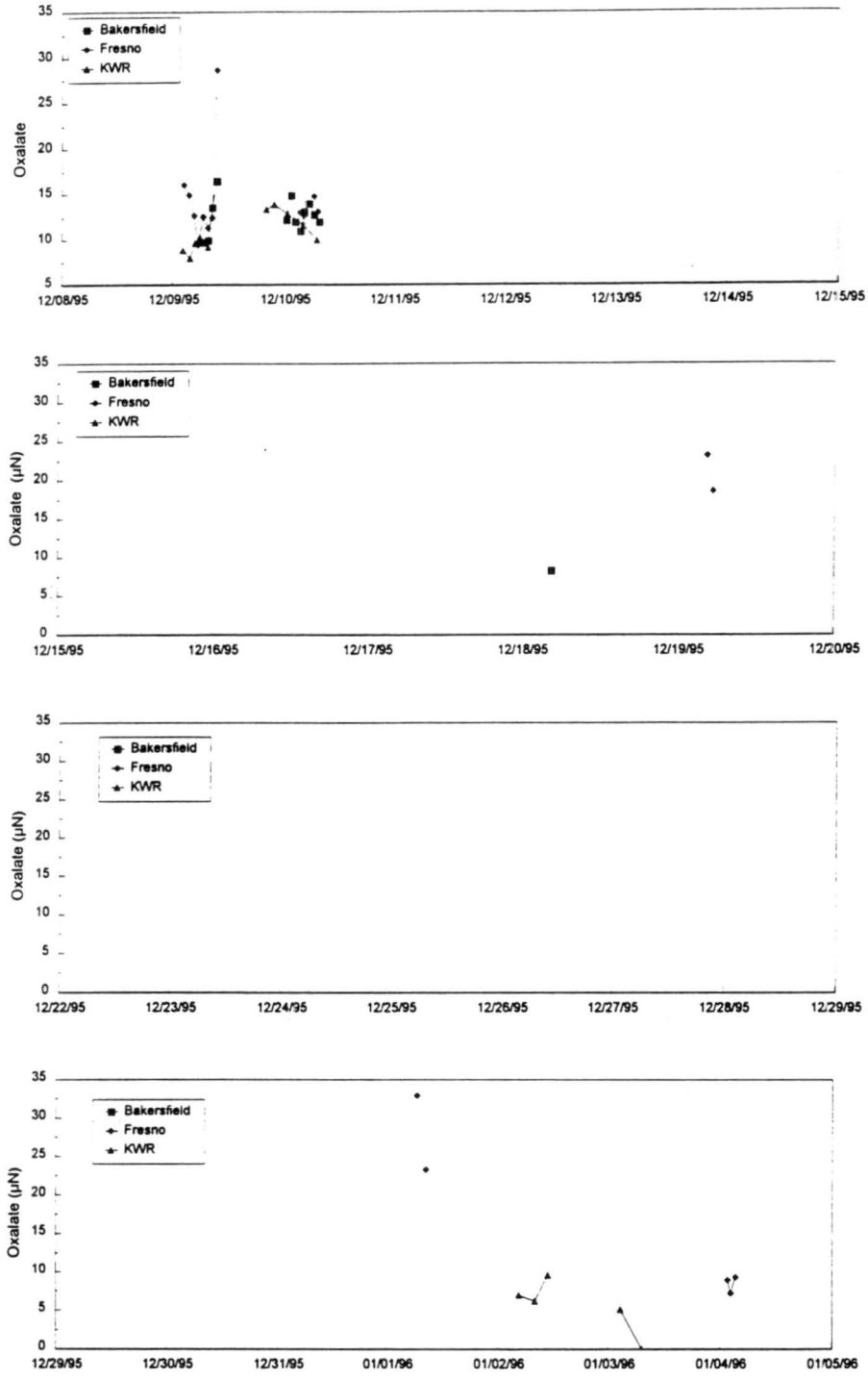

Figure A-13. Oxalate concentrations measured in bulk fog samples collected with the CASCC2 collectors at the three IMS95 core sites.

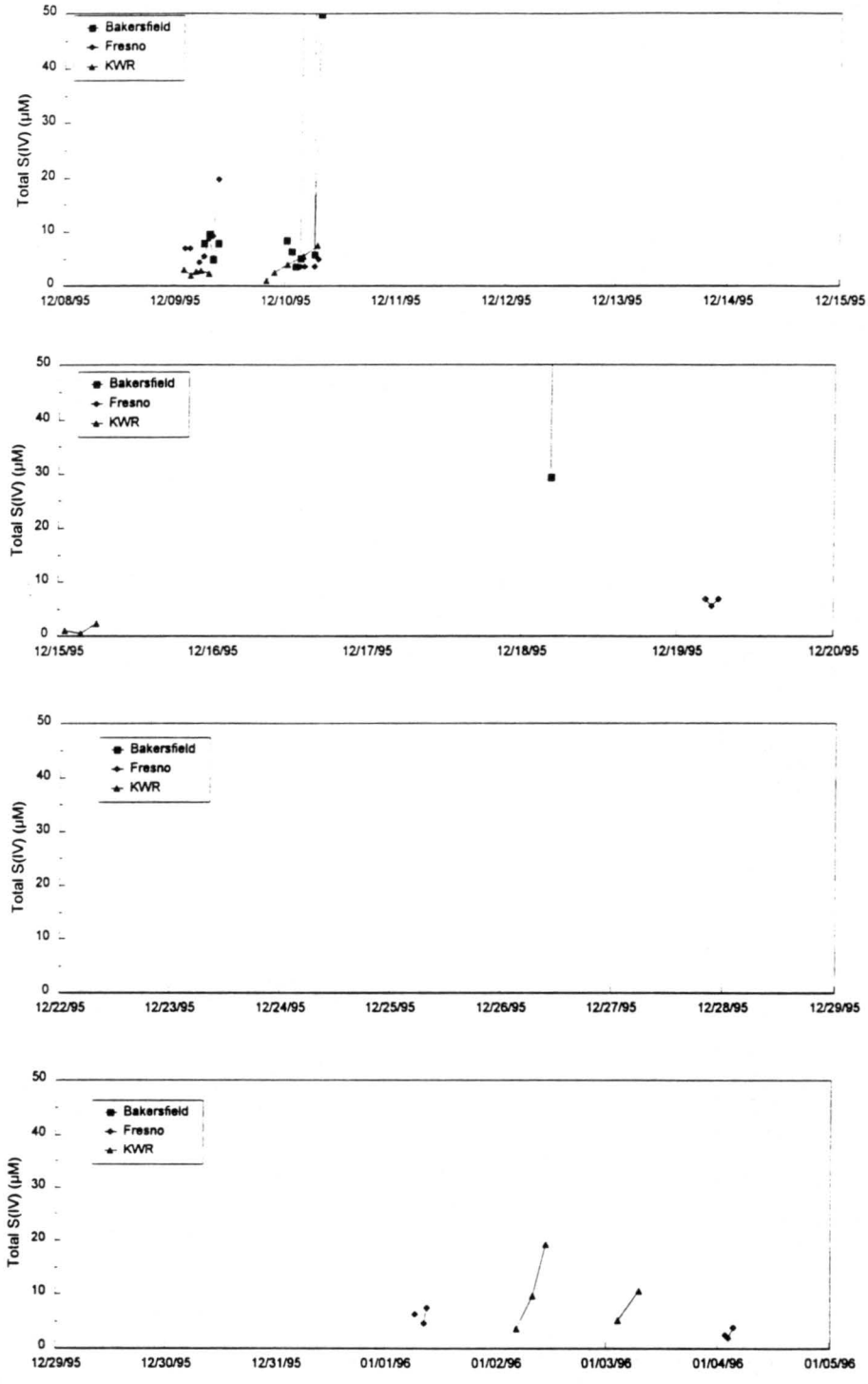

Figure A-14. Total S(IV) concentrations measured in bulk fog samples collected with the CASCC2 collectors at the three IMS95 core sites.

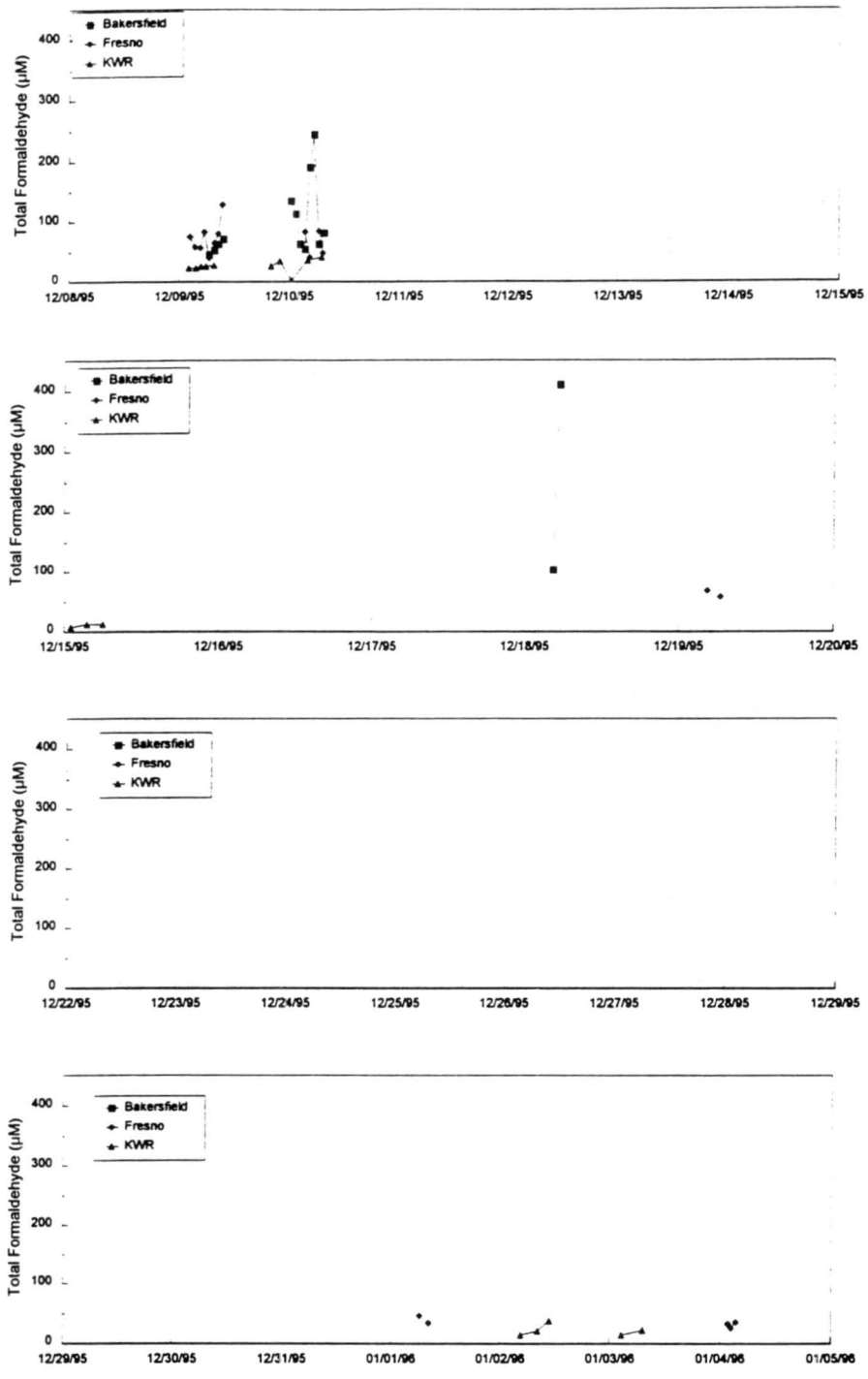

Figure A-15. Total formaldehyde concentrations measured in bulk fog samples collected with the CASCC2 collectors at the three IMS95 core sites.

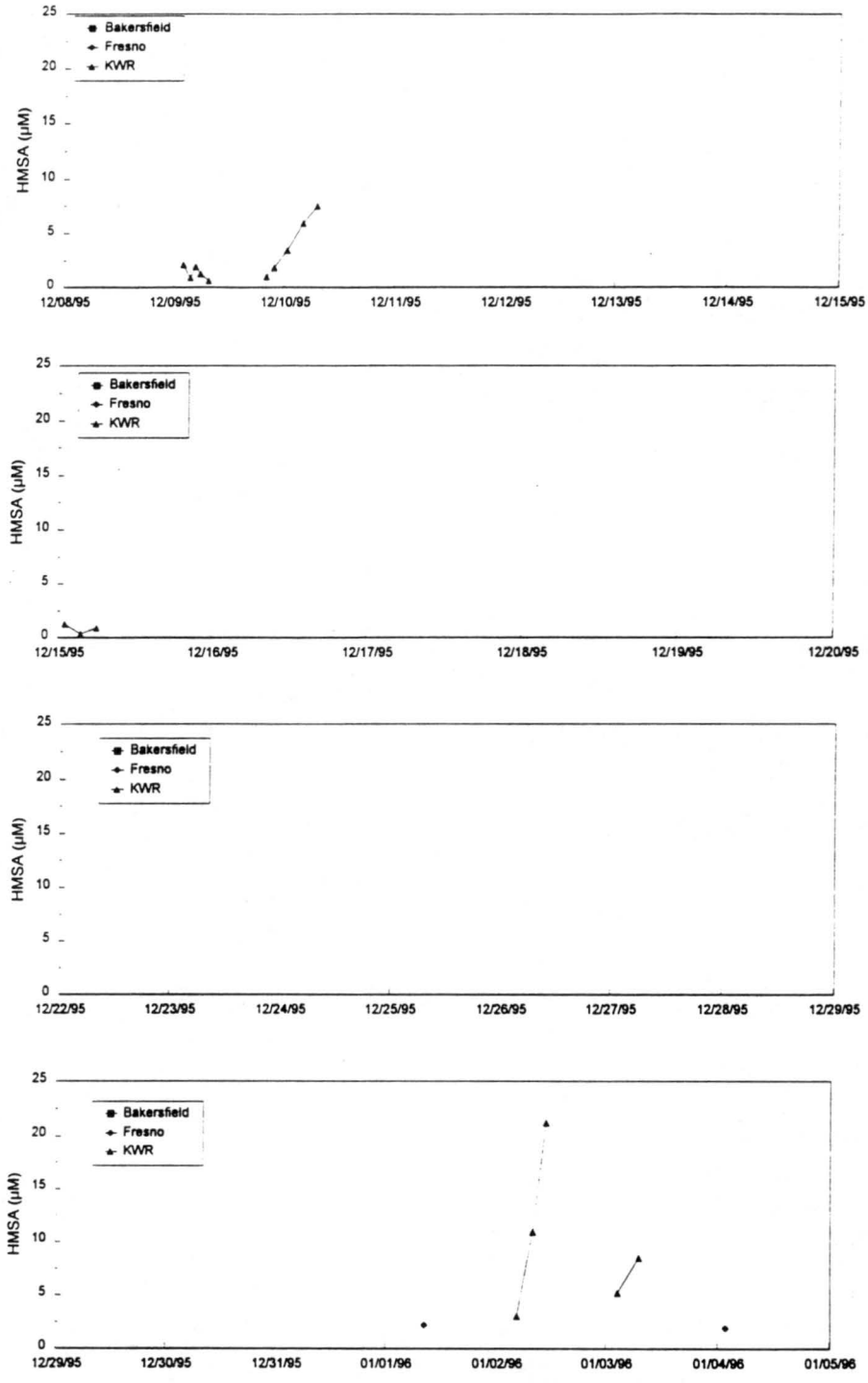

Figure A-16. Hydroxymethanesulfonate (HMS) concentrations measured in bulk fog samples collected with the CASCC2 collectors at the three IMS95 core sites.

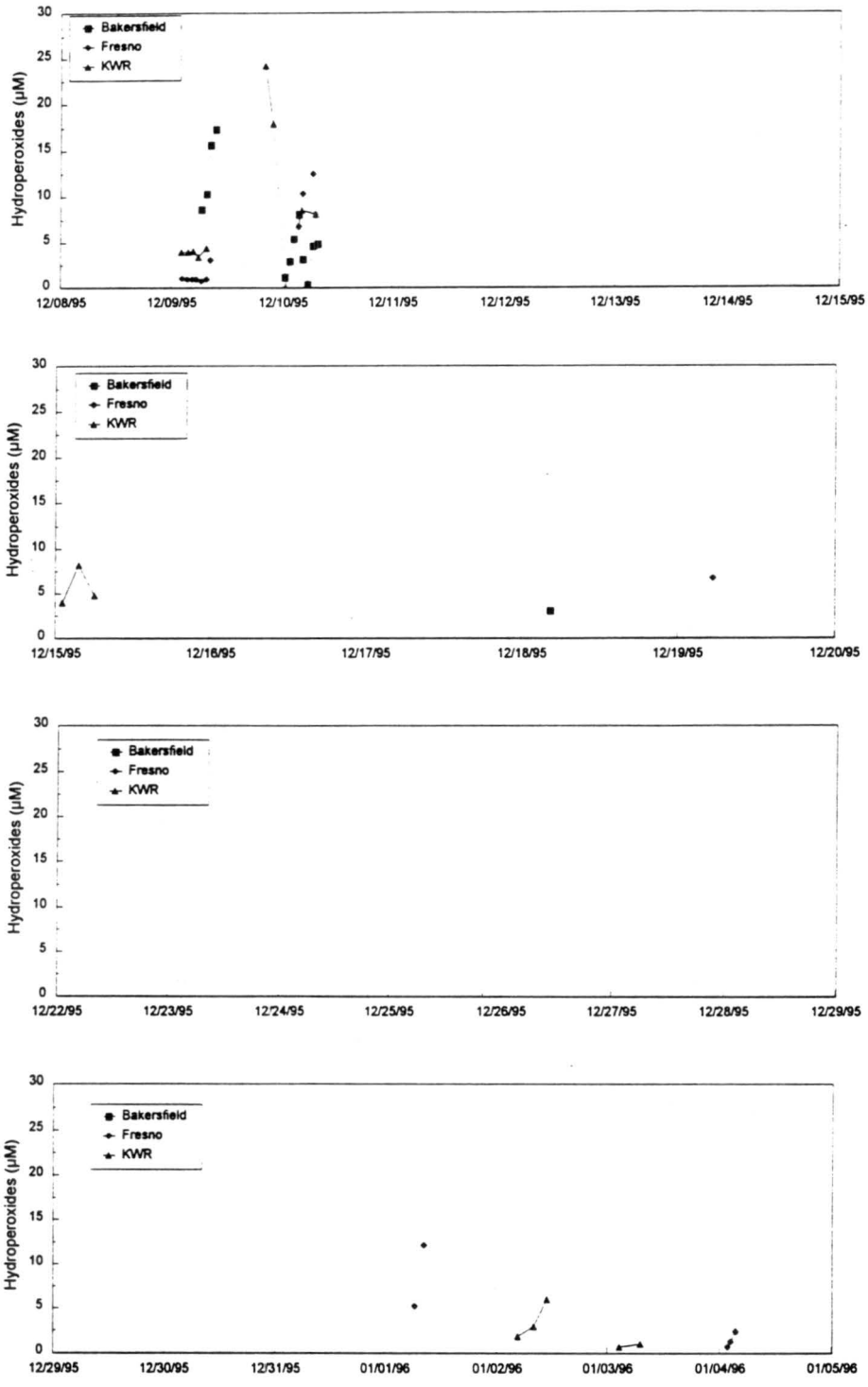

Figure A-17. Hydroperoxide concentrations measured in bulk fog samples collected with the CASCC2 collectors at the three IMS95 core sites.

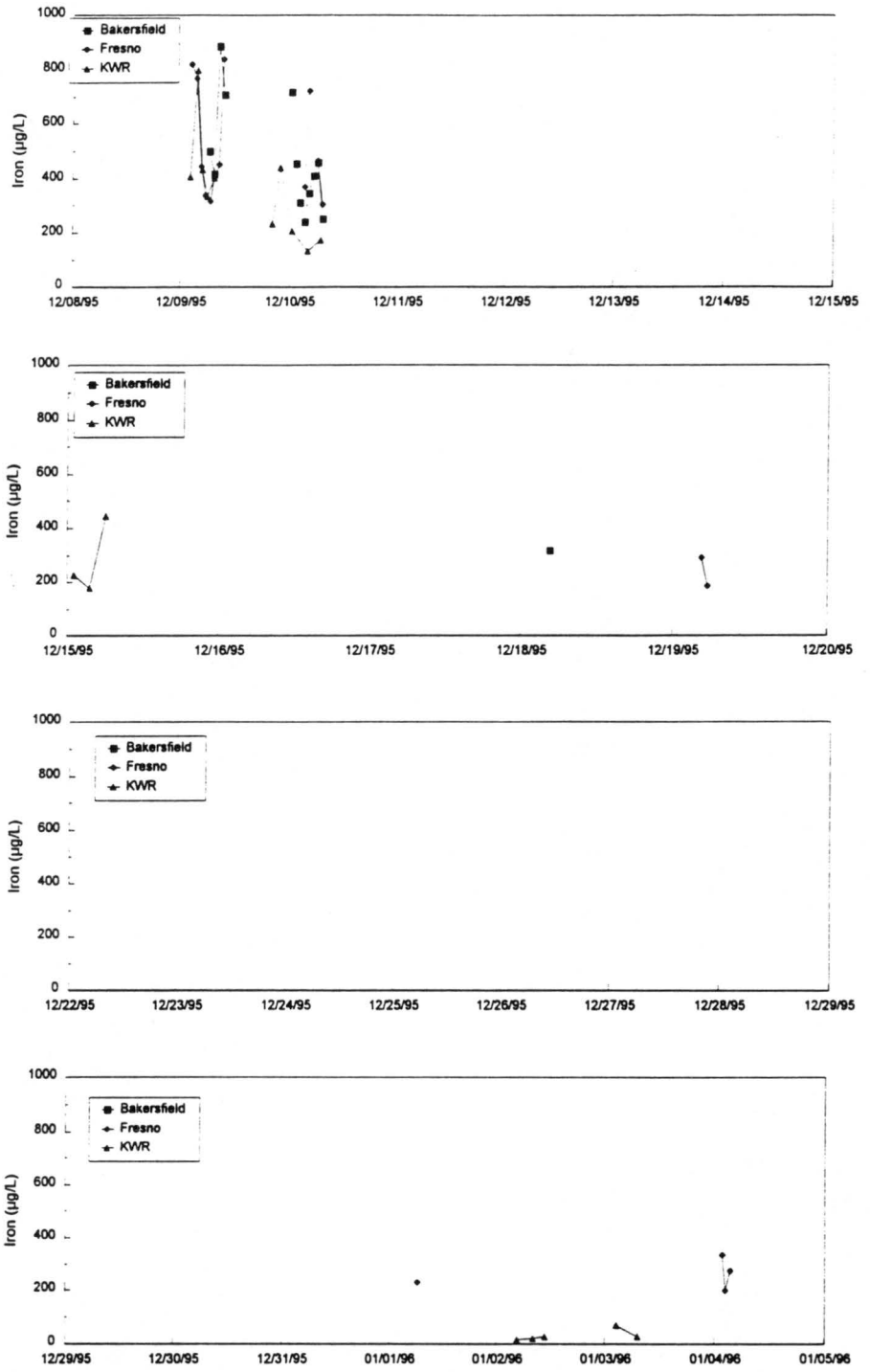

Figure A-18. Iron concentrations measured in bulk fog samples collected with the CASCC2 collectors at the three IMS95 core sites.

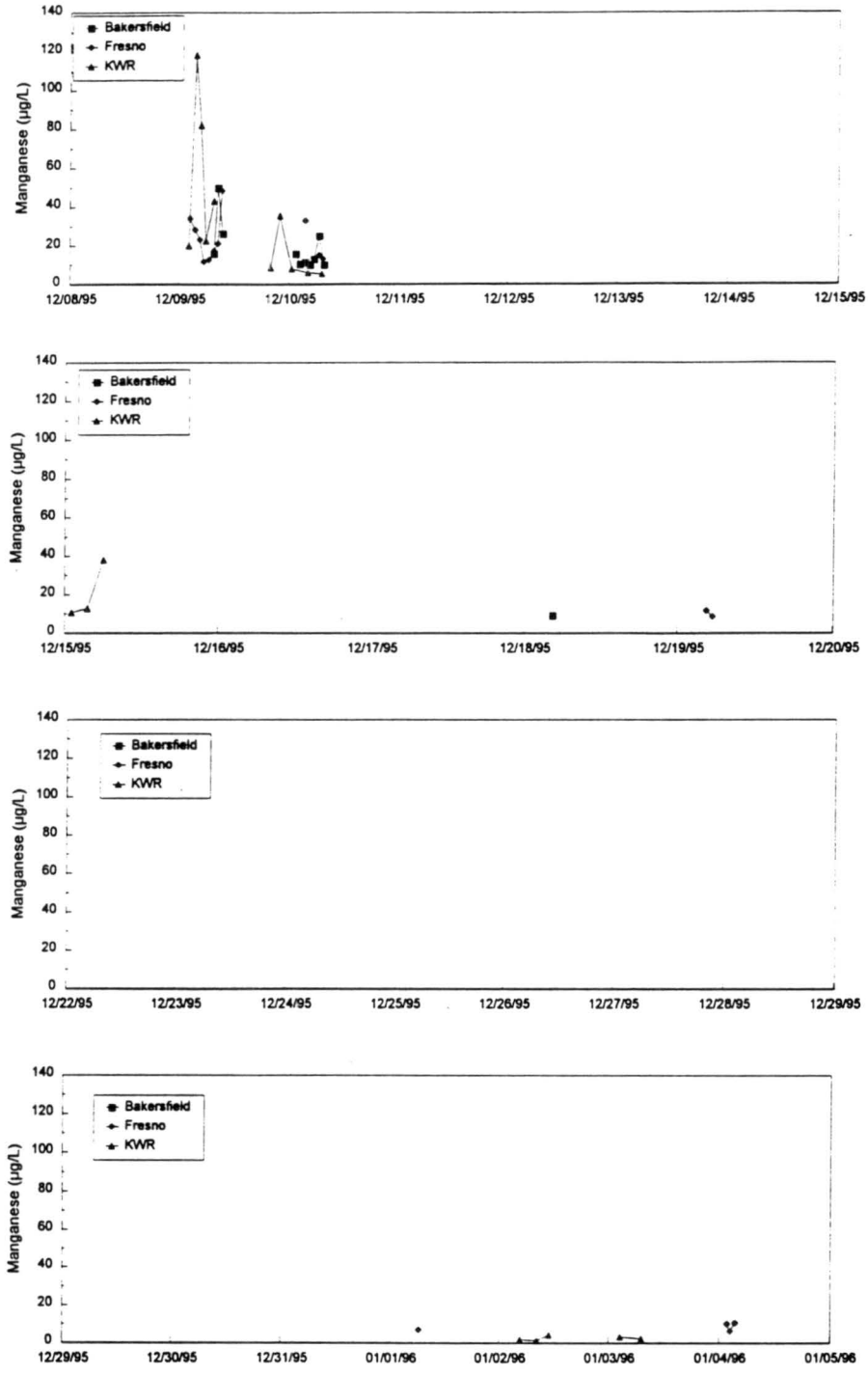

Figure A-19. Manganese concentrations measured in bulk fog samples collected with the CASCC2 collectors at the three IMS95 core sites.

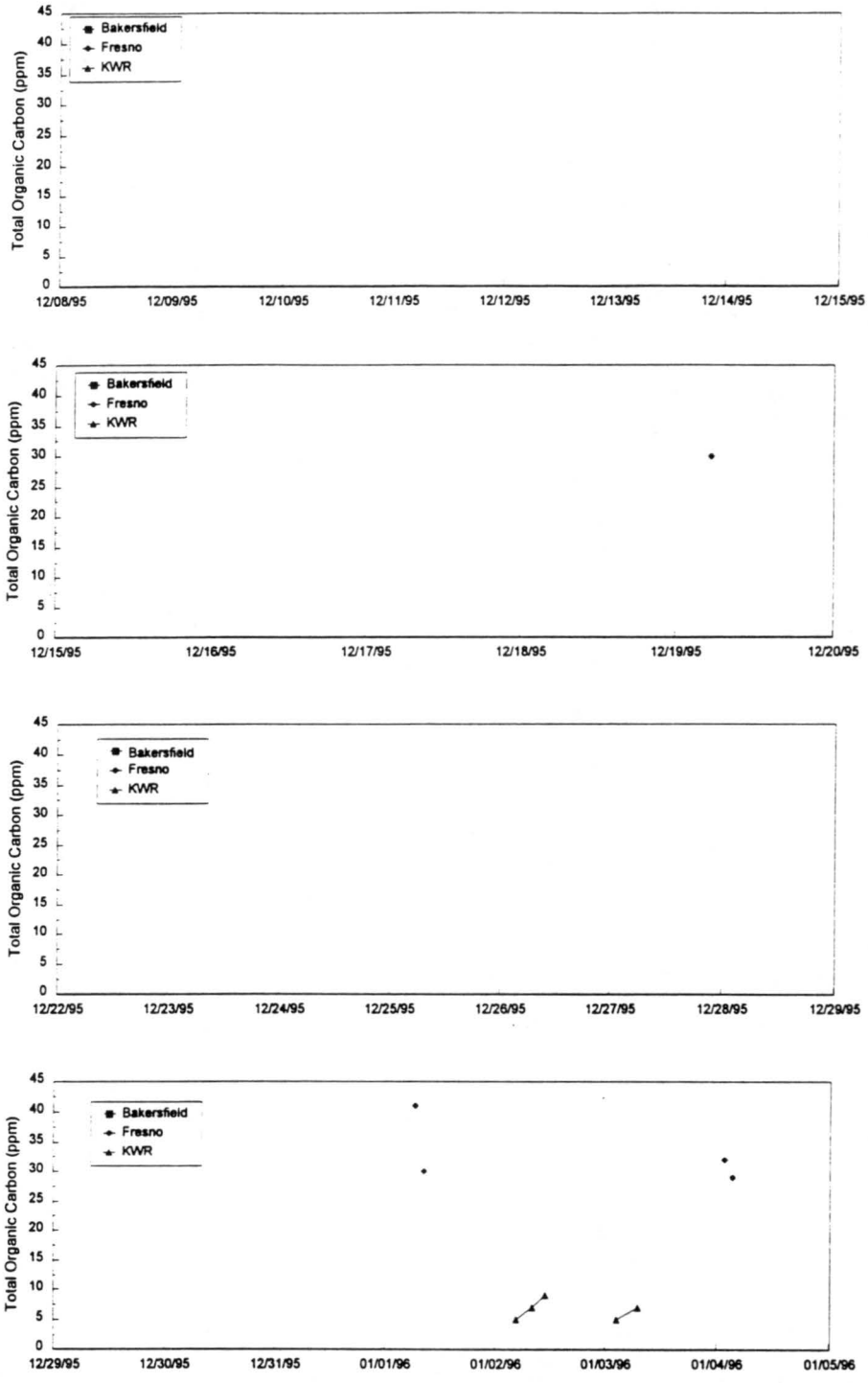

Figure A-20. Total organic carbon concentrations measured in bulk fog samples collected with the CASCC2 collectors at the three IMS95 core sites.

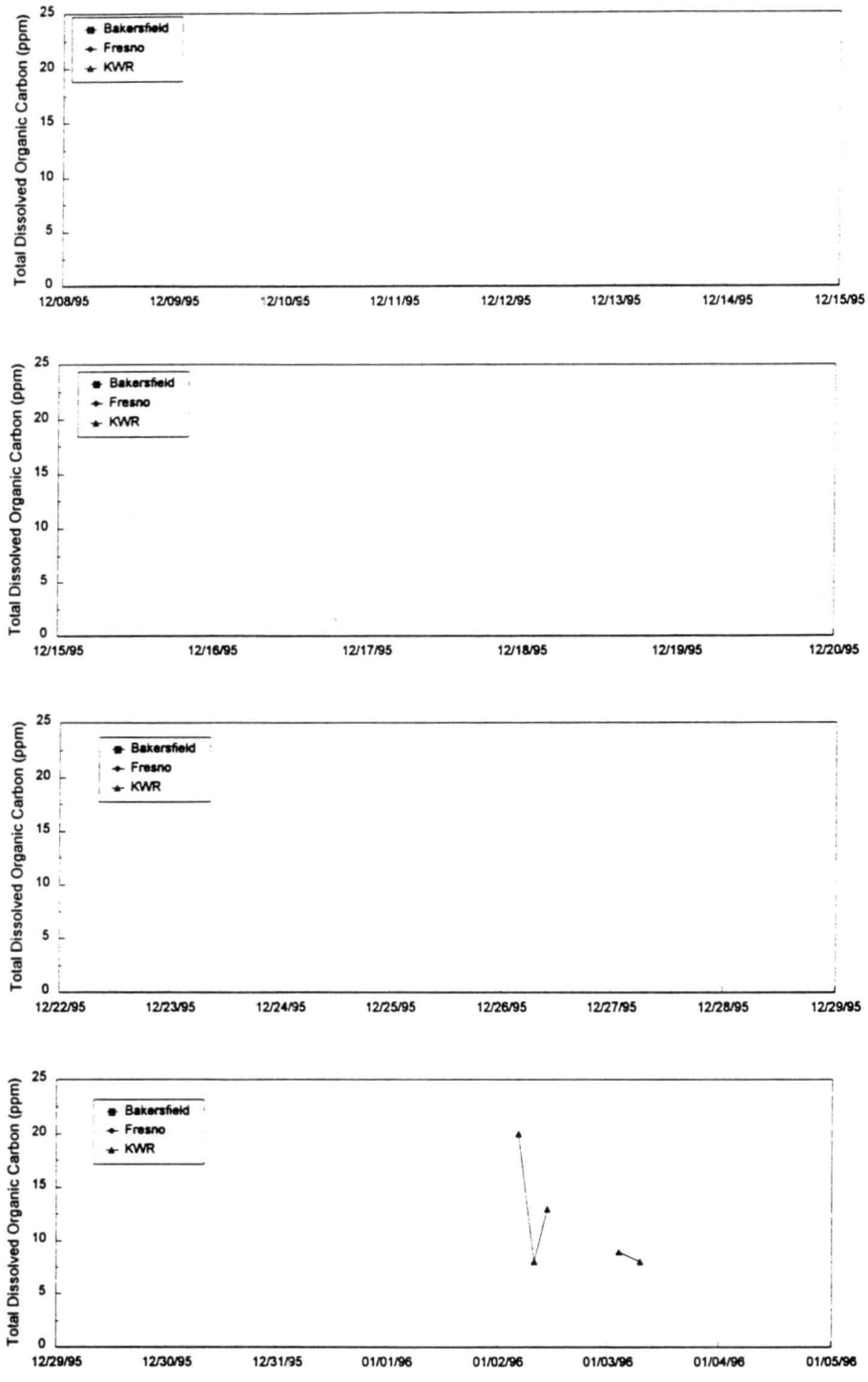

Figure A-21. Total dissolved organic carbon concentrations measured in bulk fog samples collected with the CASCC2 collectors at the three IMS95 core sites.